8-2021

Spatial Analyses of Gray Fossil Site Vertebrate Remains: Implications for Depositional Setting and Site Formation Processes

David Carney
East Tennessee State University

Spatial Analyses of Gray Fossil Site Vertebrate Remains: Implications for Depositional Setting

and Site Formation Processes

_____

A thesis

presented to

the faculty of the Department of Geosciences

East Tennessee State University

In partial fulfillment

of the requirements for the degree

Master of Science in Geosciences, Paleontology concentration

_____

by

David Carney

August 2021

_____

Dr. Andrew Joyner, Co-Chair

Dr. Chris Widga, Co-Chair

Dr. Steven Wallace

Keywords: taphonomy, fabric analysis, GIS, UAV

ABSTRACT

Spatial Analyses of Gray Fossil Site Vertebrate Remains: Implications for Depositional Setting

and Site Formation Processes

by

David Carney

This project uses exploratory 3D geospatial analyses to assess the taphonomy of the Gray Fossil

Site (GFS). During the Pliocene, the GFS was a forested, inundated sinkhole that accumulated

biological materials between 4.9-4.5 mya. This deposit contains fossils exhibiting different

preservation modes: from low energy lacustrine settings to high energy colluvial deposits. All

macro-paleontological materials have been mapped *in situ* using survey-grade instrumentation.

Vertebrate skeletal material from the site is well-preserved, but the degree of skeletal articulation

varies spatially within the deposit. This analysis uses geographic information systems (GIS) to

analyze the distribution of mapped specimens at different spatial scales. Factors underpinning

spatial association, skeletal completeness, and positioning of specimens were examined. At the

scale of the individual skeleton, analyses of the Mastodon Pit explore how element completeness

and orientation/inclination of the mastodon reflect post-depositional processes.

DEDICATION

This project is dedicated to a young naturalist that we lost too soon, Ty Harrison.

TABLE OF CONTENTS

LIST OF TABLES

LIST OF FIGURES

CHAPTER 1. INTRODUCTION TO THE PROJECT

Gray Fossil Site

The Gray Fossil Site of Washington County, Tennessee is a paleontological site that was discovered in 2000 by the Tennessee Department of Transportation during re-routing of a highway corridor near the town of Gray, Tennessee. Sediments that infilled the sinkhole date to the early Pliocene (4.9-4.5 Ma) and would have filled the sinkhole deposit over 4.5-11 Ka (Wallace and Wang, 2004; Shunk et al. 2009; Samuels et al., 2018). Ecologically, GFS is interpreted as an inundated sinkhole surrounded by a hardwood deciduous forest (Whitelaw et al. 2008; Shunk et al. 2009; Zobaa et al. 2011; Ochoa et al. 2016). Paleontological materials from these deposits include a diverse range of floral and faunal remains (e.g., Wallace and Wang 2004; Liu and Jacques 2010; Bourque and Schubert 2015; Jasinski 2018; Samuels et al. 2018).

Vertebrate remains at the GFS are extremely well-preserved, a condition that can be attributed to the low energy depositional environment (Shunk et al. 2006). These sediments are highly organic, and in some areas are thought to represent a subaqueous, anoxic depositional environment (Shunk et al. 2009; Keenan and Engal 2017).

In 2015, GFS researchers began excavation of a large mastodon. This deposit contained poorly sorted and oxidized sediments exhibiting a wide range of clast sizes, features that are uncharacteristic of the rhythmites found in other areas of the site. Particle sizes ranged from clays to boulders. A species of Dwarf Tapir, *Tapirus polkensis*, commonly found in the GFS rhythmite deposits were also found in abundance in the poorly sorted sediments of the Mastodon Pit. Poorly sorted sediments can be attributed to mass wasting events. Therefore, one possible hypothesis that explains this depositional setting is that a mastodon (or a group of mastodons)

may have become entrapped in a mass wasting event. This thesis aims to shed light on this event, and to reconstruct a taphonomic scenario that is consistent with field observations and the distribution of mapped paleontological materials.

Vertebrate Taphonomy

Within paleontology, taphonomy is defined as the study of processes acting on an individual organism after death, including decay, transport, burial, and diagenesis (Lyman 1994). This information helps researchers understand how a fossil assemblage was formed, potentially providing estimates of the length of time a site was open (Badgley 1986; Behrensmeyer, 1982; Eberth 1990; Rogers and Kidwell 2000), insight into taxonomic representation (Voorhies 1969; Behrensmeyer 1991; Lyman 1994), and spatial distribution of vertebrate materials within a site (Gilmore 1936; Dodson 1973; Hill 1979).

During the latter half of the 20th century, many taphonomists explored a variety of phenomena through patterns noted in fossil assemblages. For example, Voorhies (1969), investigated the impact of flowing water on the representation of skeletal elements. These neo-taphonomic experiments were designed to investigate how bones are transported in flowing water and empirically demonstrated preferred orientation and transport potential of various skeletal elements. These processes were further explored by Behrensmeyer (1975). Voorhies noted that bones with a distinct long axis will often orient themselves either parallel or perpendicular to the current flow depending on the flow's rate and the asymmetry of the bone in the current. Behrensmeyer (1975) used Voorhies' (1969) studies of skeletal element transport potential to create groupings of elements that she termed "Voorhies Groups". Preferential orientation of bones with a long axis, along with the frequencies of Voorhies Group elements have been used by taphonomists to infer fluvial impacts on an assemblage (Dodson 1973;

13

Berhensmeyer 1975; Blob 1997; Alberdi et al. 2001). Both fluvial and lacustrine deposits are present in the GFS sinkhole, therefore analyses traditionally applied to fluvial and lacustrine settings were used to decipher taphonomic processes occurring at the GFS. This project also incorporates new data analysis and visualization techniques that augment traditional mapping and documentation activities.

Digital Mapping and Spatial Analyses in Paleontology

Due to the transient nature of the paleontological record, accurate field documentation is critical to ethical paleontological excavation (Rogers, 1994). Historically, mapping of vertebrate fossil deposits incorporated a grid system. Excavated specimens are drawn by hand, sometimes using a gridded mapping square (Abler, 1984). Hand drawn maps are two-dimensional (2D), lacking the three-dimensional (3D) detail present in the sedimentary record, such as when fossil material is covered by other material (Brown et al. 2020). These maps are useful for site visualization, however, they do not provide key information in the analysis of the sedimentary media such as volume, inclination, elevation, or spatial association in 3D.

As digital mapping gained popularity through computer applications such as computer-aided design (CAD) and geographic information systems (GIS), it became clear to some paleontological researchers that GIS-based mapping could be invaluable to their studies. With this in mind, there was a push to incorporate into fieldwork high precision mapping techniques that are more appropriate for working in digital environments. Currently, paleontological mapping utilizes three approaches (not mutually exclusive): 1) create maps by hand that are subsequently digitized (Bramble 2014), 2) mapping specimens with GPS (Brown 2020), and/or 3) mapping specimens with survey-grade total stations (Lien et al. 2002; Albert et al. 2018). Each technique has advantages and disadvantages, however, a total station has been used to map

specimens at GFS since 2001 (Burdick et al. 2002; Nave et al. 2005;). Although it is an investment in time, money, and expertise, a total station system allows field researchers to map and document paleontological materials quickly and accurately. These data are easily transferred to a GIS for visualization and analysis.

Layout of study

This study has two objectives. First, this thesis will describe a digital approach to documenting paleontological sites using modern geospatial tools and techniques. Second, these techniques are applied to taphonomic questions at two distinct spatial scales, site-wide and pit-based. Chapters topically reflect these two objectives. Chapter two describes the workflows for using GIS to map objects and surfaces identified during field excavation. Chapter three uses exploratory 3D GIS analyses to examine taphonomic processes at work in the GFS to delineate intra-site spatial differences between low-energy rhythmite depositional settings and poorly sorted, high energy deposits where the mastodon was found.

CHAPTER 2. A WORKFLOW FOR THE DOCUMENTATION AND ANALYSES OF GEOSPATIAL FEATURES AT PALEONTOLOGICAL SITES

DAVID CARNEY

East Tennessee State University, Department of Geosciences, Johnson City, Tennessee, 37604, USA

Abstract

Maps of paleontological localities provide invaluable information for understanding ancient life and past environments. Mapping has been an important tool employed by paleontologists for decades, though the methods have changed through time. Thorough mapping of fossils and documentation of their depositional context is required for spatial taphonomic investigation, which must be completed prior to making interpretations of the site's paleoecology. Over the past few decades, palaeontological site mapping has incorporated emerging digital technologies to facilitate the mapping process and expand its capabilities. 3D mapping is now possible with various tools, including high-precision surveying equipment and geographic information systems (GIS). The dataset of mapped specimens (N > 30,000 points) from the Gray Fossil Site (GFS) provides an excellent platform for testing new 3D methods. This project provides workflows for processing raw collected data into meaningful digital products. Mapped objects are converted into features and drone-collected aerial imagery of one of the site's excavation pits are converted into raster-based files. Together, these digital products provide an interactive environment for exploring and testing spatial aspects of hypothesized depositional environments.

2.1 Introduction

Mapping the natural world has become an integral part of many studies, as the "where" is often just as important as the "what". Maps have evolved into a collection of databases that are maintained, visualized, and quantitatively analyzed within Geographic Information Systems (GIS). Recent advances in computing power, remote sensing, spatial analytics, and 3D visualization have made spatial analyses important tools for asking increasingly sophisticated geospatial questions (Grieves 2019). Such spatial tools provide a robust, comprehensive approach to the analysis of real-world spatial phenomena (Batty 2018). The concept of a real-world system that is digitally replicated has been referred to as a digital twin (Grieves 2014). The goal of a digital twin is to improve predictions, automation, and models of real-world systems for better analysis (Grieves 2019). These ideas have been applied in industrial and urban planning contexts and show promising results (Schrotter and Hürzeler 2020).

While the natural world functions differently than built environments, it also functions in predictable ways. Maps have aided in visualizing natural phenomena, but the idea of a digital twin can add a predictive aspect to these applications through spatial analytics.

Geological applications present a unique challenge to spatial analyses as the subject of study is often underground. Paleontology is one area where mapping has proven to be valuable, though particularly challenging. Spatial analyses of paleontological localities provide quantitative and empirical data that support in *in situ* observations as well as document phenomena that is unobservable in the field (Albert et al. 2018; Behrensmeyer 1975; Friscia et al. 2008; Giusti et al. 2018; Mackie et al. 2020; Voorhies 1969). These are but some of the reasons why the idea of a digital twin--a realistic digital representation capable of evolving with the collection of new data--is well suited to answer paleontological research questions.

17

Fossil-bearing deposits are geologically, stratigraphically, and taphonomically complex. Taphonomic analyses help reveal the depositional history of a site, which is important to understanding the preserved flora and fauna (Alberdi et al. 2001; Friscia et al. 2008; Lyman 1994; Voorhies 1969). Taphonomy, or the study of the fossilization process (Behrensmeyer 1988), relies heavily on the context of fossils within a sedimentary matrix. This association between fossils and the sediments in which they are preserved can reveal past landscape processes (Voorhies 1969). These relationships must be understood before paleoecological or chronological analyses reach their full potential (Akersten et al. 1983).

The process of excavation is inherently destructive. Despite the research potential of excavated paleontological materials, the removal of *in situ* materials ultimately erases information about the depositional history of the site. Specimen size, orientation, arrangement, and completeness are some of the attributes of mapped data that can be used in taphonomic analyses to reveal patterns in the preservation of the fossil material (Lyman 1994). It is therefore critical to document taphonomic patterns during field excavation through accurate mapping of materials removed from a site.

Historically, mapping of paleontological sites relies on the establishment of a local grid coordinate system (Rogers 1994). Throughout excavation, the location of macrofossils and sedimentary features are hand-drawn within this coordinate system (Bramble et al. 2014). Local grid systems can be geo-referenced and transformed to regional-scale coordinate systems such as state plane or UTM to place them within the context of independently collected topographic or geological data (Hill et al. 2020). However, the process of conversion introduces several inaccuracies into the spatial dataset. Hand-drawn maps may not consider the 3D length and

positioning of fossil material as they are drawn in only two dimensions. This can lead to scaling errors in georeferenced maps.

Some researchers have digitized hand-drawn maps by scanning and manipulating them with computer software (Bramble et al. 2014; Eberth and Getty 2005; Ryan et al. 2001). These techniques are time-consuming and provide limited analytical power. This approach provides a 2D rendition of the site, which potentially limits the visualization of complex topographic or stratigraphic relationships. Fossils and their surrounding matrix are 3D phenomena and presenting them two dimensionally reduces the observable topological interactions inherently present in the deposit.

In recent years, paleontologists have begun to integrate geospatial survey instruments, such as high accuracy global positioning systems (GPS) and total stations, into their mapping procedures (Albert et al. 2018; Brown et al. 2020; Nave et al. 2005; Burdick et al. 2002). Digital and GPS-enabled survey instrumentation improves accuracy, precision, and speed when collecting geospatial data. Additionally, these methods are more compatible with digital post-processing procedures as they remove many of the manual steps required to digitally replicate traditional site maps and minimize transcription errors. Geospatial data can be directly incorporated into a GIS using software such as Esri's ArcGIS Pro. GIS can display complex spatial data and incorporate spatial tools for data analysis. GIS programs now support 3D interfaces (e.g., called "scenes" in ArcGIS), which can be used to interpret the complex 3D nature of geologic deposits and mapped fossils preserved within. 3D tools are particularly useful in the mapping and documentation of below-ground resources. Digital site mapping has been carried out at archeological sites for decades (Apollonio et al. 2012; Estrada-Belli 1999; Giusti et al. 2018; Kvamme 1995; Mackie et al. 2020; Nigro et al. 2003), but is still rare in paleontology.

The Gray Fossil Site (GFS) provides the opportunity to assess these 3D applications since excavators have routinely used a total station to document the location of paleontological materials for the last 20 years. Mapped data are stored in a geodatabase and provide a large sample for rigorous taphonomic analyses. Methods for geospatial documentation, geostatistical analyses, and 3D visualization are described herein. These methods include techniques for mapping fossil materials, topographic, and geological features; as well as subsequent data conversion for integration into a 3D GIS platform. Together, these analyses offer insight into the potential of geospatial 3D modelling for intensive and efficient taphonomic studies.

2.2 Site Background

The GFS is located in Washington County, Tennessee (Figure 2.1) and was discovered by the Tennessee Department of Transportation (TDOT) in 2000 (Wallace et al. 2002). As TDOT began rerouting State Route 75, they uncovered fossils and brought the site to the attention of paleontologists. The GFS covers a lateral area of about 2.6 ha and reaches depths of about 40 m below ground surface (Shunk 2006; Whitelaw et al. 2008).
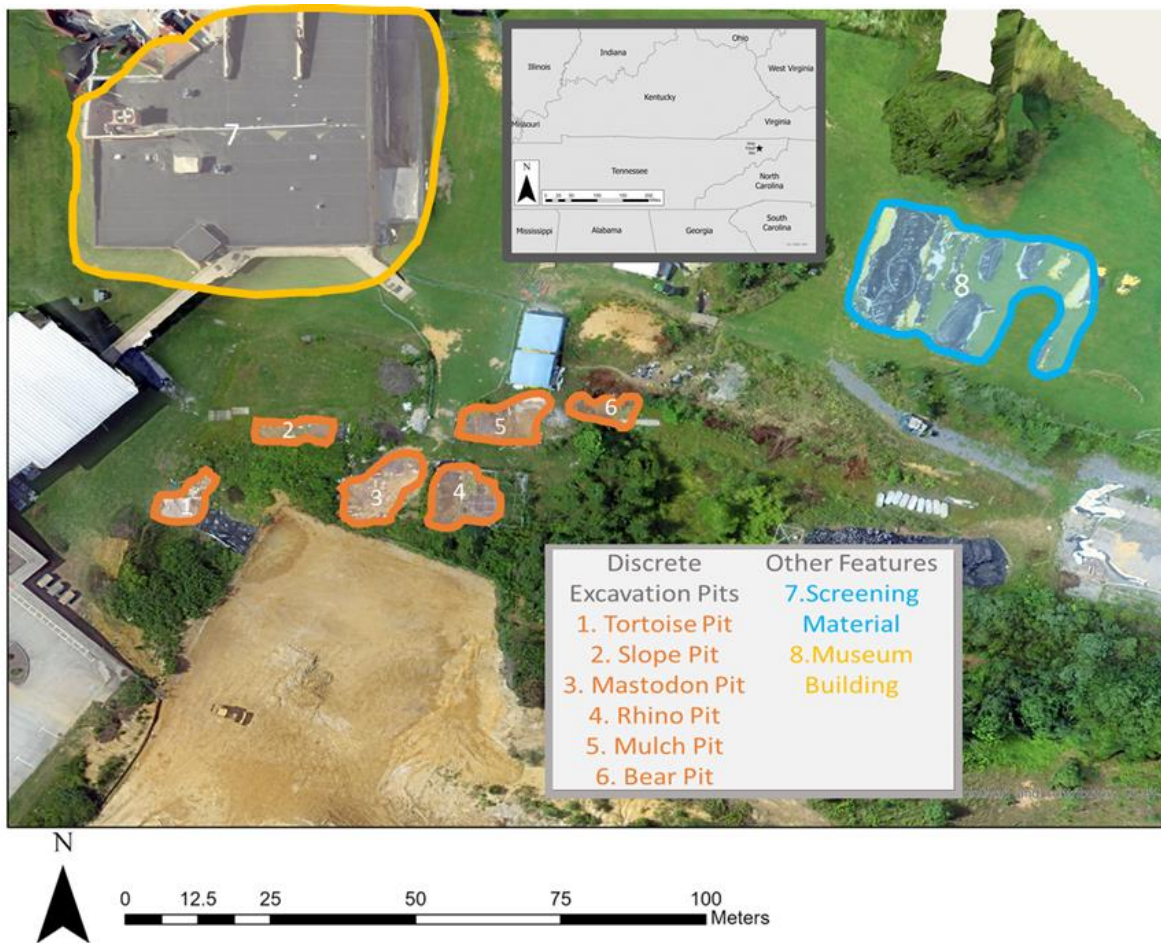
Figure 2.1 Aerial view of the Gray Fossil Site in Gray, Tennessee. Excavation pits are highlighted in orange. Excavations have been ongoing since 2000.

Paleontological materials at the GFS date to the early Pliocene (4.9-4.5 Ma) (Samuels et al. 2018; Wallace and Wang 2004). At this time, the GFS was an inundated sinkhole that infilled with fossiliferous deposits (Ochoa et al. 2016; Shunk et al. 2009). Nave et al. (2005) described a method of paleontological documentation using high-accuracy, survey-grade instrumentation. This system has been in place since 2001. Surveying each fossil is valuable for rigorous geostatistical analyses of site formation and taphonomic patterns (Ketchum 2011; Nave et al. 2005; Burdick et al. 2002). Survey data are maintained in a geodatabase.

In 2015, field crews at GFS began the excavation of a relatively complete mastodon skeleton, the largest animal yet to be discovered at the site. Sedimentological characteristics of the area where the mastodon was found were unlike the fine-grained clay deposits that characterize other excavated areas at the GFS (Shunk 2006). Sediments of the Mastodon Pit are poorly sorted with highly variable particle sizes, from clay to boulders. The taphonomic pathway for the material in this pit is very different from other areas of the site and warrants further investigation.

This study offers a workflow for analysis and visualization of the distribution of paleontological materials at the GFS at two spatial scales: 1) small-scale relationships of bones with related geological phenomena in the 63 m^2 Mastodon Pit, as well as 2) overall trends in skeletal completeness and specimen positions across the 2.6 ha GFS site. With the 3D coordinates collected by surveyors at GFS, a 3D scene -constructed from many, georeferenced 3D models is created in ArcGIS Pro. These methods also incorporate analyses of attribute information tied to mapped specimen.

2.3 Materials

All mapped paleontological materials are from GFS deposits. Fossil-bearing matrix is hand-excavated in 1x1 m squares to facilitate complete recovery of macro and micro fossils. Excavated sediments are collected from each square, their location noted, then water-screened through 1.7 mm mesh screens. Screened matrix is invaluable to paleontological research as it provides systematic recovery of microfossils, which has led to the description of several new taxa of plants and animals from the site (Bourque and Schubert 2015; Jasinski 2018; Liu and Jacques 2010; Mead et al. 2012; Ochoa et al. 2016; Parmalee et al. 2002). Vertebrate macrofossils are flagged, surveyed with the total station, then removed. All fossil specimens, field notes, and digital field data are stored in the GFS Museum. These data were incorporated into our study (Figure 2.2).
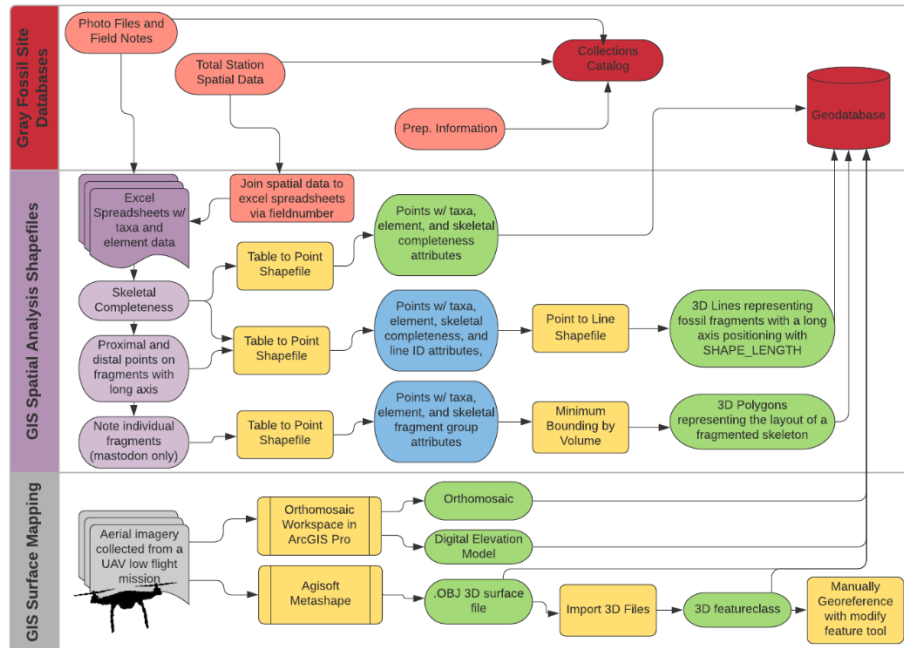
Figure 2.2 Three separate primary data sources (red) were incorporated into our study.

Spreadsheets (purple) used as a basis for shapefiles were generated from field notes and joined to

the total station spatial data using the field number. Surface mapping of the site's excavations

used aerial imagery collected from an unmanned aerial vehicle (UAV) (gray). Shapefiles and

raster-based data were saved in a geodatabase and also stored in the GFS Museum (red).

2.4 Methods

These methods describe the creation of a digital twin of the GFS. A digital twin improves asset management and facilitates geoanalytical analyses at multiple spatial scales to better understand natural phenomena preserved within.

2.4.1 Mapping the Site

2.4.1.1 Total Station Object Mapping

Total Station Procedure. A total station with attached data collector is used for mapping at the GFS. Between 2002 and 2016, spatial coordinates of paleontological objects and geological features was collected using a Topcon GPT 3002. Since 2017, all spatial data have been collected using a Sokkia CX-105. Raw spatial data are downloaded from the data collector as a .csv for subsequent archiving and analysis. Each record contains a field number, along with the Northing, Easting, and Elevation recorded in the Tennessee State Plane coordinate system.

Total station data are point-based and well-suited for point-based shapefiles in a GIS. The horizontal and vertical accuracy of points collected by the total station is within a few millimeters (Nave et al. 2005), while some of the most accurate GPS systems such as Real-time Kinematic (RTK) GPS systems are accurate within centimeters (Safrel et al. 2018). It should be noted that a total station requires a hardware operator as well as a "rod person" responsible for situating the target prism. Reflectorless total stations only need one surveyor and are capable of placing points on hard surfaces, but these systems are more costly and sacrifice some accuracy (Ali et al. 2016). It should also be noted that unlike GPS units, a total station does not need to connect to satellites to locate a point in a 3D grid. Other features such as boulders or other

geologic phenomena can also be mapped and given discrete identifiers in the dataset. To date, researchers at GFS have mapped over 30,000 points at the site.

   Total Station Dataset. At GFS, spatial datapoints represent morphological landmarks on fossil material (Nave et al., 2005). Elements with a long axis are mapped with a minimum of two points, one at each end. However, elements that are more complex shapes can be represented by dozens of points.

   Although a total station is capable of mapping points, lines, and polygons, the system in place at the GFS has evolved to treat each mapped specimen as a series of associated points that reflect multi-dimensional polygons. Each data point is assigned a unique Field Number with embedded information about the mapped specimen (Figure 2.3) (Nave et al. 2005). Importantly, field numbers tether the spatial data to hand-written field notes and provide a framework for documenting the relationships between data points at the fragment, skeletal element, and individual skeleton levels. Individual fragments are not identifiable in the developed system, however, sketch maps created in the field denote where points are placed on a fragment (Figure 2.4).
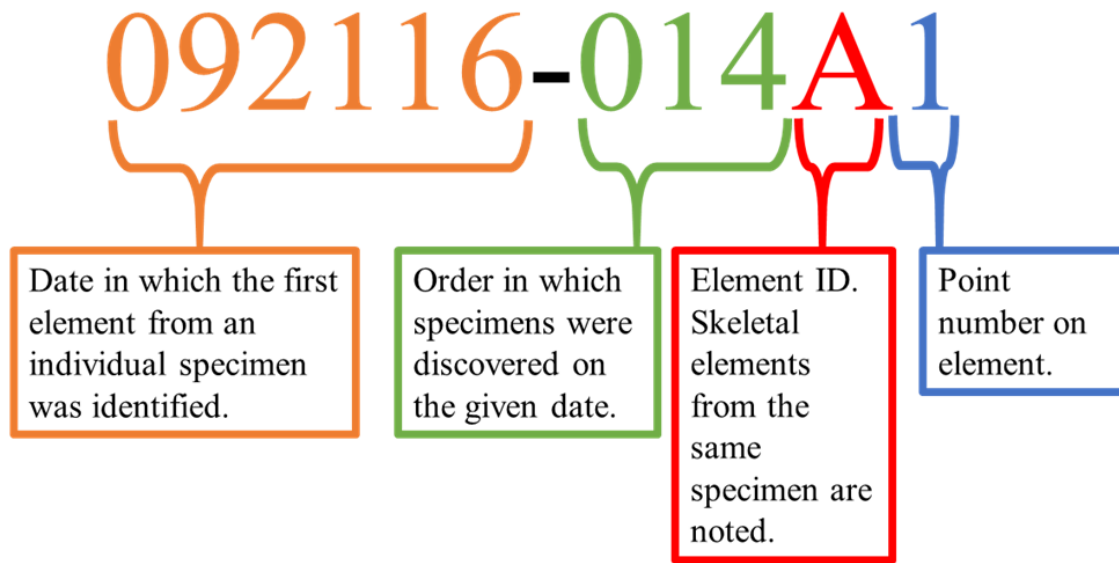
Figure 2.3 A breakdown of the field number format entered for each survey shot stored in the

total station. The first portion (orange) is the date in which the specimen was found. The second

portion (green) represents the order in which specimens were found on the given day. This

portion always has 3 digits associated with it to keep character length consistent. If these two

portions are identical on two different survey shots, the two shots represent the same individual

animal. The third portion (red) of the field number indicates the skeletal element represented by

the survey shot. If the first three portions of the field number are identical between two survey

shots, the survey shots (and coinciding field numbers) represent the same skeletal element from

the same individual. The fourth portion (blue) represents the survey shot number that was placed

on a skeletal element and is a unique, site-level identifier.
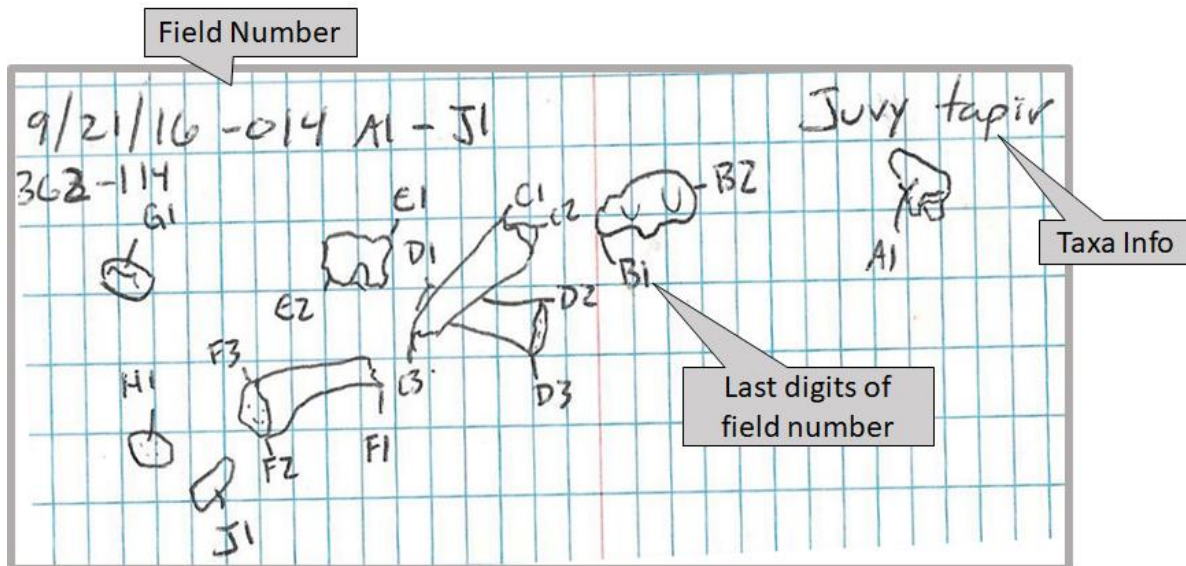
Figure 2.4 Field notes recorded to supplement the total station point-based dataset. The field number is recorded along with the rough sketches of the fossils and point placement.

Field Notes. The Sokkia total station is used to record one line of information per mapped point. The system allows more detailed inputs as opposed to one line, however the GFS workflow is designed with field expediency in mind. Field notes are recorded with a system in place to link this information to the feature recorded in the total station. Field notes contain field numbers with associated taxonomic and anatomical information, as well as a sketch map of the location of mapped morphological landmarks. Taxonomic information was also checked against post-preparation records for accuracy. For isolated elements, 1 - 2 survey points are adequate; however, complex associated specimens are mapped in a manner that preserves spatial relationships. Field sketches that illustrate *in situ* skeletal elements along with the location of mapped points placed on the element can help keep the layout of a complex specimen organized.

Because fossils are prepared and stored on site, plaster field jackets are rarely used to transport material. If field jackets are used, jacketed specimens are surveyed both before (upper

surface) and after (lower surface) removal. Specimens are typically bagged in the field and the

field number is written on the bag.

The field number written on the bags can be identified in the rough schematic sketch of

the associated skeleton. The notes and schematic sketches can be referred to during the

preparation of fragmented specimens. Figure 2.4 illustrates the field documentation of a

complex *in situ* specimen. A spreadsheet containing what associates the field number with

taxonomic and anatomical details from the field notes is a necessary precursor to integration with

the spatial geodatabase. This spreadsheet is then joined to the geodatabase using the "field

number" providing the real-world location of a specimen.

2.4.1.2 UAV Flight Surface Mapping

Although plane or satellite-based elevation datasets (e.g., LIDAR) may be available for a

site, they do not reflect local, short-lived surface changes resulting from paleontological

excavations (Brown et al., 2020), nor are they accurate enough to delineate the sub-meter

topographic differences that are often important to paleontological analyses. Unmanned aerial

vehicle (UAV) flights can occur at defined intervals throughout an excavation season, or

annually to document all changes that take place during a year. This procedure tested the

capabilities of UAVs to map mid-scale (1-5 Ha) and large-scale (<100 m^2) surface features.

UAV Specifications. The DJI Mavic Pro UAV is controlled by a remote device which is

linked to the DJI Pilot App for Android. The app allows the user to plan automated flights for

mid-scale mapping. However, mapping small areas at elevations <12 m requires manual piloting.

As the UAV completes its flight, the pilot in command takes photos using the DJI pilot app

feature and camera mounted on the UAV. The UAV records GPS coordinates and real-time

flight imagery. The Mavic Pro camera features a 35mm lens with 20 million effective pixels.

Each image taken during flight then has GPS data associated with it and can be uploaded into a GIS.

GFS Flight Missions. Surface mapping of GFS was completed with a DJI Mavic Pro UAV equipped with a gimbal-mounted camera. The DJI Pilot app for Android was used to create pre-planned missions. This automated flight feature was used for a flight that mapped approximately all 2.6 ha of GFS at an altitude of 30m. The flight acquired over 350 photos and took less than 18 minutes.

A second flight at lower altitude captured high resolution photos of the mastodon excavation pit. The UAV was manually flown in a grid pattern, approximately 3-4 meters above the ground, and acquired over 300 photos. Photos were taken with the camera facing in a downward vertical direction and also at an oblique angle to the horizontal surface in an attempt to highlight the vertical walls of the excavation pit.

For site-scale mapping, vertical UAV images were required to reduce skewing of the surface during post processing. However, for accurate 3D photogrammetry of small-scale features such as excavation pits, oblique-angle photos help to highlight features with high slopes (such as the excavation pit walls). Photos are saved on a micro-SD card and uploaded to a computer for post-processing.

2.4.2 Software Procedures for Mapped GFS Data

ArcGIS Pro (version 2.6.3) and the associated 3D Analyst extension were used to create shapefiles from the datasets representing mapped objects. The Ortho Mapping Workspace was used to process the aerial photos taken by the UAV to create mapped surfaces.

Agisoft Metashape (version 1.6.5) was used to create geo-referenced 3D meshes from UAV images. Rendered DEMs and orthomosaic photos were both incorporated into 3D scenes in ArcGIS Pro. Surficial 3D models were created and exported as .OBJ files with associated textures. This format is incorporated into 3D scenes in ArcGIS Pro, but is also compatible with 3D modeling programs including a variety of open-source software available for printing, editing, modelling, and distributing 3D models (e.g., Sketchfab, CloudCompare, Meshlab, Blender).

2.4.2.1 Procedure A. Volumetric Analyses of 3D Objects

Data Preparation. Datasets were edited and cleaned in Excel. Data hygiene is time-consuming, but a critical and necessary step in the integration of spatial and field datasets. Database fields include "Field Number", "Northing Value", "Easting Value", "Elevation", "Taxa", and "Anatomical Element". Additional fields such as "Skeletal Completeness" (total number of skeletal elements preserved for a given individual), and "Axial vs. Appendicular (left/right)" were also incorporated into the datasets for additional analyses of preservation patterns at the GFS depending on the analysis.

Fields incorporating hierarchies of anatomical information (i.e. skeletal element, body portion, and symmetry) were reserved for highly complete and associated specimens of interest. With fields organized in this fashion, "Select by Attribute" queries in ArcGIS Pro were executed to select particular elements of a skeleton (i.e., highlight all elements associated to the left side of an individual). The "Select by Attributes" tool was particularly helpful when creating a Minimum Bounding by Volume (MBV) for the entire mastodon as it could be used to ensure points were incorporated into the correct MBV object. The field number format stored in the total station spatial dataset can also link points together depending on if they are referring to the

same individual and even the individual's anatomical element. This information can support

analyses investigating degrees of association and articulation, which are known to

have taphonomic implications (Lyman 1994).

GIS Products. Three shapefile products were created in this assessment, including 3D

point-based, 3D vector-based, and 3D polygon-based shapefiles.

3D Point Shapefiles: The "XY Table to Point" tool within the data management

toolbox was used to create a shapefile containing all points of interest. This tool requires inputs

for "Northing", "Easting", and "Elevation" (optional for 3D) that must be organized as fields on

the input table. The coordinate system used here must match the coordinate system tied to the

total station's dataset for the points to appear in the correct space. The shapefile created from this

tool provides a basic visualization of where things are located as represented by points. The

points can reveal information about the proximity of specimens to one another in 3D space.

3D Vector Shapefiles for Fragments with a Long Axis: Regardless of how flat a bone

fragment sits *in situ*, the orientations of bone fragments with a long axis have implications for

interpretation of the depositional environment (Shipman 1981; Varricchio et al. 1995; Voorhies

1969). Fragment depictions in the field notes were scrutinized to ensure that they displayed a

distinct long axis. Survey points were collected at the ends of *in*

situ specimens exhibiting a distinct long axis. Vector-based shapefiles were created by

connecting these endpoints on the surveyed bones. A vector-based map display will not show the

fragment volume but is a way of visualizing trends in orientation (Eberth et al. 2007; Rogers

1994). Some authors have even argued that these types of theoretical maps are easier to

visualize than detailed bonebed maps (Eberth et al. 2007).

A new dataset that exclusively includes the points associated to bone fragments with a long axis (e.g., limb bones, ribs) was created using the "XY Table to Point" tool. This point-based shapefile is then used in the "Points to Line" (PTL) tool which treats points as vertices on a line. A "Line Field" was added to the attributes of the point-based shapefile before it is used as the PTL input feature. The "Line Field" is what the tool uses to associate a proximal point to a distal point. When run, the PTL tool creates a new vector-based shapefile. This shapefile contains a new field; "Shape Length". The units of the "Shape Length" depend on the coordinate system of the shapefile, but this value represents the length of the fossil's long axis. We used NAD 1983 (2011) State Plane Tennessee FIPS 4100 (Meters) which used meters for the "Shape_Length" field. This information is fundamentally valuable to a taphonomic study and can be calculated by ArcGIS as opposed to physically collecting this information in the field (Bramble 2014). The length of a bone's long axis also facilitates trigonometric calculations of the inclination and the orientation. These data are visualized using rose plots and stereonets (Shipman 1981).

3D Volumetric Shapefiles: The MBV tool can be used to create 3D shapes of point cloud data. Surface area and volume of each 3D entity is added to the attribute tables of newly created shapefiles. 3D volumes created with the MBV tool are used to examine complex topological relationships between field objects (e.g., vertebrate skeletons, boulders); however, all elements must have a minimum of 3-4 points per fragment. When editing the MBV parameters, "convex hull" was selected for the output feature class type. This resulted in a shape limited to the smallest possible space that surrounds all grouped points. The "group by" parameter is also important, as this relies on a field in the attributes that groups points to be bundled to create a

single shape much like the line field when using the PTL tool. This field used to group points must be edited so that there are no points excluded from the groups.

The procedure involved with creating a dataset for the MBV tool is time-consuming and recommended only for relatively complete individual skeletons. The ArcGIS Pro 3D Analyst extension continuously adds to its capabilities and functions but there are some limitations (Albert et al. 2018). Currently, raw point-based shapefiles have much of the same utility as 3D polygon-based shapefiles. 3D polygon-based shapefiles will become important for volumetric analyses as the 3D Analyst extension is further developed.

2.4.2.2 Procedure B. Documentation of Paleontological Sites Using UAVs

Two separate software platforms were used to process the aerial UAV photos. These photos were imported and aligned in Metashape to create a 3D model that was exported to textured 3D file formats (e.g., .OBJ/.PLY). ArcGIS was used to export a DEM and accompanying orthomosaic of the excavation pit. An .OBJ file is connected to a texture file that contains color for the object/surface. A DEM is a raster file which contains pixels that have elevation values associated with them. An orthomosaic is also a raster file where the pixels represent colors. A DEM represents a 3D surface while an orthomosaic is an image that overlays the DEM.

Metashape: Metashape was used to import and align 86 spatially-referenced UAV photos of the Mastodon Pit. These photos were initially used to create a sparse point cloud. A dense point cloud was then created by filling in the spaces between the points of the sparse point cloud with more points. A texture or mesh can then be applied to the dense cloud to see the overlain images in a 3D environment. This 3D model is exported as a .OBJ file.

The .OBJ file can be imported to ArcGIS Pro using the Import 3D Files tool. The placement of the file is marked by a placement point file, which is set to represent the center of the .OBJ feature. The feature may need to be shifted, which will require a change in the location of the placement point or manual editing with tools accessible in the "Modify Features" pane (Hill et al. 2020). Hill et al. (2020) used the same tool to import 3D scans of fossils from La Brea Tar Pits, Los Angeles, showing that scanned fossil material can be imported into a GIS and arranged to be oriented as they were when *in situ*. This method works well if the scanned fossil material is similar to how it looked when *in situ*. If scanned material was fragmented in the field and re-assembled, it will not reflect its *in situ* appearance, size, or orientation.

Ortho Mapping Workspace in ArcGIS Pro: The same spatially referenced photos were imported into ArcGIS Pro's Ortho Mapping Workspace. The workspace is used to adjust (similar to alignment) and refine the images. Once this is done, the images can be used to create DEM and orthoimagery raster files. The layer may require raster math editing if integrated with other DEMs in the site GIS.

2.5.1 Mapped Objects

    2.5.1.1 Point-Based Analyses

    Shapefiles consisting of points on anatomical landmarks include the following fields: "Field Number", "Northing", "Easting", "Elevation", "Preliminary Taxonomic Identification", and a metric reflecting the number of associated skeletal elements in a group (i.e., "Skeletal Completeness"). Figure 2.5 is a layout view of the shapefile with the symbology set to display points with graduating color intensity based on the given individual's amount of skeletal completeness.
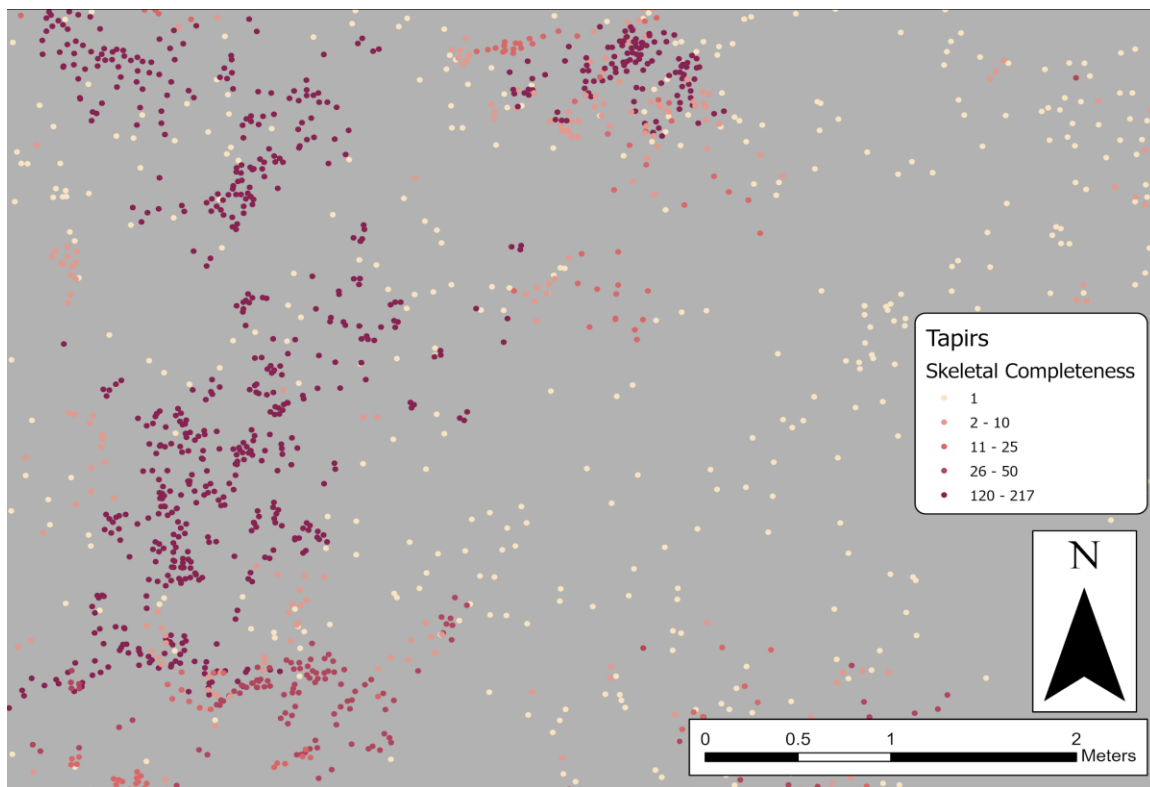
Figure 2.5. A point-based shapefile layer containing all points associated with tapir specimens. The field number can be used to sum elements associated with a given individual. The symbology of the shapefile was set to graduated colors based on the Skeletal Completeness

attribute field. Highly articulated tapir individuals are represented by dark purple points while isolated tapir fragments (Skeletal Completeness = 1) are represented by lighter colored points.

2.5.1.2 Vector-Based Analyses

Vector shapefiles represent the length, location, and positioning of bones with a long axis (Figure 2.6). Attributes include "Field Number", "Northing", "Easting", and "Elevation" for uppermost and lowermost endpoints. These data are associated with fields reflecting "Skeletal Element, "Preliminary Taxonomic Identification", and "Vector Length". Elements can be queried by taxon, individual skeleton, or skeletal element class.
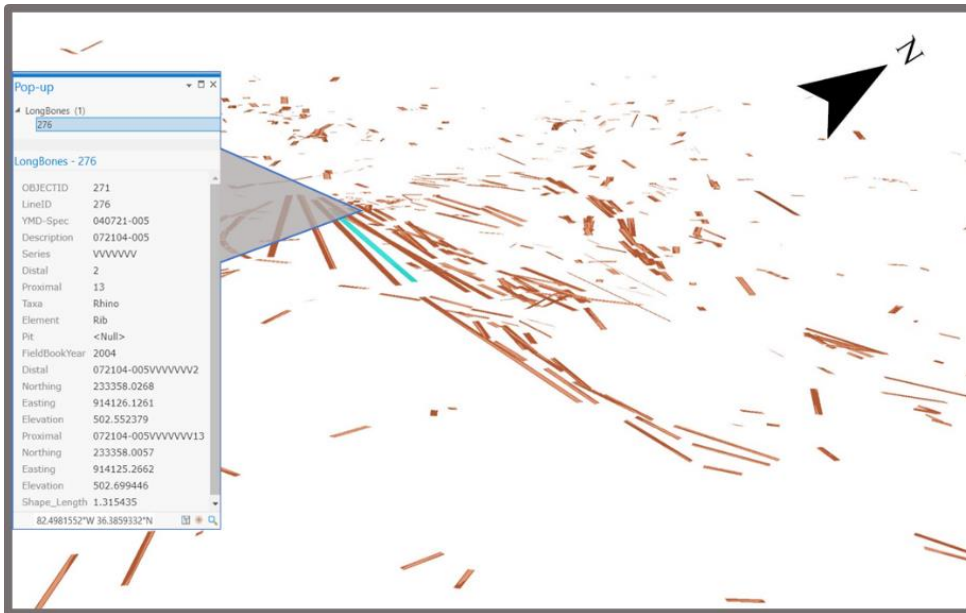
Figure 2.6 A vector-based shapefile layer with vectors representing the longest length of bones with a long axis. This layer was added to a blank 3D local scene. The view is set with an oblique view to highlight the 3D orientation of the vectors. One vector was selected to reveal the attributes associated with it.

2.5.1.3 Volumetric Analyses

A near complete mastodon skeleton was discovered at GFS in 2015, and has been thoroughly surveyed during excavation. This skeleton was discovered in an oxidized matrix consisting of poorly sorted sediments with clasts ranging in size from clays to boulders. The *in situ* location of all mastodon specimens and boulders was recorded (Figure 2.7). Considering the complexity of the deposit, time was taken to add detailed anatomical attribute fields to the shapefile. Fields include "Field Number", "Spatial Coordinates", "Skeletal Element", "Body Portion", and "Symmetry", as well as surface area and volume of the MBV polygon.
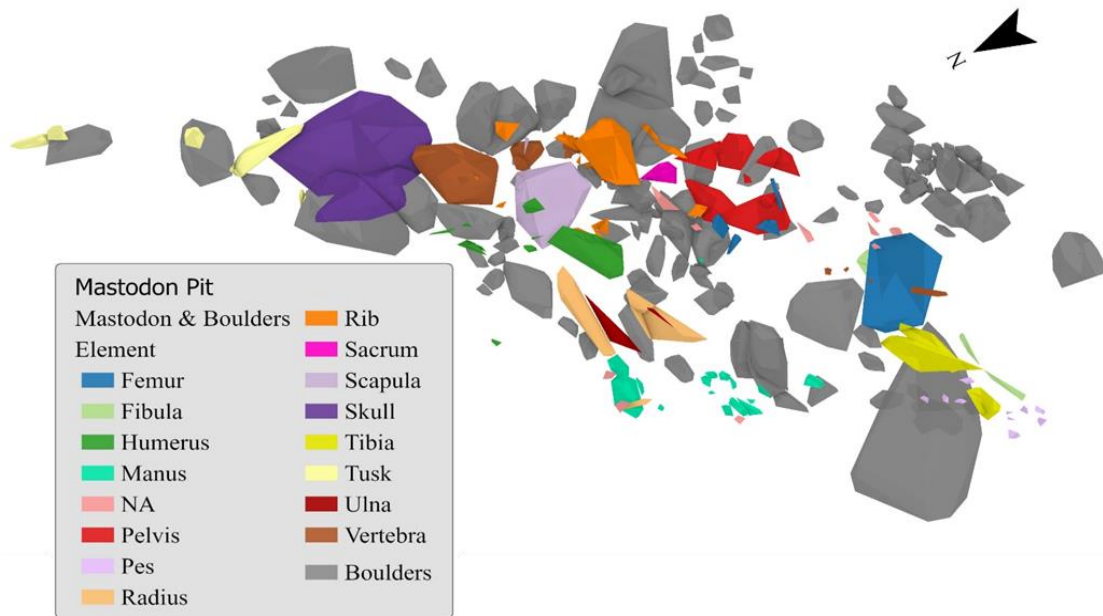
Figure 2.7 3D polygon-based shapefiles of the mastodon and boulders excavated in the Mastodon Pit. This excavation pit features a complex geology that is uncharacteristic compared to the geologies of other pits. 3D objects were created using the Minimum Bounding Volume tool in the 3D Analyst extension with mastodon and boulder point-based shapefiles used as inputs. Pit model can be viewed in an ArcGIS Online 3D interface at https://arcg.is/1T5mqL0.

2.5.2 Mapped Surfaces

Surfaces can be portrayed as a raster file layer that uses pixel values to display information. Surfaces can also be portrayed as complex 3D objects.

2.5.2.1 3D Surface (UAV Structure-From-Motion)

The photogrammetric 3D surface model was imported into an ArcGIS Pro Local Scene as an .OBJ. The dimensions of the .OBJ reflected the real-world dimensions of the excavation pit as this information was preserved during Metashape processing. The imported feature can be edited using the "Modify Feature" tool to manually georeference the file within the 3D scene. Once imported to ArcGIS Pro, the .OBJ dimensions remain intact, but the feature loses its texture (3D color) as it is imported. ArcGIS Pro currently does not have an option to add the texture files to the imported file.

The Ortho Mapping Workspace feature in ArcGIS Pro was used to create a high-resolution, large-scale DEM and orthomosaic aerial photo of an excavation pit (Figure 2.8). The Raster Calculator tool was used to compile this large-scale DEM to a lower-resolution DEM of the entire site. The compiled DEMs are not matched up perfectly in a vertical sense, but the larger-scale high-resolution DEM's real-world horizontal location is accurate. This orthomosaic can then be added as a 2D layer in the scene. The orthomosaic will drape the DEM, adding texture to the topography.
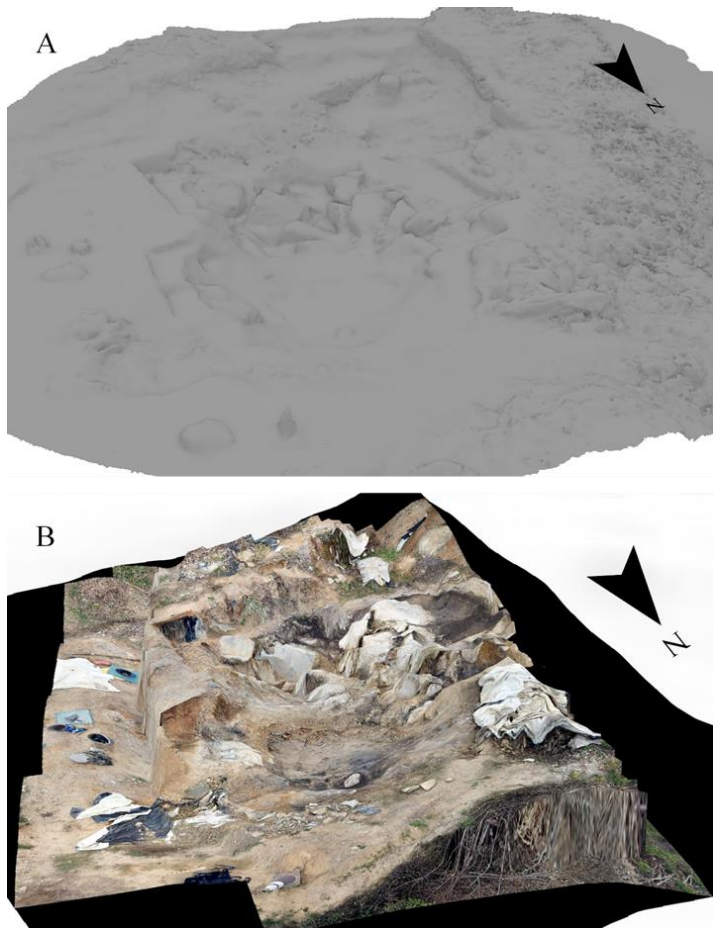
Figure 2.8 A comparison between the two surface maps of the Mastodon Pit at GFS created from UAV aerial orthophotos. (A) is a texture-less feature that was created in Agisoft Metashape and imported into ArcGIS Pro using the Import 3D Files tool. The shading feature in ArcGIS Pro allows one to see the complexity of the topography of the Mastodon Pit. Surface map (B) is a two-part map with a DEM used as an elevation surface within a 3D local scene. An orthomosaic photo is then added as a 2D layer overlaying the 3D DEM. The two interlinked layers were both created using the Ortho Mapping Workspace in ArcGIS Pro.

2.5.2.2 Integration of Point, Vector, and Volume Datasets with High-Resolution Surface Mapping

Once the surfaces have been mapped, shapefiles can be added to the scene (Figure 2.9). Shapefiles should be displayed using their "Absolute Height" in the elevation tab of the

shapefile's properties. The cartographic offset can be used to vertically refine shapefiles to a similar elevation as mapped surfaces.
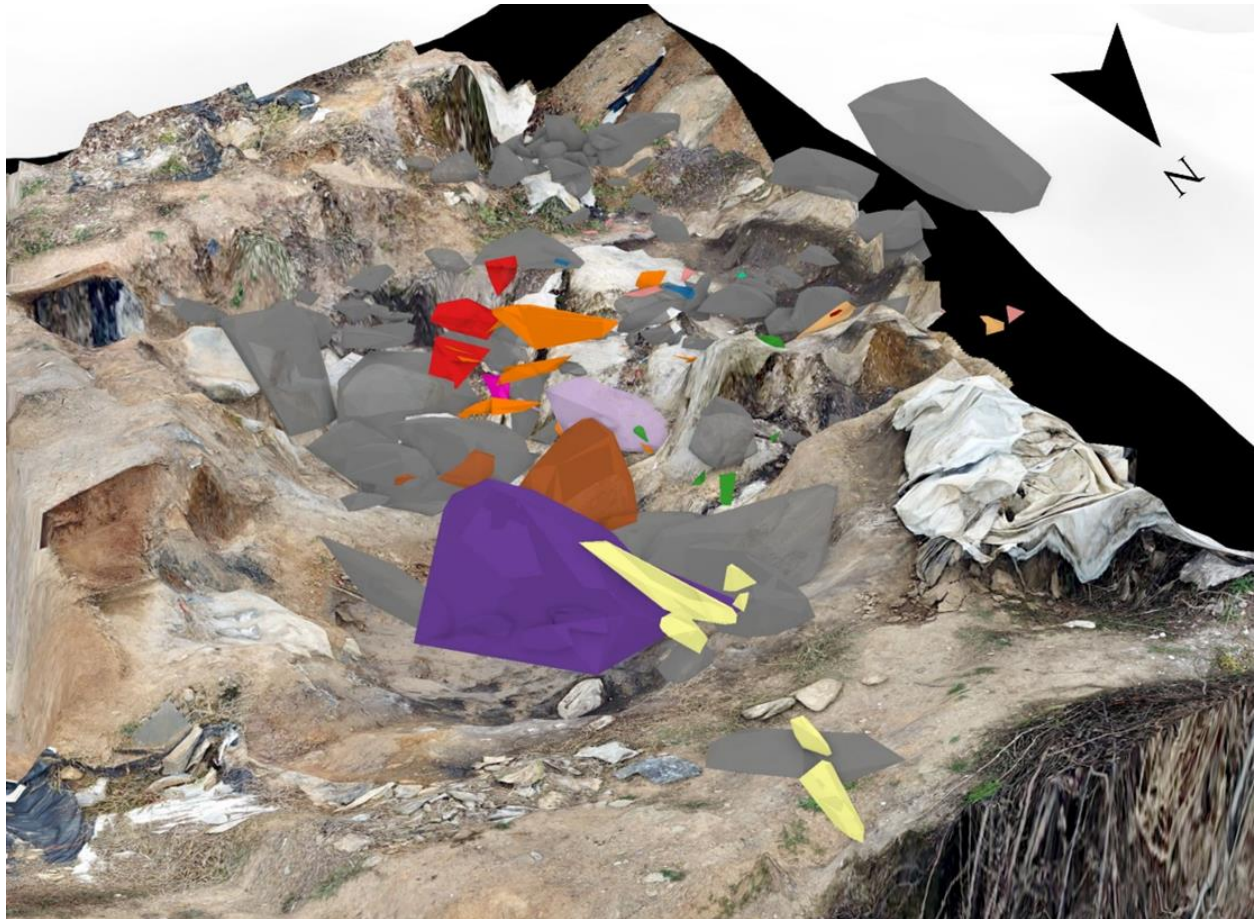
Figure 2.9 A 3D local scene featuring both the mapped surface of the Mastodon Pit along with the articulated mastodon and boulder objects. The elevation of the 3D shapefile objects can be edited to ensure they are sitting at the correct level on the 3D surface.

2.6 Discussion

2.6.1 The Utility of GIS and Spatial Analytics in the Analysis of Paleontological Sites

Workflows within this study provide an avenue for integration of paleontological spatial data into GIS analyses. Fossils at the GFS are mapped with a total station to preserve the *in situ* position of fossils. This information is organized in a database and attribute information from hand-written field notes is appended to the database. These data can be visualized in 3D scenes as raw point-based shapefiles and can also serve as a basis for more complex shapefile types such as vector-based and 3D polygon-based shapefiles. Each one of these shapefiles stores spatial and attribute information, which can be incorporated into spatial analyses. The 3D Analyst extension provides tools to analyze spatial patterns within 3D features, but the stored attributes can also be analyzed in other programs such as R statistics.

This research demonstrates how a suite of GIS and GIS-aligned tools can be used to create, visualize, query and store paleontological data. This approach is not new to paleontology, though the analytical potential of a 3D GIS remains largely unexplored. Hill et al. (2020) also developed methods for incorporating fossil material into a GIS at the La Brea Tar Pits of Las Angeles, CA. Their approach utilized 3D scans of fossils and imported them to a GIS. This method provided highly accurate renditions of the fossils, but there are some caveats including manual positioning of the imported files in GIS and somewhat limited analytical power. Additionally, 3D scans of prepared fossils may not reflect their *in situ* appearance because fossils are often preserved as fragments. The taphonomic pathway of fossils at the GFS is quite different from the pathway of Rancho La Brea specimens. These pathways lead to differences between fossil assemblages that may require different solutions.

Hill et al. (2020) also attempted to evaluate the positional accuracy of their 3D models. These positions were in reference to manual grid measurements tied to a local grid system. Mapping with a total station removes this procedure and provides higher accuracy than manual grid mapping systems. 3D models must be imported and manually positioned one at a time, while creating 3D point shapefiles using geoprocessing tools in ArcGIS Pro can be quickly performed on all mapped fossils.

2.6.2 Considering the GFS Mastodon Pit

Visualizing the *in situ,* tapho-fabric of a site has interested paleontologists since the founding of taphonomic science (Efremov 1940; Voorhies 1969). The Mastodon Pit is a complex deposit requiring further investigation to elucidate taphonomic pathways. Though we have not done that here (see chapter 4), we note that having the ability to view the spatial complexity of a deposit in 3D will assist in the interpretation of its taphonomic history. There is a clear relation between the boulders and mastodon preserved in the deposit, and volumetric mapping of these features may lead to an understanding of topological relationships that is not possible with point-based shapefiles.

Examining the 3D model of the mastodon and boulders in the deposit (Figure 2.7) begins to highlight irregularities noted in the mastodon remains. It is clear that these features are entangled within a 3D space. However, can we also use the model to come to a more complete understanding of the site's depositional history? The MBV models of the GFS mastodon illustrate that the animal was preserved in relative anatomical order. Most bone fragments are in anatomical order and are near other elements that articulate with them. Exceptions to this pattern include the head of a femur that is over a meter away from the nearest pelvis fragments. Additionally, the sacrum has been shifted to a position anterior to the pelvis, and rib and vertebra

fragments accumulated at an elevation below the mastodon's main fossil horizon. This is a preliminary look at the mastodon skeleton and, though it seems clear that it was deposited simultaneously with the boulders, there are irregularities within the skeleton that need to be addressed before the depositional history comes into clearer focus.

2.6.3 Excavations Mapped as Surfaces

Metashape and ArcGIS Pro both have workflows for spatially referenced UAV photos. UAV technology has drastically improved within the last five years, and both platforms are capable of using captured imagery to create high-resolution geospatial products that were previously unavailable, or unavailable at cost and scale. When working at small spatial scales such as excavation pits at paleontological sites, UAV-based digital elevation products still require manual editing. Both programs were able to make these excavation pit-sized surfaces capturing the vertical walls of the pits. The orthomosaic and DEM provided by the ArcGIS Pro workflow provided high resolution imagery, but the DEM's resolution captured less spatial complexities than Metashape's .OBJ file. A caveat with .OBJ files is that associated textures could not be imported into ArcGIS Pro. It should be noted that all surfaces created had to be manually edited in ArcGIS Pro to improve their vertical accuracy using raster math. With this in mind, Metashape's .OBJ file was preferred for visualization. Not only did the file seem to have better resolution, but it was converted to a shapefile, which was easier to edit using the "Modify Feature" tool. The raster-based DEM will be more useful for spatial analytics as raster files are commonly incorporated into spatial analytics.

2.6.4 Future Research

Workflows described in this study are valuable as digital spatial products become more accurate and precise, and are also more editable, interactive, and analytically useful (Albert et al.

2018). Maps detailing the anatomical morphology of mapped bones may be visually appealing, but simple maps featuring lines and basic shapes work well to display taphonomic information (Brown et al. 2020) and are scale-able from meters to hectares.

Overall, these procedures take little time once data are organized into spreadsheets. This process could be more efficient through the incorporation of digital field notes. Digital field notes could be formatted in a program such as Survey123 (3.12, ArcGIS), simplifying and streamlining fieldwork. Hand-drawn sketches were incredibly useful when deciphering the remains of complex associated individuals. Digital field notes could even incorporate a picture of the hand-drawn field notes or an annotated photo of the excavation to capture advantages of both field note methods. Digital notes could then be exported into a geodatabase for statistical analyses and incorporated into ArcGIS Pro.

High resolution spatial data can aid in better understanding the relationships in fossil materials preserved in complex deposits (Albert et al. 2018; Guisti et al. 2018; Mackie et al. 2020). These new studies have incorporated highly accurate, point-based data to calculate metrics such as length, surface area, and volume. This study provides a proof of concept, allowing paleontologists the ability to ask questions they were not able to ask before as 3D geostatistics can be applied to models of *in situ* carcasses. Vector- and volume-based shapefiles add topological data to points, unlocking many new avenues of research. As 3D spatial analyst tools continue to mature, new analyses will be possible.

2.7 Conclusion

Digital object mapping of paleontological sites is made possible by survey grade field technology such as GPS, total stations, and UAVs. These mapped objects can be analyzed and visualized as 3D point-based, 3D vector-based, and 3D polygon-based shapefiles. The utility of created shapefiles is directly related to the quality of the mapped and documented field data. The intent of the analysis and preservation qualities of the assemblage will warrant the implementation of these different shapefile types. A small assemblage of unarticulated bones may incorporate a point-based or vector-based analysis whereas a more complex assemblage with associated skeletons may warrant a polygon-based analysis.

Digital surface mapping has improved in ease and accuracy with the maturation of UAV technology. Mapping paleontological sites requires large-scale mapping techniques that were not possible without a UAV. They can take high resolution photographs and apply spatial tags so that the photos can be processed by 3D-capable software such as Agisoft Metashape or ArcGIS Pro. High resolution DEMs may be available for certain sites, but these data do not reflect short time scales of excavation and landscape alteration.

Every paleontological site is spatially complex. These complexities are what researchers strive to understand as *in situ* arrangements are mapped. Complexities of a site may frame how the spatial field data are collected. The mapping approaches described here are flexible, time-efficient, and analytically powerful which will benefit complex mapping projects. Shapefiles are also editable, allowing new data to be appended as it is collected at the site. Excavation surfaces can be mapped every year to observe annual site changes. Altogether, this suite of map products moves towards the theoretical goal of creating a digital twin of a fossil site that can evolve as new information is acquired. These qualities make this approach excellent for spatial taphonomic

analyses of the site, and can also be implemented in future resource management and research

objectives.

References

Agisoft Metashape. https://www.agisoft.com/pdf/PS_1.3%20-Tutorial%20(BL)%20-%20Orthophoto,%20DEM%20(GCPs).pdf

Akersten W, Shaw C A, and Jefferson G T. 1983. Rancho La Brea: Status and future. Paleobiology. 9: 211–217.

Alberdi M T, Alonso M A, Azanza B., Hoyos✠ M, and Morales J. 2001. Vertebrate taphonomy in circum-lake environments: Three cases in the Guadix-Baza Basin (Granada, Spain). Palaeogeography, Palaeoclimatology, Palaeoecology, 165(1-2): 1-26. doi:10.1016/s0031-0182(00)00151-6.

Albert G, Botfalvai G, and Ősi A. 2018. Mapping the past: GIS and intrasite spatial analyses of fossil deposits in paleontological sites and their applications in taxonomy, taphonomy and paleoecology. Palaeontologia Electronica, 21(3). doi:10.26879/8120031-0182(00)00151-6

Ali S H, Omar N Q, and Abujayyab S K. 2016. Investigation of the accuracy of surveying and buildings with the pulse (non-prism) total station. International Journal of Advanced Research, 4(3): 2320-5407.

Apollonio F I, Gaiani M, and Benedetto Benedetti B. 2012. 3D Reality-Based Artefact Models for the Management of Archaeological Sites Using 3D GIS: A Framework Starting from the Case Study of the Pompeii Archaeological Area. Journal of Archaeological Science 39(5): 1271-1287. https://doi.org/10.1016/j.jas.2011.12.034

Batty M. 2018. Inventing future cities. doi:10.7551/mitpress/11923.001.0001

Behrensmeyer A K. 1975. The taphonomy and paleoecology of Plio-Pleistocene vertebrate assemblages east of Lake Rudolph, Kenya. Bulletin of the Museum of Comparative Zoology. 146:473–578.

Behrensmeyer A. 1988. Fossils in the making. Chicago: Chicago Univ. Press.

Bourque J R and Schubert B W. 2015. Fossil Musk Turtles (Kinosternidae, Sternotherus) from the Late Miocene-Early Pliocene (Hemphillian) of Tennessee and Florida. Journal of Vertebrate Paleontology 35(1):1–19.

Bramble K, Burns M E, and Currie P J. 2014. Enhancing bonebed mapping with GIS technology using the Danek Bonebed (Upper Cretaceous Horseshoe Canyon Formation, Edmonton, Alberta, Canada) as a case study. Canadian Journal of Earth Sciences. 51(11): 987-991. doi:10.1139/cjes-2014-0056

Brown C M, Herridge-Berry S, Chiba K, Vitkus A, and Eberth D A. 2020. High-resolution (centimetre-scale) GPS/GIS-based 3D mapping and spatial analysis of in situ fossils in two horned-dinosaur bonebeds in the Dinosaur Park Formation (Upper Cretaceous) at Dinosaur Provincial Park, Alberta, Canada. Canadian Journal of Earth Sciences. 1-22. doi:10.1139/cjes-2019-0183

Burdick K, Wallace SC, Nave J. 2002. State of the art GIS applications at the Miocene age fossil site in Gray, Tennessee. Journal of Vertebrate Paleontology 22(3, supplement):117A.

Eberth D A and Getty M A. 2005. Ceratopsian bonebeds: occurrence, origins, and significance. In Currie P J and Koppelhus E B (eds.). Dinosaur Provincial Park: a spectacular ancient ecosystem revealed. Indiana University Press, Bloomington, Indiana. p. 501–536.

Eberth D A, Rogers R R, and Fiorillo A R. 2007. A Practical Approach to the Study of Bonebeds. In Bonebeds: Genesis, analysis, and paleobiological significance. Chicago: University of Chicago Press.

Efremov I A. 1940. Taphonomy: a new branch o f paleontology. Pan-American Geologist 74: 81-93.

Esri 3D GIS. ArcGIS Capabilities. Available: https://www.esri.com/en-us/arcgis/3d-gis/overview.

Esri Orthomosaic workflow. https://doc.arcgis.com/en/imagery/workflows/tutorials/create-drone-imagery-products-ortho-mapping.htm

Estrada Belli F. 1999. The archaeology of complex societies in Southeastern Pacific coastal GUATEMALA: A Regional GIS Approach. doi:10.30861/9781841711195

Friscia A, Van Valkenburgh B, Spencer L, and Harris J. 2008. Chronology and Spatial Distribution of Large Mammal Bones in Pit 91, Rancho Le Brea. Palaios. 23(1): 35-42.

Giusti D, Tourloukis V, Konidaris E, Thompson N, Karkanas P, Panagopoulou E, and Harvati K. 2018. Beyond hill Maps: Patterns of Formation Processes at the Middle Pleistocene Open-Air Site of Marathousa 1, Megalopolis Basin, Greece. Quaternary International. 497:137–53.

Grieves M. 2014. Digital Twin: Manufacturing Excellence through Virtual Factory Replication. Digit Twin White Pap. Accessed November 17, 2019.

Grieves, M. 2019. "Digital Twin."Arup 18:80.

Hill K, Swift J N, Howard C, Farrell A, and Lindsey E L. 2020. 3D Visualization of Subsurface Objects from La Brea Tar Pits, Los Angeles, CA. Digital Applications in Archaeology and Cultural Heritage. doi:10.1016/j.daach.2020.e00167

Jasinski S E. 2018. A New Slider Turtle (Testudines: Emydidae: Deirochelyinae: Trachemys) from the Late Hemphillian (Late Miocene/Early Pliocene) of Eastern Tennessee and the Evolution of the Deirochelyines. PeerJ, 6. doi:10.7717/peerj.4338

Ketchum W. 2011. Using Geographical Information Systems to Investigate Spatial Patterns in Fossils of *Tapirus polkenis* from the Gray Fossil Site, Washington County, Tennessee. (Master's Thesis). East Tennessee State University. Johnson City, TN.

Kvamme K L. 1995. A view from across the water: the North American experience in archaeological GIS. In Archaeology and Geographical Information Systems: A European Perspective. Pennsylvania: Taylor & Francis. p. 1–14.

Liu Y and Jacques F M. 2010. *Sinomenium macrocarpum* sp. nov. (Menispermaceae) from the Miocene–Pliocene transition of gray, northeast Tennessee, USA. Review of Palaeobotany and Palynology. 159(1-2): 112-122. doi:10.1016/j.revpalbo.2009.11.005

Lyman R L. 1994. Vertebrate taphonomy. Cambridge manuals in archaeology. Cambridge University Press, Cambridge.

Mackie M E, Surovell T A, O'Brien M, Kelly R L, Pelton S, Haynes C V, Mahan S. 2020. Confirming a cultural Association at the la Prele Mammoth Site (48CO1401), converse County, Wyoming. American Antiquity. 85(3): 554-572. doi:10.1017/aaq.2020.8

Mead J I, Schubert B W, Wallace S C, Swift S L. 2012. Helodermatid lizard from the Mio-Pliocene oak-hickory forest of Tennessee, eastern USA, and a review of monstersaurian osteoderms. Acta Palaeontologica Polonica. 57:111–121 doi:10.4202/app.2010.0083

Nave J W, Ali T A, and Wallace S C. 2005. Developing a GIS Database for the Gray Fossil Site, Tennessee, Based on Modern Surveying. Surveying & Land Information Science. 65(4): 259–264.

Nigro J D, Ungar P S, Ruiter D J, and Berger L R. 2003. Developing a Geographic Information System (GIS) for Mapping and Analysing Fossil Deposits at Swartkrans, Gauteng Province, South Africa. Journal of Archaeological Science. 30(3): 317-324. doi:10.1006/jasc.2002.0839

Ochoa D, Zavada M, Liu Y, and Farlow J. 2016. Floristic implications of two contemporaneous inland upper Neogene sites in the eastern US: Pipe Creek Sinkhole, Indiana, and the Gray Fossil Site, Tennessee (USA). Palaeobiodiversity and Palaeoenvironments. 96: 239-254.

Parmalee P W, Klippel WE, Meylan P A, and Holman J A. 2002. A late Miocene–early Pliocene population of Trachemys (Testudines: Emydidae) from east Tennessee. Annals of Carnegie Museum. 71: 233–239.

Rogers R R. 1994. Vertebrate paleontological techniques. In Leiggi P. and May P. (eds.).

> Vertebrate paleontological techniques. Cambridge England: Cambridge University Press.
>
> p. 47-58.

Ryan M J, Russell A P, Eberth D A, and Currie P J. 2001. The taphonomy of a *Centrosaurus*

> (Ornithischia: Ceratopsidae) bone bed from the Dinosaur Park Formation (Upper
>
> Campanian), Alberta, Canada, with comments on cranial ontogeny. Palaios. 16: 482–506.

Safrel I, Julianto E N, and Usman N Q. 2018. Accuracy Comparison between GPS Real Time

> Kinematic (RTK) Method and Total Station to Determine the Coordinate of an Area.
>
> Unnes Journals. 20(2): 123-130. doi:10.15294/jtsp.v20i2.16284

Samuels J, Bredehoeft K, and Wallace S. 2018. A new species of Gulo from the Early Pliocene

> Gray Fossil Site (Eastern United States); rethinking the evolution of wolverines. PeerJ. 6.
>
> doi:10.7717/peerj.4648

Schrotter G and Hürzeler C. 2020. The digital twin of the city of Zurich for urban planning. PFG

> – Journal of Photogrammetry, Remote Sensing and Geoinformation Science. 88(1): 99-
>
> 112. doi:10.1007/s41064-020-00092-2

Shipman P G. 1981. Life history of a fossil: An introduction to taphonomy and paleoecology.

> Harvard University Press, Cambridge.

Shunk A J, Driese S G, and Clark G M. 2006. Latest Miocene to earliest Pliocene sedimentation

> and climate record derived from paleosinkhole fill deposits, Gray Fossil Site,

northeastern Tennessee, U.S.A. Palaeogeography, Palaeoclimatology, Palaeoecology. 231(3): 265–278.

Shunk A, Driese S, and Dunbar J. 2009. Late Tertiary paleoclimatic interpretation from lacustrine rhythmites in the Gray Fossil Site, northeastern Tennessee, USA. Journal of Paleolimnol. 42(1): 11–24. https://doi.org/10.1007/s10933-008-9244-0

Varricchio D J. 1995. Taphonomy of Jack's Birthday Site, a diverse dinosaur bonebed from the Upper Cretaceous Two Medicine Formation of Montana. Palaeogeography, Palaeoclimatology, Palaeoecology. 114:297–323.

Voorhies M R. 1969. Taphonomy and population dynamics of an early Pliocene fauna, Knox County, Nebraska. University of Wyoming Contributions to Geology, Special Papers. 1: 1-69.

Wallace S C, Nave J W and Burdick K M. 2002. Preliminary report on the recently discovered Gray Fossil Site (Miocene), Washington Co., Tennessee: with comments on observed paleopathologies–The advantages of a large sample. Journal of Vertebrate Paleontology. 22: 117.

Wallace S and Wang X. 2004. Two new carnivores from an unusual late Tertiary forest biota in eastern North America. Nature. 431(7008): 556-559.

Whitelaw J L, Mickus K, Whitelaw M J, and Nave J. 2008. High-resolution gravity study of the Gray Fossil Site. Geophysics. 73(2). doi:10.1190/1.2829987

CHAPTER 3. SPATIAL TAPHONOMY OF LARGE VERTEBRATES FROM THE GRAY FOSSIL SITE

DAVID CARNEY

East Tennessee State University, Department of Geosciences, Johnson City, Tennessee, 37604, USA

email: davecarney03@gmail.com

RRH: SPATIAL TAPHONOMY OF THE GRAY FOSSIL SITE

LRH: D. Carney and C. Widga

ABSTRACT

This project uses exploratory 3D geospatial analyses to assess the taphonomy of the Gray Fossil Site (GFS). During the Pliocene, the GFS was a forested, inundated sinkhole that accumulated biological materials between 4.9-4.5 mya. This deposit contains fossils exhibiting different preservation modes: from low energy lacustrine settings to high energy colluvial deposits. All macro-paleontological materials have been mapped *in situ* using survey-grade instrumentation. Vertebrate skeletal material from the site is well-preserved, but the degree of skeletal articulation varies spatially within the deposit. This analysis uses geographic information systems (GIS) to analyze the distribution of mapped specimens at different spatial scales. Factors underpinning spatial association, skeletal completeness, and positioning of specimens were examined. At the scale of the individual skeleton, analyses of the Mastodon Pit explore how element completeness and orientation/inclination of the mastodon reflect post-depositional processes.

3.1 INTRODUCTION

Taphonomic interpretations are heavily influenced by the spatial distribution and topological relationships of fossils preserved within a site (Voorhies 1969; Hill and Behrensmeyer 1984). Macro-scale taphonomic and geologic data provide insight into the amount of time represented within a fossil assemblage and associated post-depositional processes (Behrensmeyer 1991). Large paleontological sites may encompass many different depositional settings, potentially benefiting from analyses at multiple spatial scales (Alberdi et al. 2001; Albert et al. 2018; Guisti et al. 2018). Exploring differences between sedimentary environments within a site (i.e., meso-scale) may provide additional nuance and ultimately increases the strength of taphonomic interpretations.

The field of taphonomy incorporates knowledge and observations from many different disciplines that focus on the postmortem, pre-, and post-burial histories of organic remains (Lyman, 1994). A common denominator among these approaches is the importance of spatial organization (Voorhies 1969; Behrensmeyer 1975; Hill 1979; Eberth et al. 2000). Spatial statistics can reinforce and quantify visual observations. Comprehensive spatial analytic approaches have been broadly incorporated into archaeological site analyses (Giusti and Arzarello 2016; Organista et al. 2017; Mackie et al. 2020), yet these approaches are rarely applied to paleontological sites (Albert et al., 2018).

Creation of maps that show the distribution of paleontological remains is standard practice for paleontological excavations (Abler 1984; Eberth 2007), yet the purpose of these maps is often limited to site documentation and qualitative visual observations. Newer techniques that incorporate high-precision mapping hardware such as GPS and total station systems have the potential to document spatial phenomena with improved accuracy. Although

56

these techniques are becoming more common in paleontology (Lien et al. 2002; Eberth and Getty 2005; Nave et al. 2005; Albert et al. 2018; Brown et al. 2020; Hill et al. 2020), there remain few applications where the full potential of geospatial statistics has been realized. Incorporating metrics such as elevation, volume, and matrix characteristics into site mapping strategies shows promise for hypothesis-driven spatial analytics (Alberdi et al 2001; Friscia et al. 2008; Bramble et al. 2014; Bertog et al. 2014; Albert et al. 2018; Giusti et al. 2018; Mackie et al. 2020). To this end, this study leverages a high-resolution geospatial dataset acquired with a total station over many years and modern geostatistical tools to better understand the spatial underpinnings of site depositional processes at a Pliocene lagerstatte in northeastern Tennessee.

The Gray Fossil Site (GFS) is a 2.6 ha paleontological site located in Gray, Tennessee (Figure 3.1). Fossiliferous deposits reach depths of about 40 m below ground surface (Shunk 2006; Whitelaw et al. 2008). The site formed over the course of 4.5-11.0 Ka (Shunk 2009) and offers a rare glimpse into forested ecosystems of the southeastern United States during the Early Pliocene. Macro and microfossils are well-preserved at the GFS (Wallace and Wang 2004; Liu and Jacques 2010; Bourque and Schubert 2015; Jasinski 2018; Samuels et al. 2018). The sedimentary matrix is composed of organic rich clays (i.e., rhythmites) that infilled the sinkhole and preserved floral and faunal remains (Shunk 2006) (Figure 3.2). Generally, more complete skeletons are mixed with isolated fragments. All material is fragmented to some degree as a result of sediment crushing by overburden (following Lyman 1994). The remains of flora and fauna were preserved in an anoxic environment (Keenan and Engel 2017; Keenan et al. 2018), at least in some areas of the sinkhole. Dwarf Tapirs (*Tapirus polkensis*) are especially common and are present in all excavation pits thus far (Gibson, 2011).
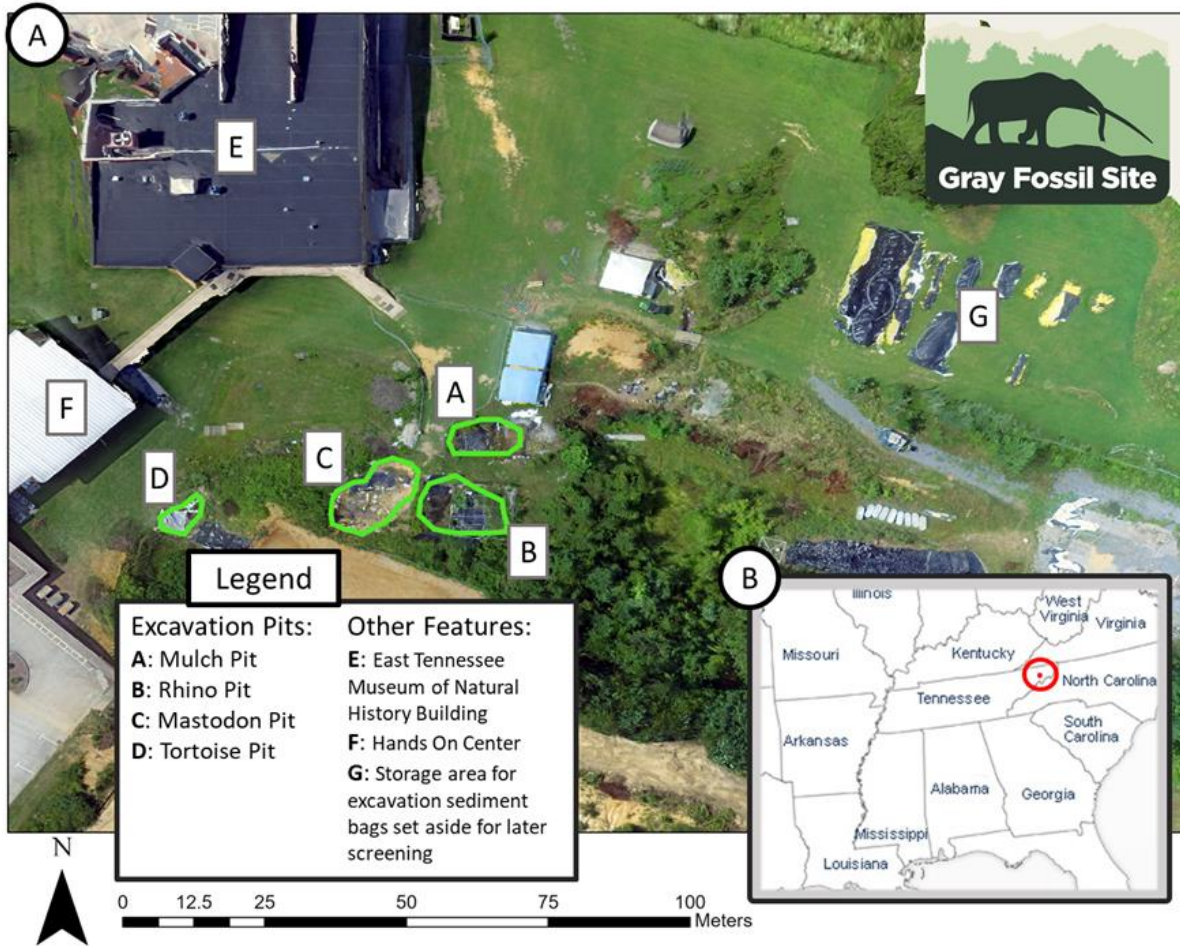
Figure 3.1. (A) The "backyard" of GFS showing excavation pits that are included in this study (green). (B) Location of site within the state of Tennessee. GFS is in Northeastern Tennessee in the Valley and Ridge physiographic province.

A spatial concentration of tusk fragments was noted in early investigations at the site. In 2015, the origin of these fragments was linked to a proboscidean tusk buried near the surface, which led to the opening of a new excavation pit. The tusk material belonged to a mostly complete, semi-articulated mastodon skeleton (ETMNH 305), the largest animal discovered at the GFS thus far (Figure 3.2). Keenan et al. (2018) proposed that this individual was killed and buried in a single catastrophic event. Fresh breaks observed in the animal's bones were used to support this claim, however their study did not investigate the *in situ* observations that provide further support to the catastrophic event hypothesis. This excavation, called the Mastodon Pit, exhibits a depositional environment unlike the clay rhythmites found in other areas of the site (Shunk, 2006). The sedimentary matrix encasing ETMNH 305 is poorly sorted and oxidized. The deposit is dominated by intermixed clay and sand along with many large, limestone boulders (Figure 3.2). Poorly sorted sediments, like the ones observed in the Mastodon Pit, are often attributed to mass wasting events (Schuster and Highland, 2007). Furthermore, mass wasting deposits that contain high clay content increase the coherence of the flow (Marr et al., 2001), which may impact the organization of the skeletons in the deposit.
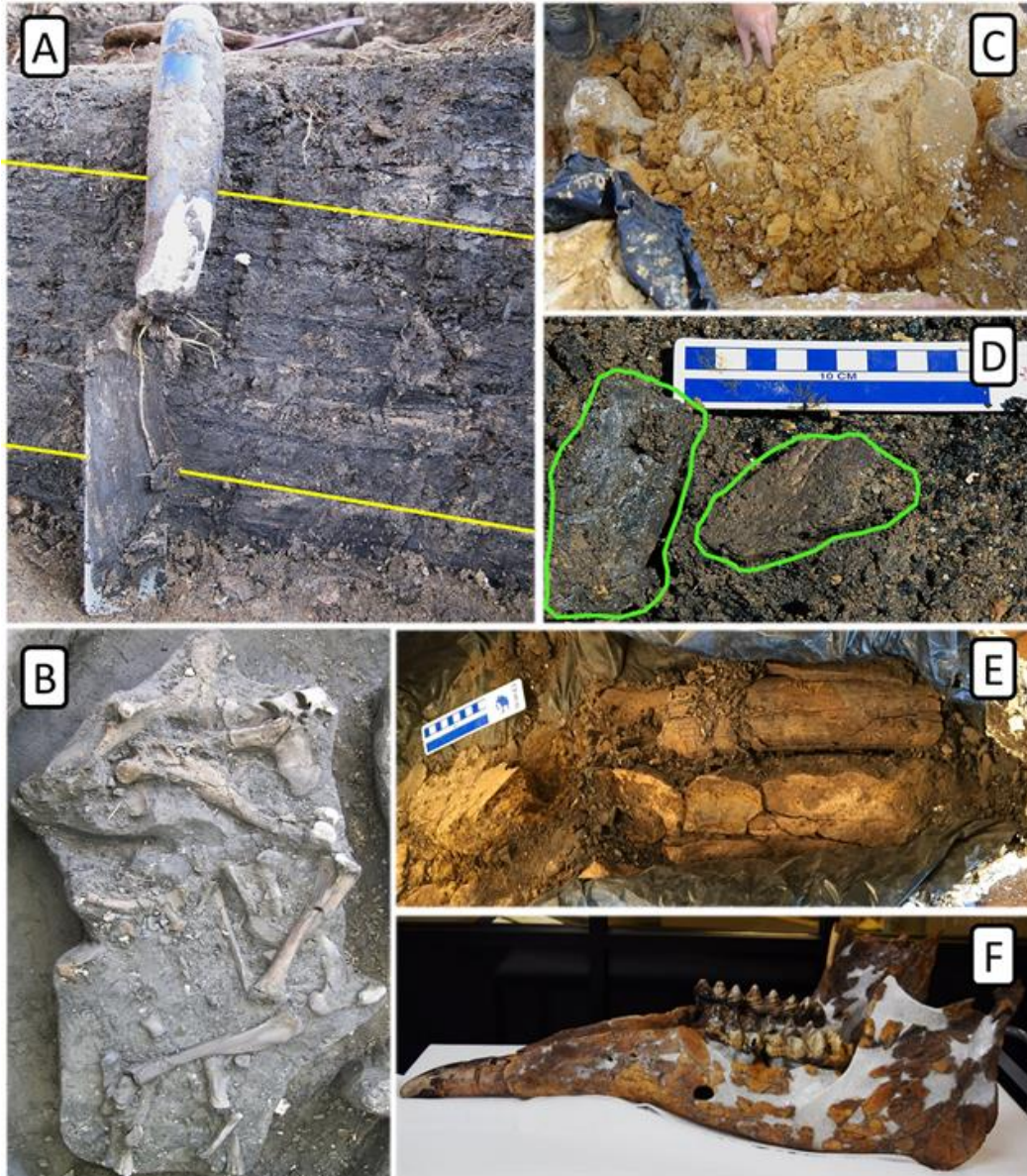
Figure 3.2. (A) Stratigraphy of the infill rhythmites. Yellow lines indicate orientation of the beds, trowel for scale. (B) An articulated tapir individual preserved in the black clay. (C) Sediments associated with the Mastodon Pit. Sediments are poorly sorted and contain boulders of varying size. (D) Closeup of poorly sorted sediments. Note mastodon material circled in green and the variability of the sediment's grain sizes and color. (E) Jacketed elements from the Mastodon

(ETMNH 305). Elements are crushed, in situ. (F) The prepared mandible of ETMNH 305. The Left side of the mandible is less complete and slightly lighter in color.

Analytical Framework

This study examines spatial phenomena at two scales. Meso-scale phenomena are examined through comparisons between different excavation pits at the GFS (Figure 3.3) to better understand spatial differences in depositional histories across the entire site. Micro-scale phenomena such as the spatial relationships between specimens and mapped boulders in the Mastodon Pit will also be explored.
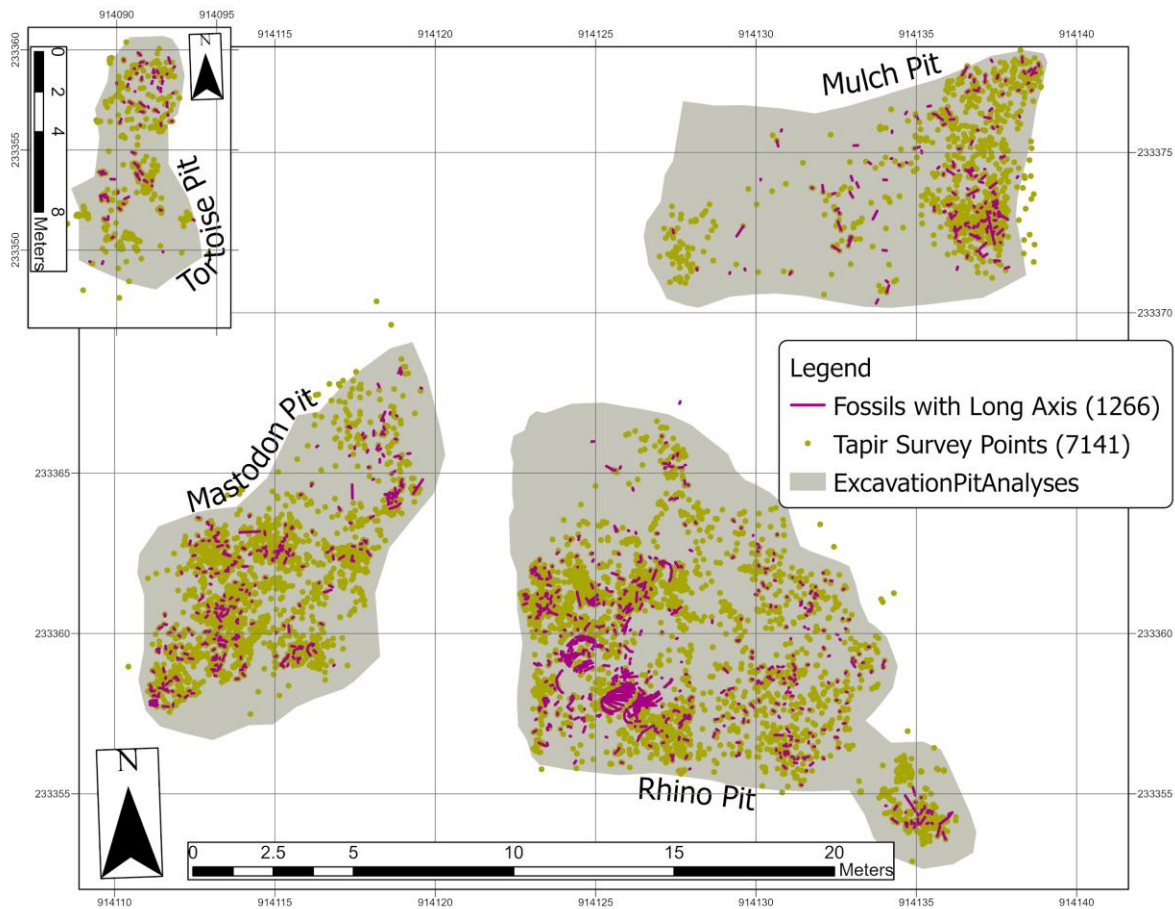
Figure 3.3 Schematic of the GIS layers used for our taphonomic fabric analysis. Layers contain spatially discrete areas of fossil material located with the excavation pits. Three pits are adjacent to one another while the Tortoise Pit is located 23 meters to the west of the Mastodon Pit's western side.

Spatial analyses are focused on the following:

1. Intra and Inter-pit analyses of long-axis orientation and inclination.

2. Analyses of relationships between preserved tapir elements and fluvial transport potential (i.e., Voorhies Groups) within each pit.

3. Analyses of meso-scale spatial trends in skeletal completeness.

4. Tests of vertical association between mastodon remains and large boulders

Although there are visual differences between excavation pits in terms of depositional environments, spatial analyses will assist in quantifying these differences. These analyses are important to understanding larger-scale site formation processes at work within the sinkhole. The GFS sinkhole was a lacustrine environment, and therefore, the depositional environments present are hypothesized to be lacustrine in nature. These environments include lake bottom (low energy deposition) and lake margins where a mixture of high and low energy depositional processes are expected (Guisti et al., 2018).

Spatial analyses will also help to analyze the complex depositional environment present in the Mastodon Pit and provide better resolution of depositional processes at work in this area of

the site. The organization of the fossil material along with preliminary, anecdotal observations of sediment characteristics within the Mastodon Pit will be used to test the mass wasting hypothesis as positioning of fossil material may reflect reworking, an observed result of mass wasting (Rogers, 2005).

3.2 MATERIALS & METHODS

The GFS has been systematically excavated since 2001 by paleontologists from East Tennessee State University. Spatially discrete foci of paleontological research at the GFS are referred to as excavation 'pits', and are informally identified on the basis of major finds (e.g., Mastodon Pit). All identifiable vertebrate macrofossils are mapped using a total station. This method records the Northing, Easting, and Elevation of a point (survey shot) on the object within the Tennessee State Plane Coordinate System. These points reflect anatomical landmarks on a bone fragment (whenever possible) and are associated with an object's field number. Currently, the GFS spatial database contains over 30,000 points, each with a unique field number. This database is cross-referenced with field notes which document what each field number represents.

Field numbers are organized in a way to indicate the number of skeletal elements associated with recovered individuals. This was the basis for a dataset that measures Skeletal Completeness (SC), where skeletal elements are summed for each spatially discrete group of associated specimens. Isolated fragments were treated individually and assigned a SC of 1. The same SC value was applied to each survey point of any given individual.

Fragments with a distinct long axis receive a minimum of two survey points, one at each end of the specimen. Once integrated into the GIS, these points are converted to 3d vectors using the Point to Line (PTL) tool in ArcGIS Pro. Vectors represent the length, inclination and orientation of an element in 3D space. This was the basis for our Fragment with Long Axis (FLA) Dataset. The SC number field was joined to the fragments in the FLA dataset to distinguish material coming from unassociated (SC<5) and associated (SC>5) specimens. The SC dataset was restricted solely to tapir remains to control for species-specific biological and

body size variability. This allows exploration of the relationships between SC and depositional environments within the GFS sinkhole.

A third dataset was created for mastodon skeletal remains and large limestone clasts (i.e., boulders) of the Mastodon Pit. Mastodon bones and boulders were mapped in detail (2164 mastodon points, 2548 boulder points). Mastodon points were grouped at the fragment level, with each fragment associated with individual skeletal elements. The mastodon and boulder datasets were converted to 3D shapes in GIS using the Minimum Bounding Volume (MBV) tool (Figure 3.4). The 3D polygon-based shapefile was used to explore the relationship between Northing and Elevation within the Mastodon Pit, and to note parts of the articulated mastodon skeleton where skeletal elements have been unarticulated and displaced.
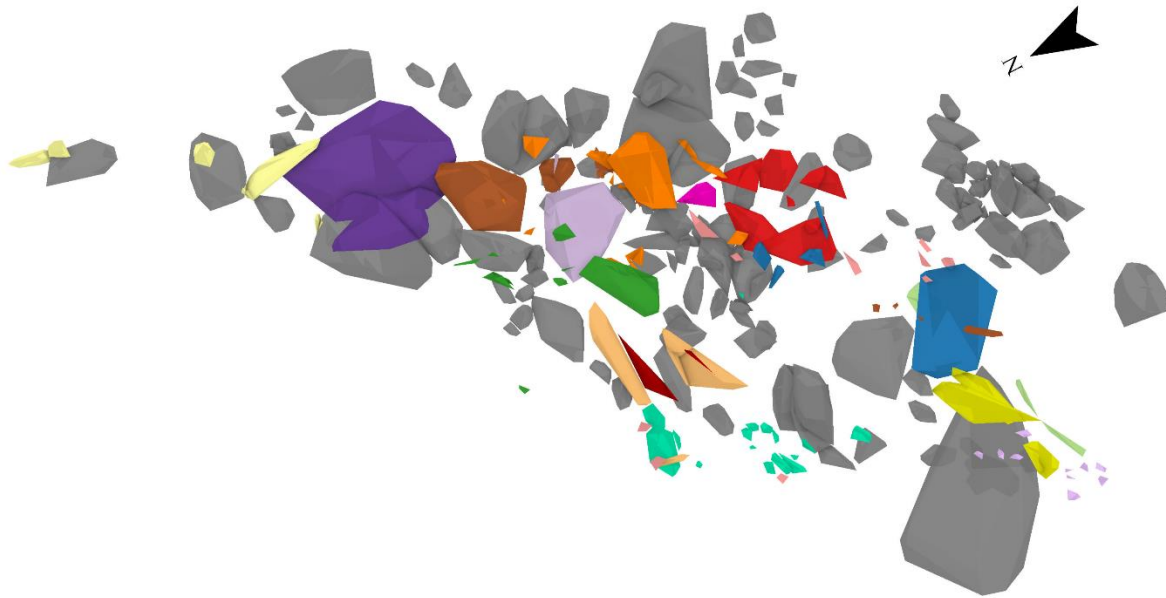
Figure 3.4 An image of the 3D Minimum Bounded by Volume (MBV) shapefile of the mastodon and associated boulders created in GIS. This view is vertical. Green circle highlights spatial abnormalities discussed in the qualitative spatial analysis of the mastodon's skeleton. An interactive model can be accessed in an ArcGIS Online 3D interface at https://arcg.is/1T5mqL0.

3.2.1 Meso-Scale Spatial Analyses Between Excavation Pits

3.2.1.1 Skeletal Completeness. — The SC index reflects the degree of disarticulation within an individual skeleton. Skeletons represented by disarticulated fragments may indicate an individual has been transported after death (Shotwell 1955), but the degree of disarticulation may also reflect the amount of time between death and burial (Dodson 1971; Behrensmeyer 1991; Currie 2000) or the diversity and energy of taphonomic processes (Fiorillo 1991; Varricchio 1995). Rogers (2005) also reports varying degrees of skeletal completeness in debris flows, a

type of mass wasting event. At the GFS, a complex mixture of skeletal remains displaying varying degrees of association/articulation and completeness are present in all excavation pits.

The relationship between elevation and relatively isolated (SC < 5) and skeletally associated (SC > 5) tapir remains was explored. Significant differences in the elevations of isolated and associated specimens were tested with a linear regression. A within group ANOVA was also used to examine the significance of the vertical spread of associated tapir (SC > 5) remains within each excavation pit.

3.2.1.2 Fabric Analysis. — Bone fragments with a long axis are spatially organized within a sedimentary matrix through fluvial processes (Toots 1965; Voorhies 1969; Behrensmeyer 1975; Shipman 1981; Eberth et al. 2007; Guisti et al. 2018). This organization is classified as either anisotropy or isotropy. Anisotropy is directionally dependent (linear or planar) while isotropy exhibits spatial structure that is independent of long axis direction (Figure 3.5). A preferred long axis direction (anisotropy) in mapped bones indicates a fluvial deposit (linear fabric). Fluvial energy will also sort material depending on the size, shape, and density of the material (Voorhies 1969; Dodson 1973).
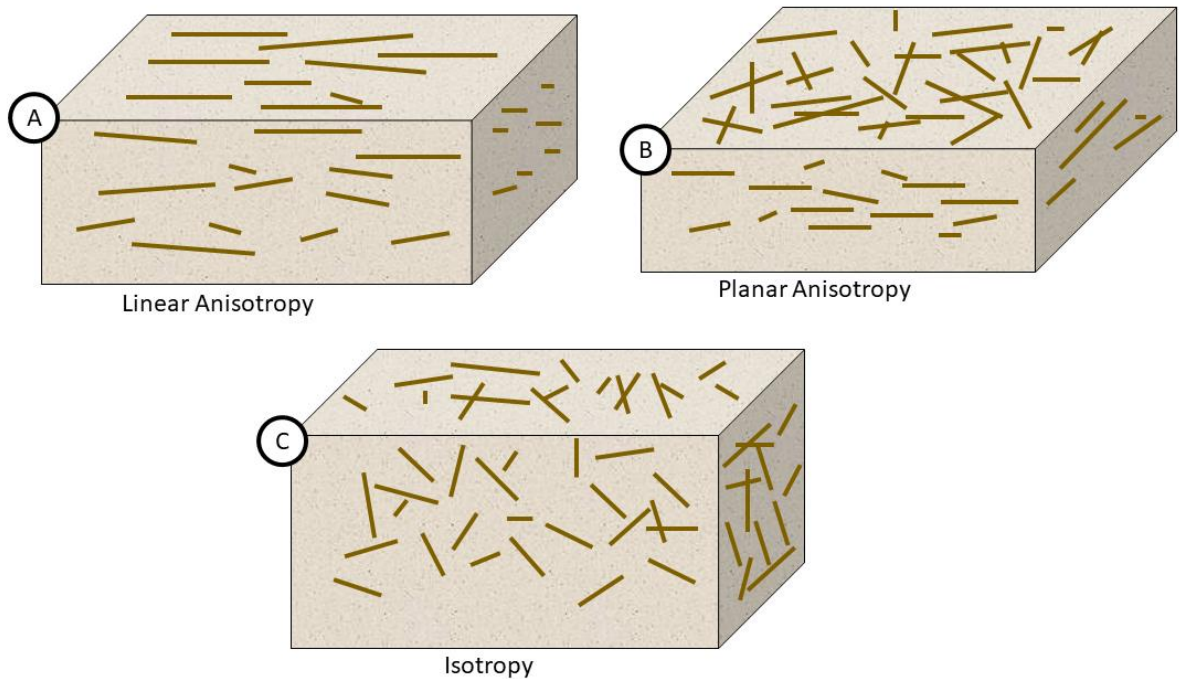
Figure 3.5. (A) Fossils with a distinct long axis representing a linear anisotropic fabric where fragments display orientation preference and similar inclinations. (B) Fossils with a distinct long axis representing a planar anisotropic fabric where fragments do not display orientation preference with similar inclinations. (C) Fossils with a distinct long axis representing isotropy where fragments do not display orientation preference nor similar inclinations.

There is also the potential for anisotropic signatures in low energy lacustrine environments. Depositional fabrics in lacustrine environments can vary widely depending on location within a lake (Guisti et al. 2018). Low energy, lake bottom deposits will often develop a planar fabric where bones with a long axis will not display a preferred orientation (Behrensmeyer 1975). However, the range of inclinations of these bones will be limited (Hunt 1990; Bertog et al. 2014) (Figure 3.5). Minimal sorting (Bertog et al. 2014) and a mixture of articulated and unarticulated skeletons (Agenbroad 1984) is also common in these settings. Material in marginal lacustrine environments may exhibit preferred orientation from changes in water level (Alberdi

et al. 2001; Cobo-Sanchez et al. 2014). Marginal lacustrine environments will likely display a mixture of high- and low-energy characteristics (Guisti et al. 2018).

Mass wasting depositional environments are often isotropic (Figure 3.5). Mass wasting materials are unsorted, randomly oriented, and randomly inclined (Pierson 2005). Mass wasting deposits have the potential to rework fluvial deposits (Lancaster et al. 2010), and have been identified at lake margins with steep banks (Miller et al. 2014).

Anisotropic and isotropic fabrics are identified through trends in orientation and inclination of specimens with a long axis. Orientation is related to azimuthal direction of fossil material. These trends are 2D and can be used to test for linear anisotropy in mapped features. Inclination trends in 3D space can then begin to support planar anisotropy where features with similar inclinations reflect the depositional surface. Finally, an isotropic deposit does not have preferred orientation and inclination. This setting may indicate a high energy depositional environment.

Orientation. The FLA dataset was divided into subsamples for each excavation pit including; all specimens (FLA-Total), associated material (SC>5) (FLA-Associated), and unassociated material (SC<5) (FLA-Unassociated). With such high frequencies of tapir material, the same FLA subsamples were also created for tapirs only (FLA-TapirTotal, FLA-TapirAssociated, FLA-TapirUnassociated). Stereonets (created in StereoNet V.11.3.0 - Allmendinger, 2020; https://www.rickallmendinger.net/stereonet) and roseplots (Created in GeoRose version 0.5.1 –Young Technology Inc., 2014; http://www.yongtechnology.com/georose/) displaying bin frequency were created for each of the subsamples.

69

All plots were multimodal, so rather than use the Raleigh's Test (for unimodal patterns), we use statistical tests for multimodal significance (Hewitt et al. 2018; Lanler et al. 2019). Two Hermans-Rasson tests were used to test statistical significance for preferred direction in the rose plots according to the methods of (Landler et al. 2019). The new (HR2) and original (HRP) Hermans-Rasson tests from Landler et al. (2019) were used to test whether the orientation datasets were statistically different from a random distution. The tests were run within Rstudio (v2.1) which reports a *p*-value for both the new and original Hermans-Rasson tests. A *p*-value less than .05 means that the subsample is non-randomly oriented.

While the HR2 and HRP tests analyze the bin frequency of the azimuthal data, they do not consider the inclination of the fragments within the bins. To better understand the relationship between fragment inclination and orientation, a Von Mises analysis was performed using StereoNet, V.11.3.0 (Allmendinger 2020). Kappa values are interpreted based on the scale devised by Landis and Koch (1977) where a Kappa values < 0.2 have little significance, 0.2-0.4 have fair significance, 0.4-0.6 have moderate significance, and > 0.6 have substantial significance.

Inclination. The hypothesis that a mass wasting event was responsible for clasts within the Mastodon Pit was also scrutinized through the comparative analysis of mean inclinations that are recorded in the FLA subsamples. For these analyses, the direction of the inclination is not important since deposits produced by mass wasting events are unsorted and exhibit random orientation and inclination values (Pierson 2005). The mean and standard deviation of inclination were compared among the excavation pits using comparative mean statistics.

Voorhies Groups in Tapirs. Behrensmeyer (1975) grouped skeletal elements based on transport potential within a fluvial environment and coined the term "Voorhies Groups". These

groups reflect skeletal element classes that are often sorted in fluvial environments (Voorhies 1969). Voorhies Group 1 elements have the highest potential for transport within a fluvial environment, followed by Group 2 then Group 3. The percentages of these groups were identified in the three adjacent excavation pits and compared to one another. Isolated tapir material (SC<1) was exclusively considered for the analysis of Voorhies Groups because these groups are defined by the response of disarticulated elements within a fluvial environment. The relative percentages of these groups within an assemblage reflects the impact of fluvial processes on the assemblage. A Spearman's Rho test was conducted on the Voorhies Groups distributions to test for significant differences between excavation pits.

3.2.2 Micro-Scale Spatial Analyses, the Mastodon Pit

A similar set of analyses were carried out on materials from the Mastodon Pit to examine the vertical association of boulder and mastodon fragment survey points, orientation and inclination trends noted in the mastodon fragments, and qualitative anecdotal observations noted in the associations/articulations of mastodon skeletal elements and fragments.

3.2.2.1 Fabric Analysis. — The mastodon's FLA (FLA-Mastodon) orientations and inclinations were plotted and tested with the same statistical analyses as the FLA subsamples used for the meso-scale analysis. These results were then compared to all of the FLA subsample results of the Mastodon Pit.

3.2.2.2 Spatial Correspondence Between the Mastodon and Boulders. — The mastodon and boulders within the Mastodon Pit are mixed. Some boulders were large enough that they had to be removed with micro-explosives to reach the mastodon material below. Poorly sorted sediments along with this seemingly close relationship between the mastodon and the boulders has led to the hypothesis that the mastodon was entrapped in a mass wasting event. To test this

71

hypothesis, an ANOVA compared the mean elevations of the mastodon and boulder survey points.

   3.2.2.3 Articulation of the Mastodon Skeleton. — A qualitative analysis of the mastodon skeleton was carried out to assess the degree that skeletal elements have become disassociated. This was performed using the 3D model of the carcass remains created using the "Minimum Bounding Volume" tool in GIS (Figure 3.4). Areas where the skeletal elements were out of anatomical order or distantly associated are identified and reported.

3.3 RESULTS

For this study, excavation pits are treated as spatially discrete samples within a complex sinkhole deposit. Though the depositional 'situation' of an individual specimen may vary depending on where in the sinkhole the specimen was buried, comparing specimens between different excavation pits helps to identify the relative importance of different taphonomic processes, and how these processes vary spatially. The Mastodon, Mulch, and Rhino Pits are adjacent to one another while other pits are more distant and generally at lower elevations (Figure 3.6). The vertical frequency of specimens within the Rhino, Mulch, and Mastodon pits indicates that all paleontological materials within these pits are generally buried at the same elevation (Figure 3.6). The Tortoise Pit may provide a spatially distant and vertically lower comparison to the three adjacent pits. Backplots of elevation in an N/S trend also support the spatial similarity of the adjacent pits (Figure 3.6).
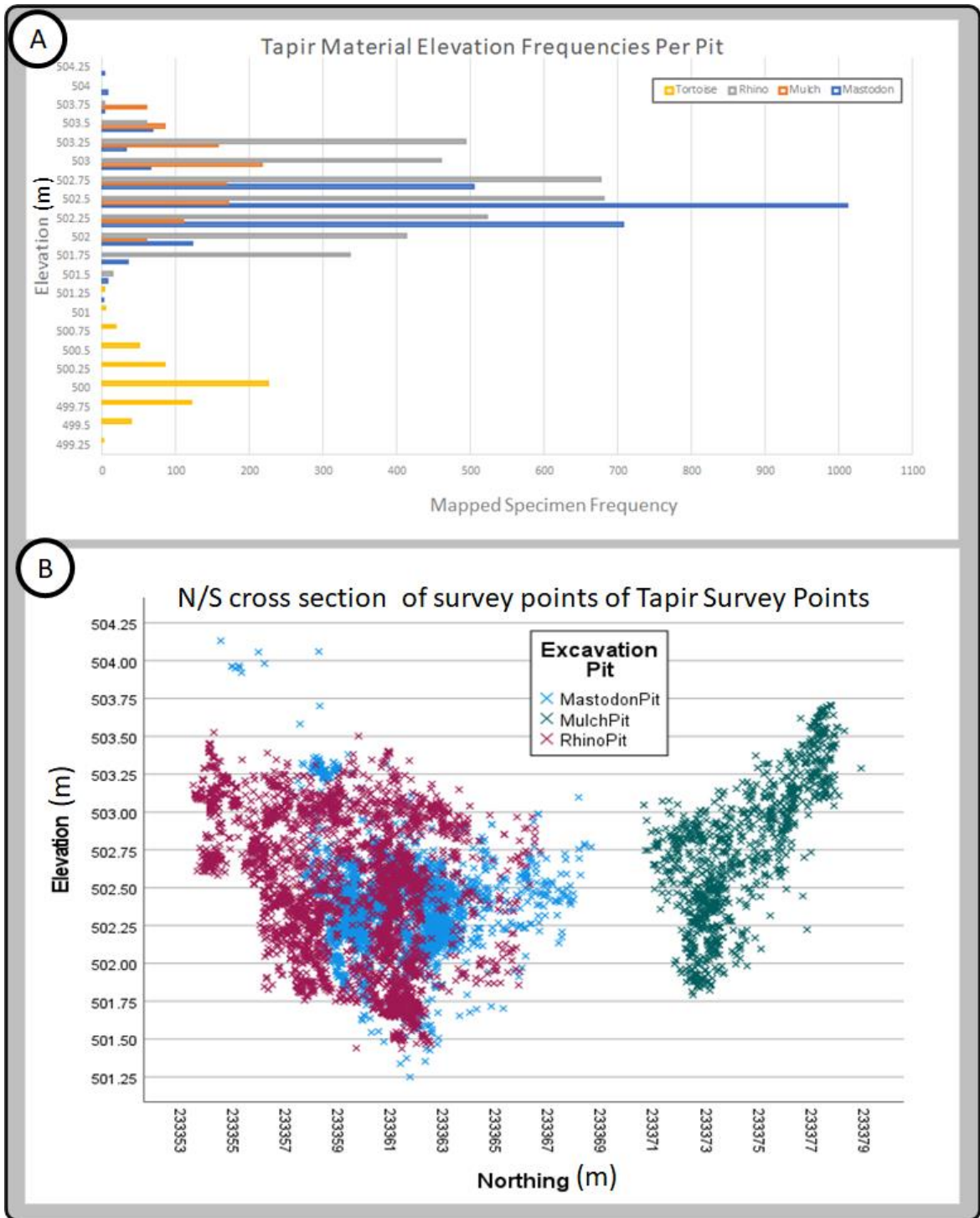
Figure 3.6 (A) Elevation of survey points (tapir only) for each discrete excavation pit incorporated in the assessment, (B) North/South backplot of survey points (tapir only) in the three adjacent excavation pits.

3.3.1 Meso-Scale Analysis

3.3.1.1 Skeletal Completeness. — SC is a metric that is intended to reflect the degree of disarticulation and transport of tapir remains. In general, higher SC values indicate skeletons that have experienced less disarticulation than skeletons with low SC values. Restricting the SC dataset to only include tapirs reduces variability due to non-depositional processes such as body size or species-specific behaviors. This analysis of SC uses the associated tapir skeleton dataset (Table 3.1). Anatomical association (SC value) is not related to elevation (Mastodon Pit R^2= 0.06; Rhino Pit $R^2 = 0.18$; Mulch Pit $R^2 = 0.03$). However, the mean elevation in associated tapirs (SC>5) between the three adjacent excavation pits is significantly different (F test statistic = 85.4; p=0.0001). The standard deviation of elevation in associated tapir groups (SC>5) in the Mastodon Pit was smaller (st. dev. = 0.28) than the standard deviations of the Mulch (st. dev. = 0.54) and Rhino Pit (st. dev. = 0.45). The spread of these values is significantly different between the Mastodon Pit and the two other pits (Levene's test statistic = 341.2; p= 0.0001).

3.3.1.2 Fabric Analysis. — *FLA Statistics.* Shipman (1981) suggests a sample size where $N > 72$ for robust analysis using rose plots. All FLA subsamples of the data from the Rhino and Mastodon Pits were greater than this minimum sample (Table 3.2 & 3.3). Half of the subsamples for material from the Mulch Pit had large enough samples and the Tortoise Pit only had sufficient sample size in the total material FLA subsample. The Tortoise Pit data were not included in subsequent analyses. Because these are subsamples of the same FLA dataset, Mulch Pit subsamples were included as they were all greater than 50.

Statistical results for circular uniformity are reported in Table 3.2 (total faunal) and Table 3.3 (tapirs). The HRP and HR2 tests generally supported preferential orientation in all subsamples ($p = 0.0001$), however unassociated datasets in the Mastodon and Mulch Pit were

randomly oriented ($p = 1.0$). The Von Mises test considers both inclination and orientation information as a single vector direction. Kappa scores for FLA subsamples ranged from 0.04 to 0.45. Generally, the scores were higher in associated subsamples than in unassociated, however even these subsamples exhibited only low significance. The Mastodon Pit's FLA-Tapir Associated (Kappa = 0.42) and the Tortoise Pit's (Kappa = 0.45) FLA-Total subsamples had the highest kappa values suggesting a moderately significant preferred orientation. Results of the HRP and HR2 tests suggest directional preference in many subsamples, however these subsamples are all multimodal. Further analyses with the Von Mises test indicate overall low scores, suggesting low to moderate significance in preferred vector direction.

Orientation. HRP and HR2 circular statistics suggest there is preferential orientation within nearly all the FLA subsamples, however, with inclination direction incorporated into the Von Mises statistics, preferential orientation was not strongly supported. Long axis orientation of the FLA subsamples was calculated for each excavation pit (i.e. unassociated and associated). Trends in long axis orientation were visualized using stereonets and roseplots (Figure 3.7). None of the four excavation pits were unimodal. FLA-Total subsamples from each pit showed no preferred orientation. FLA-Associated (SC>5) subsamples exhibited quadrant-scale unimodal directional preference, but 10° bins in the preferred quadrants had variable frequencies. The FLA-Associated subsample in the Mastodon Pit displayed a NE orientation. The Mulch Pit FLA-Associated subsample displayed SW orientation. The Rhino Pit FLA-Associated subsample displayed a multimodal NE and SW preference, and the Tortoise Pit FLA-Associated subsample displayed a multimodal W/SW preference. All FLA-Unassociated (SC<5) subsamples showed no preferred directions and had longer rose petals in most directions. The Rhino Pit's FLA-

Unassociated subsample had a preferred axis to the north, but the unassociated material was observed in all other direction bins as well.

Orientation of Tapir specimens. Reducing the plots to a single taxon reduces biological variables, which may reduce the "noise" reported in the stereonets and roseplots. This seems to be the case when comparing the stereonets and roseplots of the total faunal FLA subsamples to the FLA subsamples restricted to tapir remains (Figure 3.8). All trends noted for total faunal FLA subsamples are supported by the Tapir FLA subsamples. Generally, the FLA-Tapir Associated subsamples show higher directional preference than the FLA-Tapir Unassociated subsamples.

Although there are differences noted in the orientations of fossil material of each excavation pit and preferential orientation is supported with the HRP and HR2 tests, all subsamples display multimodal orientation preference. Fluvial systems are supported when linear anisotropy is present in the orientations of fossil material. The multimodal orientations observed in all FLA subsamples does not support deposition within a fluvial system suggesting the fossils preserved at the GFS were preserved in a different type of depositional environment.
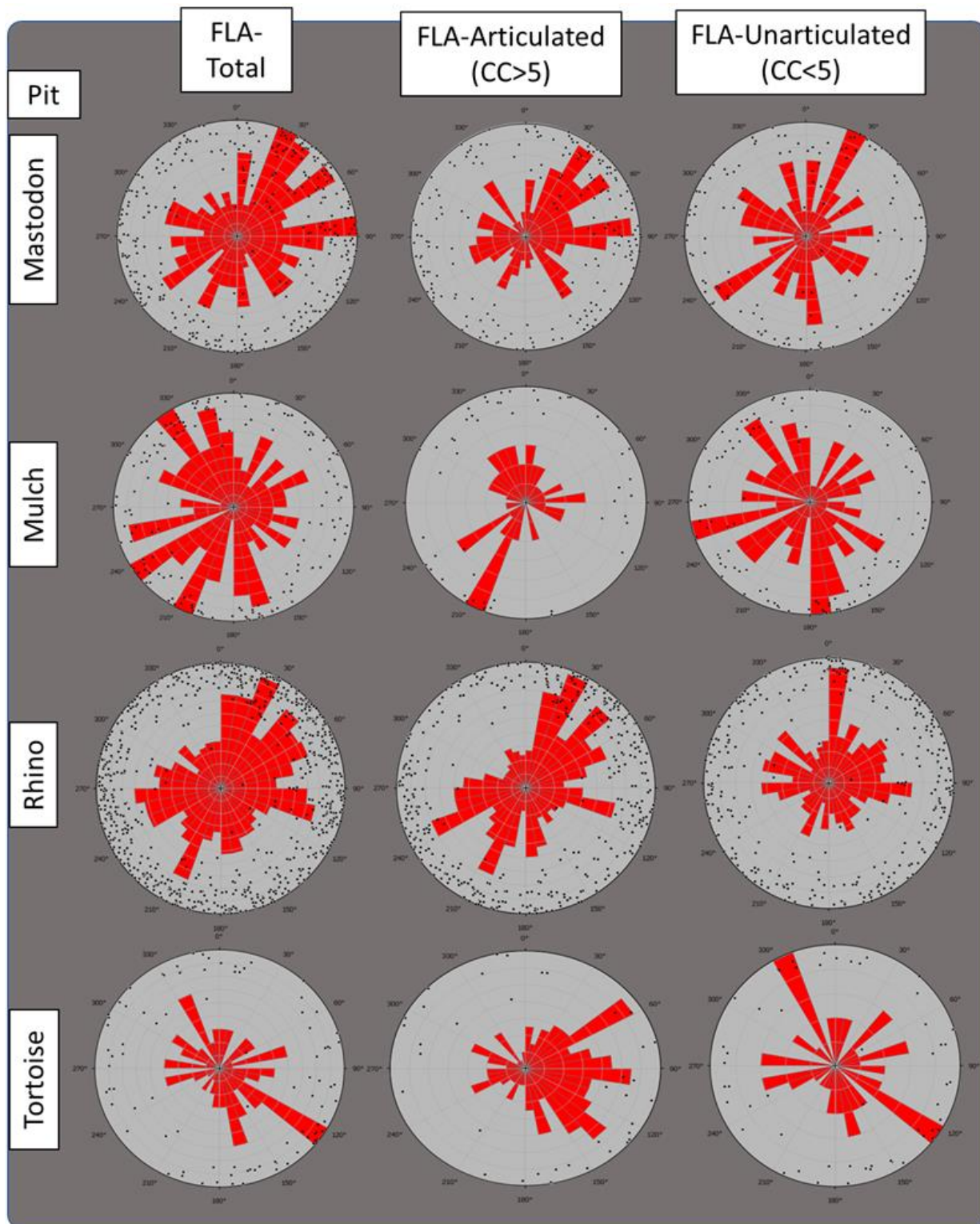
Figure 3.6 Stereonet and rose plots for FLA subsamples (FLA-Total, FLA-Associated, and FLA-Unassociated) in each excavation pit.
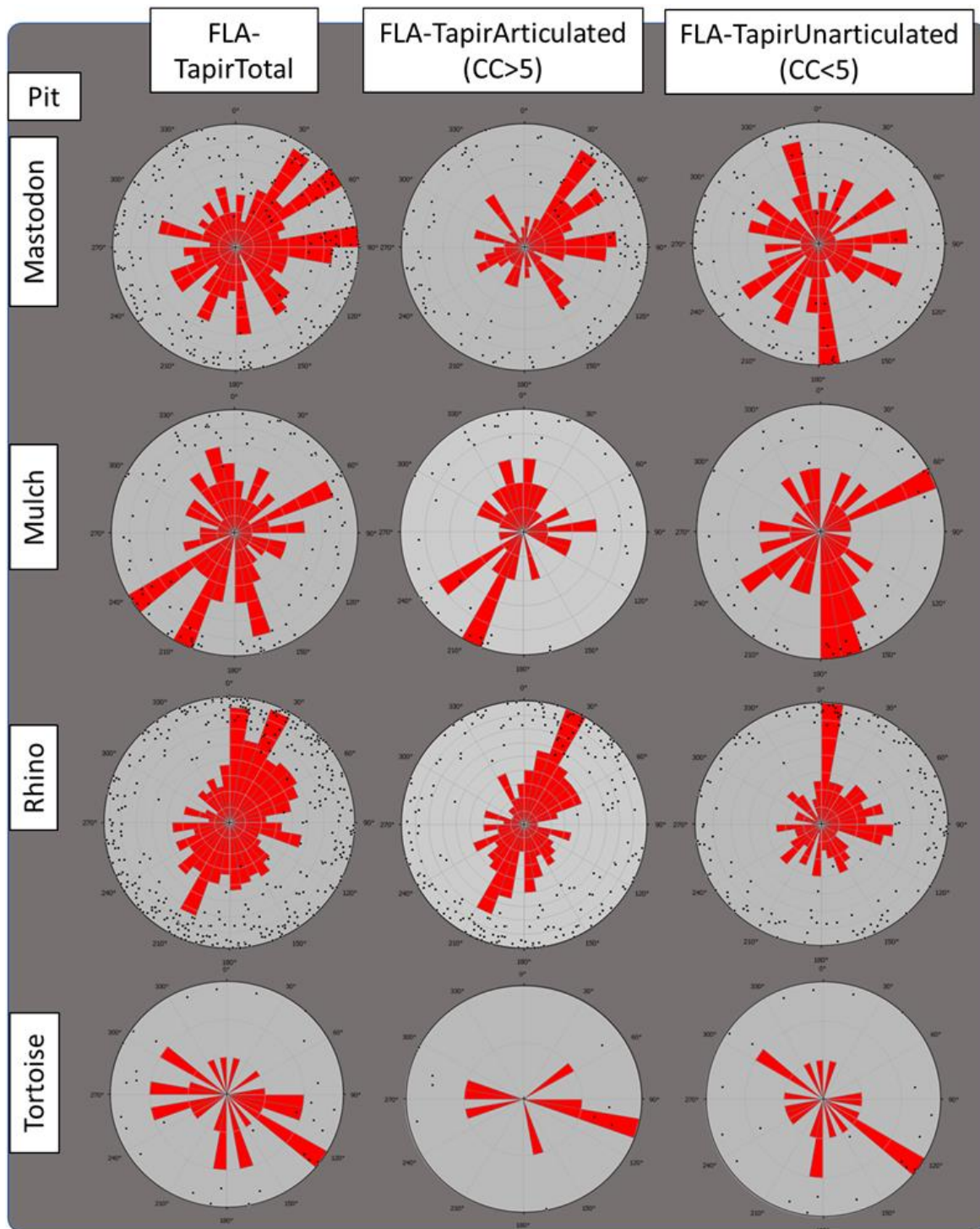
Figure 3.7 Stereonet and rose plots for Tapir FLA subsamples (FLA-Total Tapir, FLA-Tapir Associated, and FLA-Tapir Unassociated) in each excavation pit.

FLA Subsample			Excavation Pit			
			Mastodon	Mulch	Rhino	Tortoise
FLA-Total	Sample Size		336	172	766	96
	HRP P-Value		**0.0001**	**0.0001**	**0.0001**	**0.0001**
	HR2 P-Values		**0.0001**	**0.0001**	**0.0001**	**0.0001**
	Von Mises Kappa Value		0.201	0.1403	0.1403	0.2622
	Inclination	Mean	15.3°	12.3°	12.4°4	13.5°
		Standard Deviation	13.8°	9.5°	11.1°	12.1°
FLA-Associated	Sample Size		133	58	432	40
	HRP P-Value		**0.0001**	**0.0001**	**0.0001**	**0.0001**
	HR2 P-Values		**0.0001**	**0.0001**	**0.0001**	**0.0001**
	Von Mises Kappa Value		0.345	0.3034	0.1403	**0.4511**
	Inclination	Mean	15.0°	11.3°	12.5°	12.6°
		Standard Deviation	12.2°	9.2°	10.3°	11.2°
FLA-Unassociated	Sample Size		105	114	334	55
	HRP P-Value		**0.0001**	**0.0001**	**0.0001**	**0.0001**
	HR2 P-Values		1	**0.0001**	**0.0001**	1
	Von Mises Kappa Value		0.02	0.1605	0.201	0.201
	Inclination	Mean	15.8°	12.9°	12.3°	14.2°
		Standard Deviation	16.0°	9.7°	12.1°	12.6°

Table 3.1 *P*-value and Kappa reported for circular uniformity tests on Total Faunal FLA subsamples with significant results in bold. Summary statistics provided for FLA subsample inclinations.

FLA Subsample			Excavation Pit			
			Mastodon	Mulch	Rhino	Tortoise
FLA-TapirTotal	Sample Size		237	107	399	30
	HRP P-Value		**0.0001**	**0.0001**	**0.0001**	**0.0001**
	HR2 P-Values		**0.0001**	**0.0001**	**0.0001**	**0.0001**
	Von Mises Kappa Value		0.2213	0.04	0.1807	0.2418
	Inclination	Mean	15.7°	13.1°	12.2°	16.1°
		Standard Deviation	14.1°	10.0°	10.6°	13.0°
FLA-TapirAssociated	Sample Size		132	54	239	8
	HRP		**0.0001**	**0.0001**	**0.0001**	NA
	HR2		**0.0001**	**0.0001**	**0.0001**	NA
	Von Mises Kappa Value		**0.4296**	0.2622	0.1202	NA
	Inclination	Mean	15.3°	11.6°	12.8°	20.1°
		Standard Deviation	12.4°	9.2°	10.6°	11.4°
FLA-TapirUnassociated	Sample Size		106	53	160	21
	HRP P-Value		1	**0.0001**	**0.0001**	**0.0001**
	HR2 P-Values		1	**0.0001**	**0.0001**	1
	Von Mises Kappa Value		0.1001	0.3242	0.3034	0.3242
	Inclination	Mean	16.2°	14.6°	11.3°	14.5°
		Standard Deviation	16.1°	10.6°	10.6°	13.5°

Table 3.2 *P*-value and Kappa reported for circular uniformity tests on Tapir FLA subsamples with significant results in bold. Summary statistics provided for Tapir FLA subsample inclinations.

Inclination. Inclination was also analyzed. The mean of the inclinations for each FLA subsample are reported in Table 3.2. Mean inclinations of subsample datasets in the Mastodon Pit were greater than those of the Mulch and Rhino Pits. The Tortoise Pit had the most variable inclinations in its subsamples which may have been caused by small sample size. Standard deviations in the Mastodon Pit's subsamples were all higher than those reported for all other excavation pit subsamples. The FLA-Associated subsamples had lower inclinations than the FLA-Unassociated material in the Mastodon and Mulch pits. The opposite was noted in the Rhino Pit where the FLA-Associated subsample had a higher inclination than its FLA-

Unassociated subsample. The standard deviation of each excavation pit's FLA-Associated subsample was lower than the pit's FLA-Unassociated standard deviation.

Tapir Inclination. Interestingly, when mean inclinations are restricted to exclusively tapirs, identical trends are noted in each pit (Table 3.3). Total faunal FLA subsamples mostly consist of tapirs, which may play a role in the similarity. However, all of the Rhino Pit's Total faunal FLA subsamples are far larger than the pit's Tapir FLA subsamples, and similar trends are noted here with the FLA-Tapir Associated subsample having higher mean inclinations than the FLA-Tapir Unassociated subsample.

Voorhies Groups of Isolated Tapir Material. The percentage of isolated tapir bones belonging to different Voorhies Groups was calculated (Figure 3.9). The sample size of isolated tapir material in the Tortoise Pit was insufficient for meaningful analysis. The distribution of Voorhies Groups among the three adjacent excavation pits is similar. Elements belonging to Voorhies Group 2 (medium transport potential) are the most common in each pit with frequencies ranging from 60%-75%. Elements assigned to Voorhies Group 1 (high transport potential) are the second most common specimens in each group. Elements in Voorhies Group 3 (low transport potential) were the least common in each pit.
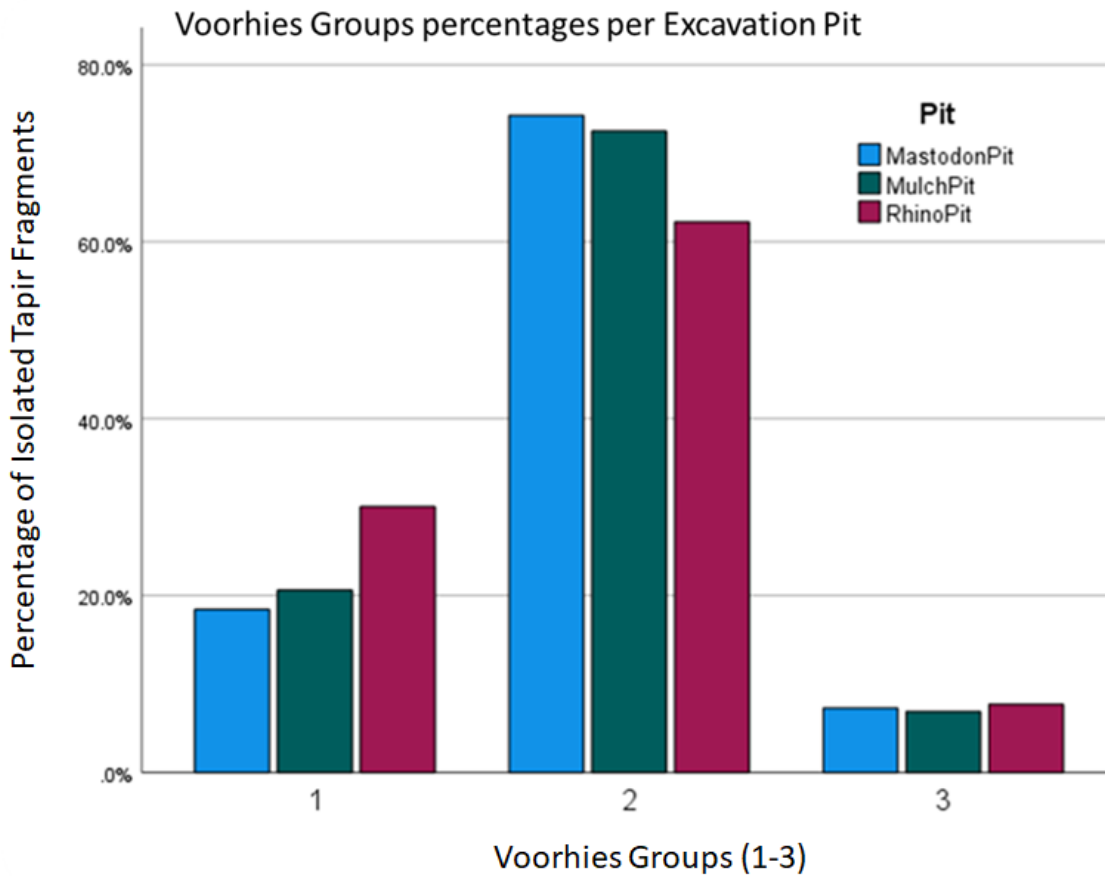
Figure 3.9 Percentages of Voorhies Groups in the three adjacent excavation pits.

A Spearman's Rho tested whether the distribution of Voorhies Groups was significantly different between the three adjacent excavation pits. The null hypothesis, that there is no relationship between the Voorhies Groups of isolated tapir fragments and excavation pit, cannot be rejected ($rs(2240) = -.027$, $p = 1$). This supports the absence of fluvial organization to deposits in this area of the GFS.

Results of the orientation analysis and the percentages of Voorhies Groups in the

excavation pits indicate that there is no fluvial organization of deposits in this area of the GFS.

Multimodal orientation preference in the FLA subsamples suggest a linear anisotropic fabric is

not present and the percentages of Voorhies Groups (based on transport potential in a fluvial

setting) are consistent through the excavation pits. Although the lack of unimodal orientation

falsifies linear anisotropy, planar anisotropy is supported where fragments with a long axis are

positioned with minimal variance in their inclinations. Planar anisotropic fabrics are noted in the

Mulch and Rhino pits where the inclinations are plotting with a small standard deviation.

Isotropic tendencies are noted in the Tortoise and Mastodon Pit. These excavation pits

had random orientation results and higher inclinations with larger standard deviations. Due to

small sample size, this inference must remain tentative in the Tortoise Pit. However, the much

larger sample size in the Mastodon Pit indicates the presence of an isotropic fabric where fossils

are randomly positioned throughout the deposit, supporting the mass wasting hypothesis for the

excavation pit.

3.3.2 Micro-Scale Analysis, the Mastodon Pit

3.3.2.1 Fabric Analysis. — Isolated tapir materials indicate an isotropic fabric is present

in the mastodon pit. This pattern is further explored through fabric analysis (orientation and

inclination) of the entire fauna from this area. Bone fragment orientation and inclination data

from the mastodon skeleton (ETMNH 305) is compared to directional trends in the entire

Mastodon Pit fauna.

Orientation. Orientation was calculated for fragments identified as part of the mastodon

(FLA-Mastodon). FLA-Mastodon orientations are plotted on stereonets and roseplots (Figure

3.10). Hermans-Rasson tests were significant (p=0.0001) suggesting a preferred, non-random

orientation (Table 3.4). The Von Mises distribution test resulted in a Kappa value of 0.41, which

is moderately significant according to Landis and Koch (1977) (Table 3.4). Interestingly,

preferred inclination values are near the opposite direction from inclination in all other Mastodon

Pit FLA subsamples. Circular uniformity tests suggest orientations of mastodon elements are

non-randomly distributed, and many of the 10° bins have similar frequencies. The highest

frequency of specimens is oriented to the southwest.
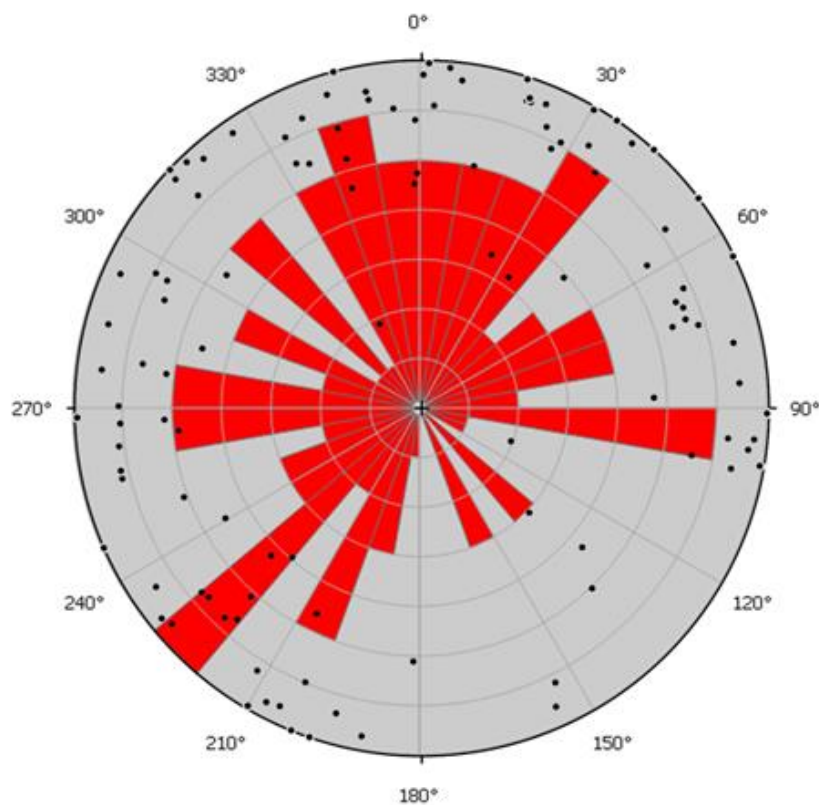
Figure 3.10 Stereonet and rose plots of mastodon bone fragments with a long axis. HR circular

statistics support a non-random distribution ($p = .0001$).

FLA-Mastodon Subsample Statistics			
Sample Size			109
HRP P-Value			**0.0001**
HR2 P-Values			**0.0001**
Von Mises Kappa Value			**0.4296**
Inclination	Mean		17.2°
	Standard Deviation		14.2°

Table 3.3 *P*-value and Kappa reported for circular uniformity tests on FLA-Mastodon subsample significant results are emboldened. Mean statistics provided for FLA-Mastodon inclinations.

Inclination. Specimen inclination was also analyzed and compared to inclinations of other Mastodon Pit specimens. There is a higher mean inclination in mastodon specimens than in all other Mastodon Pit FLA subsamples (Table 3.5). The standard deviation of the inclinations plots within those reported for Mastodon Pit FLA subsamples. The meso-scale orientation and inclination analyses support an isotropic fabric for the deposit in the Mastodon Pit. A focus on the inclinations of the mastodon fossil fragments support that it was deposited in a similar fashion.

3.3.2.2 Testing the Spatial Association Between the Mastodon and Boulders. —
Mastodon elements and boulders exhibit a close visual association within the Mastodon Pit (figure 3.11). A north/south backplot also illustrates the spatial relatedness of these two features.

The mean elevation of the boulders (502.61 m) is 30 cm higher than the mean elevation for mastodon specimens (502.30 m) (F test statistic = 585.4; p = 0.0001), which is significant. A Levene's test also supported a difference in the spread noted in the mastodon fragments and boulders (Levene's test statistic = 567.8 p = 0.0001). One caveat is that the base of the excavation pit artificially limits the vertical distribution of boulders. The Mastodon Pit boulders extend for an unknown depth below the mastodon. Once their full vertical extent is known, their mean elevation will be lower than the current estimate, which may lead to a significant association between the boulders and mastodon.

Survey Point Subsample	Sample Size	Mean Elevation (m)	Std. Deviation	Std. Error	95% Confidence Interval	
					Lower	Upper
Mastodon Fragments	2164	502.3	0.3	0.007	502.27	502.36
Boulders	2549	502.6	0.4	0.01	502.59	502.68

Table 3.4 Summary statistics of elevation differences between the boulder and mastodon datasets.
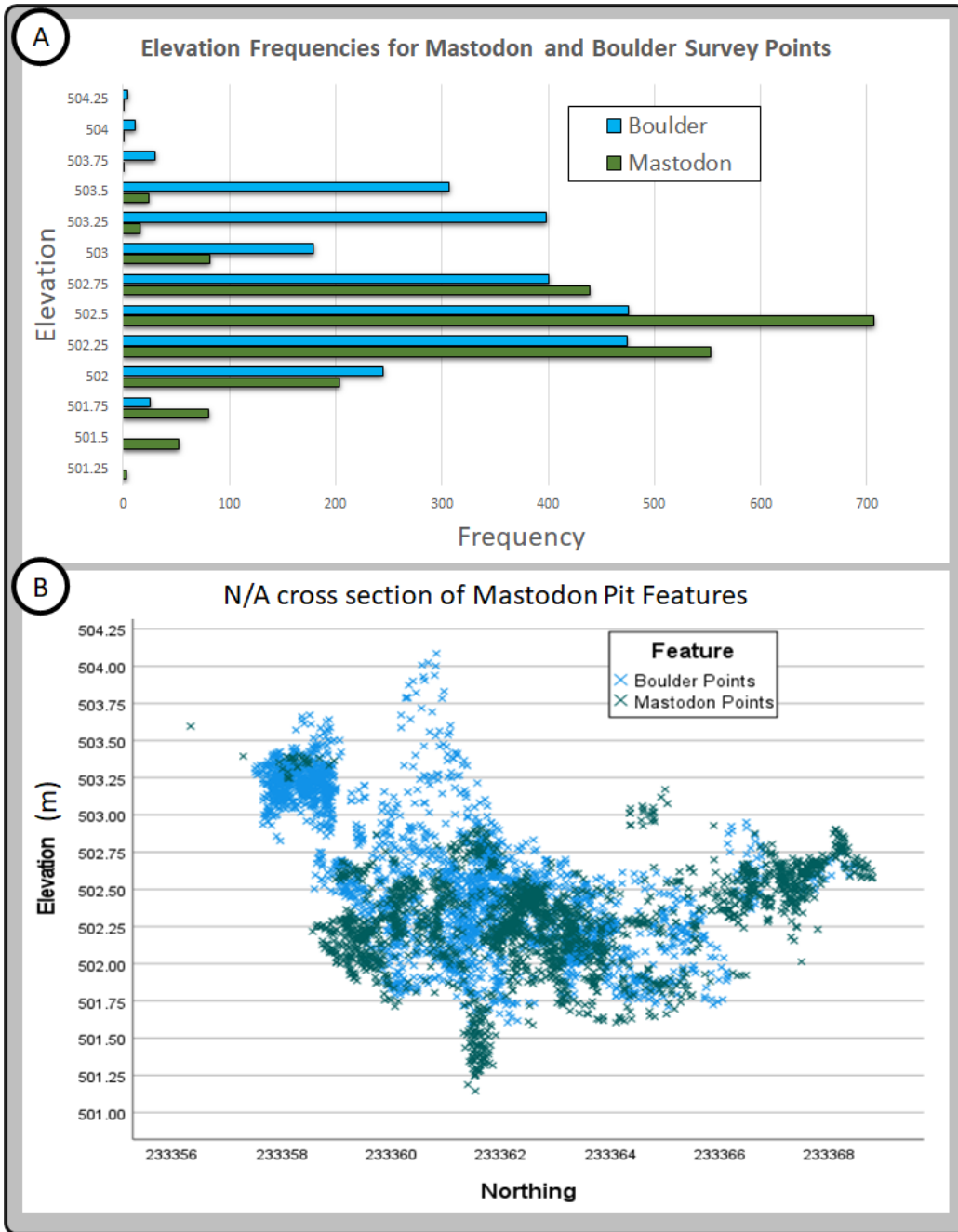
Figure 3.11 (A) Vertical frequency of mastodon and boulder survey points within the Mastodon

Pit. (B) North/South backplot of mastodon and boulder survey points in the three adjacent

excavation pits.

3.3.2.3 Qualitative Assessment of the Mastodon Skeleton. —The mastodon skeleton is highly fragmented in situ due to sediment crushing, but the right side (lower side of the carcass) is more complete than the left side. Many of the thoracic vertebrae and ribs are fragmented and mixed throughout. The limbs are highly fragmented as well, but the fragments are clustered, and are generally in relative anatomical position. There is also one place where rib and vertebra material accumulated between two boulders deeper in the pit. These specimens represent the lowest elevation (501.15 m) where the mastodon has been found (Figure 3.11).

The mastodon's most anatomically out of place element is its sacrum which appears to have been moved to a position anterior to the pelvis (where it should have been posterior to the pelvis in life). The sacrum appears to be on the edge of a gap where rib and vertebra fragments are vertically dispersed (Figure 3.12).

Other displacement in the mastodon is noted at the posterior end of the individual. The hind limbs (including femur, tibia/fibula, and pes) and caudal vertebrae are closely articulated, however this area is displaced from the rest of the body (Figure 3.4). The left femoral head is over a meter away from the closest pelvis fragment. The anterior-most caudal vertebra is only slightly closer (~0.5 m) to the pelvis, however, this caudal vertebra articulates with the displaced sacrum, which is 2.5 m from this caudal vertebra.
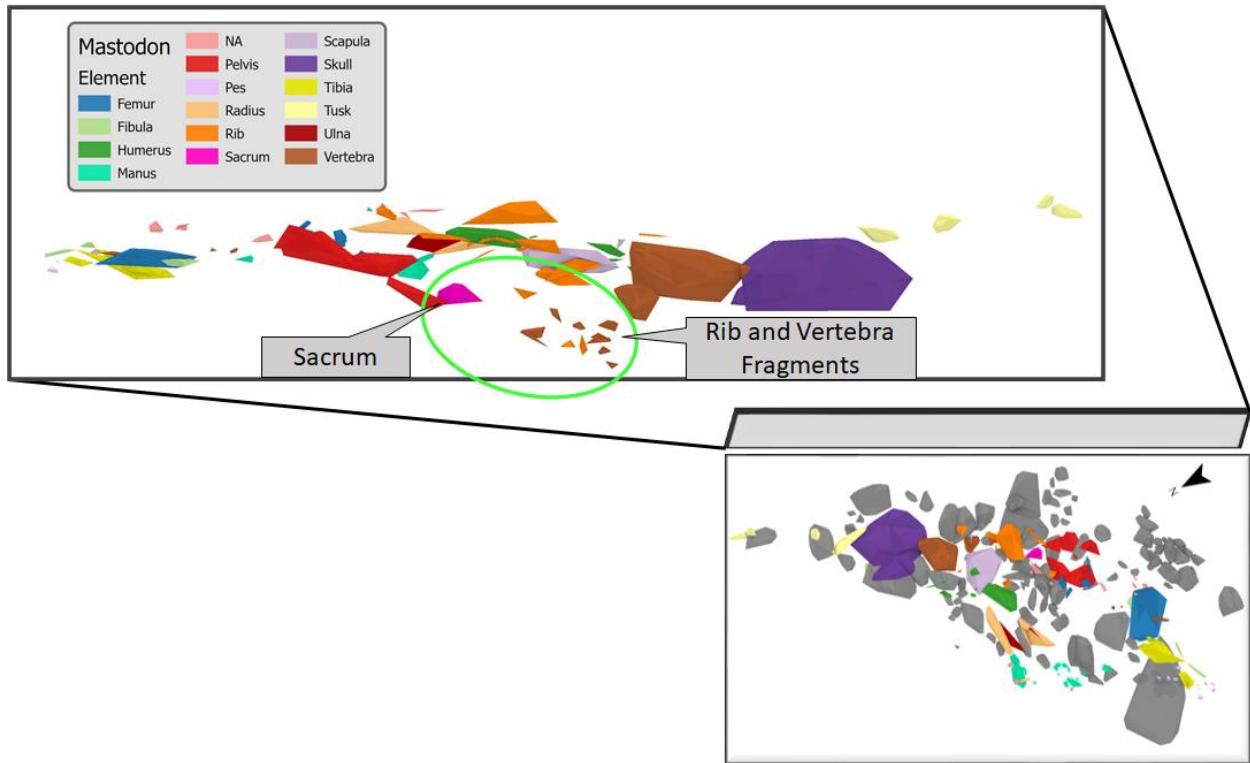
Figure 3.12 An oblique view of the dorsal side (facing the east) of the mastodon carcass *in situ*.
Sacrum is displaced anteriorly to the pelvis. Vertebra and rib fragments accumulate at the lowest
elevations. Map can be viewed in an ArcGIS online 3D interface at https://arcg.is/1T5mqL0.

3.4 DISCUSSION

3.4.1 Depositional Environments at the GFS

Fossil-bearing deposits at the GFS are the infill of a Pliocene sinkhole (Shunk 2006).

Spatially discrete excavation pits serve as comparable samples that provide meaningful

interpretation of meso-scale formation processes acting at the site level (Badgley et al. 1995;

Alberdi et al. 2001).

3.4.1.1 Spatial Variability in Disarticulation Rates. — SC is used as a proxy for the

degree of disarticulation, which can be useful for taphonomic assessment (Voorhies 1969;

Behrensmeyer 1991; Bunn 1989; Varricchio 1995). The frequencies of tapir SC values in each of

the excavation pits are very similar. Although oriented differently, the relative frequency of SC

values between unassociated (SC<5) and associated (SC>5) tapirs between pits is similar.

Unassociated and associated tapir skeletons occur at similar elevations within each pit, however,

the vertical spread of associated skeletons in the Mastodon pit (st. dev. = 0.28) is significantly

narrower than adjacent pits (Mulch st. dev. = 0.54; Rhino st. dev. = 0.45) (Levene's test statistic

= 341.2; p= 0.0001).

An isotropic fabric in the Mastodon Pit supports a mass wasting event, but one would

expect to see a greater dispersal of skeletons here than in low energy lacustrine deposits with a

planar anisotropic fabric. Rogers (2005) discusses a debris flow deposit where skeletal remains

are in various states of association and articulation. These types of deposits can transport fossils,

but interestingly these skeletons may experience minimal disarticulation. Perhaps within the

Mastodon Pit deposit, associated skeletons are acting in similar ways. Another factor here is the

size of the mass wasting deposit. The vertical spread of the boulders and mastodon fragments

suggest that the deposit is at least three meters thick while their N/S spread is approximately ten

meters. The event transported this material a relatively short distance. Perhaps the skeletal remains would have dispersed further if they travelled a longer horizontal distance.

3.4.1.2 Fabric Analysis. — FLA subsamples in the Mastodon Pit and Mulch Pit did not have a preferred direction, however the Rhino Pit showed a NE-SW directional preference in FLA-Associated and FLA-Tapir Associated subsamples. When inclination and orientation are considered together, trends become less significant as low Kappa values indicate no preferred direction in each subsample for all pit data.

Excavation pits reflect different locations within the sinkhole such as the sinkhole bottom, margins, or collapsed walls. The fossils in these areas are deposited in conditions reflecting anisotropic and isotropic fabrics. The Mulch Pit may reflect sinkhole bottom sediments as planar anisotropic fabric is present. Mulch Pit orientation data is without preference suggesting a linear fabric (fluvial organization) is not present. Inclination of associated (SC>5) subsamples have lower means than their unassociated (SC<5) counterparts suggesting they may have had different taphonomic pathways. This might be explained by a bloat and float model where carcasses become bloated, then disarticulate during decomposition (Allison and Briggs 1991; Roger and Kidwell 2007; Syme and Salisbury 2017). Syme and Salisbury (2017) observed this phenomenon in crocodile carcasses as they floated in water; once the soft tissue holding the carcass together decays, bones begin to disarticulate and result in lower rates of SC.

The FLA dataset indicated a preferred direction among many of the subsamples in the Rhino Pit. This pattern could be due to fluvial transport or general orientation of long axes parallel to the slope at the margin of the sinkhole. There is no relationship between element frequencies and Voorhies Groups, suggesting fluvial transport had little impact on specimen

distributions. Therefore, fluvial organization of material in the rhino pit seems the less likely of

two possible depositional scenarios. The mean inclination of the FLA subsamples in the Rhino

Pit were generally similar to those of the Mulch Pit, yet the standard deviation was greater.

Interestingly, the opposite trend was noted for the inclinations of the associated and unassociated

subsamples; where the associated individuals had a higher mean inclination than the

unassociated specimens, though the standard deviations were not reciprocated like the means.

The spatial attributes of the Rhino Pit suggest it is a planar anisotropic fabric with more

preferential linear direction. Perhaps the Rhino Pit represents the deposition of associated

skeletons along a lake margin that is steeper than the bottom of the sinkhole where interaction

with the water's edge may have positively impacted linear trends.

Analyses of orientation using the FLA dataset suggest similar trends in mapped

specimens between the Mastodon Pit and the Mulch Pit. However, the inclination results in the

FLA dataset, along with sedimentary characteristics in these different excavation pits are very

different. The Mulch Pit contained sediments characterized as organic rich rhythmite clay layers

(Shunk, 2006), while the Mastodon Pit sediments were oxidized and contained a poorly sorted

mixture of sediment grain sizes. The mean and standard deviation of inclinations in the

Mastodon Pit were also higher, suggesting the influence of high energy depositional processes

that would cause bones to lie at high angles. The combination of high inclinations and lack of

preferred orientation indicates an isotropic fabric is present within the Mastodon Pit.

Furthermore, poorly sorted sediments suggest rapid, high-energy deposition. These

characteristics of the Mastodon Pit deposit suggest that a mass wasting event may have been

responsible for the deposition of this sedimentary unit.

3.4.2 Depositional Environment in the Mastodon Pit

3.4.2.1 Genesis of the Mastodon Pit deposits. — The skeleton of the mastodon (ETMNH 305) is almost entirely complete and with most skeletal elements in relative anatomical position. There has been some minor displacement of elements, as noted above. The associated individual is highly fragmented, but broken edges are not abraded or weathered (Widga et al. 2018). Neither the mastodon fragments, nor other tapir material from the Mastodon Pit show a preferred orientation. Furthermore, the mean inclination for mastodon fossil fragments was >17°, one of the highest mean inclinations within the site. The standard deviation (14.21°) of inclinations of mastodon fragments is consistent with the standard deviation (14.14°) of the tapir subsample from the same pit. Much like all other Mastodon Pit material, high inclination, and no preferred orientation in fragments with a long axis support the idea that this mastodon is potentially associated with a mass wasting event.

3.4.2.2 The Association Between Mastodon Bones and Boulders. —ANOVA tests of association between the mastodon bone and boulder elevations suggest a significant difference in their vertical positions, however there are unmapped boulders lower in the deposit. Once these lower boulders are mapped and incorporated into this dataset, the mean elevation of the Mastodon Pit boulders will decrease and possibly support a significant association between them and the mastodon skeleton. The mean elevation of these datasets differ by 30 centimeters, but boulders continue below the mastodon. The visual overlap suggests that these two features were simultaneously deposited. Excavating and surveying the deeper boulders may further strengthen this interpretation.

It is difficult to determine whether the mastodon died prior to a mass wasting event, or if perhaps there was an open space between the boulders that would have allowed water to deposit material in the small space. A mastodon carcass that decayed to a point where the sacrum was

disarticulated would have mobile skeletal elements. Qualitative observations of the mastodon remains based on a reconstructed 3D model of the individual show the remains present are mostly in anatomical order. The dorsal elements of the mastodon are generally less well-preserved than ventrally located elements. There is a section where rib and vertebra fragments were collected between two boulders. This was noted by excavators and is also apparent in the 3D model. Interestingly, the mastodon element that exhibits the most displacement from its anatomical position is the sacrum which was moved to a position anterior to the pelvis. The sacral wings are still articulated, but the rest of the sacrum shifted. The sacrum may have been forcefully displaced during a mass wasting event. Another possibility is that as the soft tissue between the pelvic wings decayed, this area would have been more vulnerable to sediment crushing. Perhaps the pelvis and sacrum were articulated during the event, but as the carcass decayed and the deposit settled, the sacrum was freed from the pelvis. This scenario, however, does not explain the displacement of the sacrum to an anterior position to the pelvis. How was the sacrum able to shift anterior to the pelvis if it was buried?

If the mastodon was involved in a mass wasting event at or near the time of its death, its skeletal element's mobility would be restricted within the deposit. With such large boulders also present in the deposit, it would have been possible to have confined open spaces between them. Water and finer sediments could move through these spaces, but larger objects such as boulders and mastodon bones would not be able to. Voorhies (1969) reports that mammalian sacrums float in water until they ultimately become waterlogged and begin to sink. These ideas could explain the displacement of the sacrum, as it would have had mobility in a seemingly confined space. The mastodon could have decayed post burial, and as water made its way into the mass

wasting sediments, they could have shifted the buoyant sacrum within the confined space between boulders.

3.4.3 Site Formation Processes at the Micro and Meso Scales.

These paleontological and sedimentological results are consistent with a circum-lacustrine, swampy lacustrine depositional environment (Bertog et al. 2014). This depositional environment would consist of low energy depositional processes, areas of anoxia (low dissolved oxygen), and high organic content. This environment would be similar to Cullar de Baza (Granada, Spain), a fossil site described by Alberdi et al. (2001) which has similar frequencies of Voorhies groups (group 2 being the highest, and groups 1 and 3 are similar in size), moderate degrees of articulation, minimal weathering, terrestrial and aquatic fauna, and carbonate-based sediments. While evidence supports a swampy lacustrine depositional environment, it should be noted that the water depths of the GFS are unknown. The GFS is not often depicted as a shallow depositional environment, however it was likely a low energy environment (Shunk et al. 2009; Whitelaw et al. 2008)

Further evidence for a swamp-like setting can be supported by the absence of lithified fossils. Lithification, or material becoming increasingly lithified, can be a step in the fossilization process as organic material is replaced with minerals. As this process has been studied, it is apparent that lithification of fossils can vary. At GFS, material is relatively unlithified (Keenan and Engel 2017). Woody debris that is common in the rhythmite clays is still highly organic as opposed to petrified. Many of the site's vertebrate fossils are often fragmented, but anatomical voids in bones (e.g., trabeculae, marrow cavities) have not experienced crystal formation. Some specimens do exhibit iron carbonate formation, probably siderite. Voorhies (1969) suggests the absence of lithification may be a result of the mobility of fossil material post burial. This could

96

be a possible occurrence at the GFS as the rhythmite clays would be locally mobile in an aqueous setting (Shunk et al. 2009). This could allow the reworking of fossils and possible stratigraphic disorder through mixing of older and newer remains (Cutler and Flessa 1990).

However, if skeletons were mobile after burial, how would the articulated individuals remain articulated? Lyman (1994) combined studies of Hill and Behrensmeyer (1984) and Hill (1979) to understand the ordering in which major body parts become disarticulated during decay and found that "unusual environments" such as anoxic areas or areas with high sedimentation rates will slow decay and disarticulation. Many researchers suggest that portions of the sinkhole pond are anoxic (Shunk et al. 2009; Keenan and Engel 2017; Keenan et al. 2018). Therefore it is possible that articulated individuals are being held together with slowly decaying soft tissue (e.g., tendons, muscles) as they are being transported short distances within the sinkhole.

This reconstruction is consistent with the minimal evidence of carnivore interaction and carnivore material on tapir remains (Ketchum, 2011). Alligators at the GFS would be expected to consume tapirs. However, tapir carcasses may be deposited in an anoxic location inaccessible to the alligators at the site (as opposed to the bloat and float hypothesis where they would have been accessible).

A possible modern setting that is analogous to these taphonomic observations are meromictic lakes. Most deep lakes experience holomixis where the shallow and deep waters of varying temperature and density are seasonally mixed by wind (Lewis 1983). This cyclical process does not occur in meromictic lakes as the differences in density are too strong to support vertical exchange of surface and deep waters (meromixis) (Walker and Likens 1974). This results in meromictic lakes containing two stratified water layers; the upper oxygenated

97

mixolimnion and lower anoxic monimolimnion (Stewart et al. 2009). Stewart et al. (2009)

mention that a lake shielded from wind in mountainous or forested environments is more likely

to be meromictic. Gorham and Sanger's (1972) studies of a meromictic lake suggest that organic

materials are present at abnormally high levels throughout sampled sediments from a transect of

the lake. The organic material is present at higher percentages in inshore sediments (65%), but

was also noted to be near similar levels in the deepest water sediments (60%) (Gorham and

Sanger, 1972). They propose the highly organic material slumped to the deepest parts of the lake.

Perhaps this is a mechanism that brings organic material including vertebrates to an anoxic zone

at the GFS.

3.5 CONCLUSION

GFS is a complex sinkhole deposit system with a unique fossil assemblage. This study analyzed the spatial distribution of paleontological materials across the site in order to better understand the type and range of depositional settings that are present at the site.

Overall, paleontological materials are preserved in an anoxic environment by fine grained, organic-rich infill sediments deposited in the sinkhole under low energy. There is low potential for transport within this setting. Fabric analyses of bone orientation and inclination along with the degree of association in individual tapirs indicate that these animals are preserved in similar ways throughout the site, yet the orientation and inclinations of their skeletal remains may vary.

The Mastodon Pit is represented by fossil taxa commonly found in sediments at GFS, however there is significant evidence to suggest the Mastodon Pit material was reworked by a mass wasting event that is represented by a poorly sorted deposit and fossil fragments with a long axis displaying no preferred orientation with high mean inclination.

REFERENCES

ABLER, W. L., 1984, A three-dimensional map of a paleontological quarry: Contributions to

Geology (University of Wyoming), v. 23, p. 9-14.

AGENBROAD, L. D., 1984, Hot Springs, South Dakota: entrapment and taphonomy of Columbian

Mammoth, *in* P. S. Martin and R. G. Klein, (eds.), Quaternary extinctions: a prehistoric

revolution: University of Arizona Press, Tucson, p. 113-127.

ALBERDI, M. T., ALONSO, M. A., AZANA, B., HOYOS, M., and MORALES, J., 2001, Vertebrate

taphonomy in circum-lake environments: Three cases in the Guadix-Baza Basin

(Granada, Spain): Palaeogeography, Palaeoclimatology, Palaeoecology, v. 165, p. 1-26,

doi:10.1016/s.

ALBERT, G., BOTFALVAI, G., and ŐSI, A., 2018, Mapping the past: GIS and intrasite spatial

analyses of fossil deposits in paleontological sites and their applications in taxonomy,

taphonomy and paleoecology: Palaeontologia Electronica, v. 21, p. 1-22,

doi:10.26879/8120031-0182(00)00151-6

ALLISON, P. A., and BRIGGS, D. E., 1991, Taphonomy of Nonmineralized Tissues: Topics in

Geobiology, 25-70. doi:10.1007/978-1-4899-5034-5_2

ALLMENDINGER, R., 2020, StereoNet V.11.3.0. Rick Allmendinger's Stuff. Cornell University.

Retrieved December 30, 2020, from https://www.rickallmendinger.net/

BADGLEY, C., BARTELS, W. S., MORGAN, M. E., BEHRENSMEYER, A. K., and RAZA, S., 1995,

Taphonomy of vertebrate assemblages from the Paleogene of northwestern Wyoming and

the Neogene of northern Pakistan: Palaeogeography, Palaeoclimatology, Palaeoecology, v. 115, p. 157-180, doi:10.1016/0031-0182(94)00110-t.

BEHRENSMEYER, A.K., 1975, The taphonomy and paleoecology of Plio-Pleistocene vertebrate assemblages east of Lake Rudolph, Kenya: Bulletin of the Museum of Comparative Zoology, v. 146, p. 473–578.

BEHRENSMEYER, A.K., 1991, Terrestrial vertebrate accumulations, *in* Allison P.A. and Briggs D.E.G. (eds.), Taphonomy: Releasing the data locked in the fossil record, Blackwell Scientific Publications, Oxford, p. 291–335.

BEROG, J., JEFFREY, D., COODE, K., HESTER, W., ROBINSON, D., and BISHOP, J., 2014, Taphonomic patterns of a dinosaur accumulation in a lacustrine delta system in the Jurassic Morrison Formation, San Rafael Swell, Utah, USA: Palaeontologia Electronica, v. 17, p. 1-19, doi:10.26879/372.

BOURQUE, J. R. and SCHUBERT, B. W., 2015. Fossil Musk Turtles (Kinosternidae, Sternotherus) from the Late Miocene-Early Pliocene (Hemphillian) of Tennessee and Florida: Journal of Vertebrate Paleontology, v.35(1), p. 1–19.

BRAMBLE, K., BURNS, M. E., and CURRIE, P. J., 2014, Enhancing bonebed mapping with gis technology using The Danek Bonebed (UPPER cretaceous Horseshoe canyon Formation, Edmonton, Alberta, CANADA) as a case study: Canadian Journal of Earth Sciences, v. 51, p. 987-991. doi:10.1139/cjes-2014-0056.

BROWN, C. M., HERRIDGE-BERRY, S., CHIBA, K., VITKUS, A., and EBERTH, D. A. 2020, High-resolution (centimetre-scale) GPS/GIS-based 3D mapping and spatial analysis of in situ fossils in two horned-dinosaur bonebeds in the Dinosaur Park Formation (Upper Cretaceous) at Dinosaur Provincial Park, Alberta, Canada: Canadian Journal of Earth Sciences, p. 1-22. doi:10.1139/cjes-2019-0183.

BUNN, H.T. 1989, Diagnosing Plio-Pleistocene hominid activity with bone fracture evidence, *in* Bonnichsen, R. and Sorg, M. H. (eds.), Bone modification: University of Maine Center for the Study of the First Americans, Orono, p. 299-315.

COBO-SÁNCHEZ L., ARAMENDI J., and DOMÍNGUEZ-RODRIGO M. 2014, Orientation patterns of wildebeest bones on the lake masek floodplain (Serengeti, Tanzania) and their relevance to interpret anisotropy in the Olduvai Lacustrine Floodplain: Quaternary International, v. 497, p. 137-153, doi:10.1016/j.quaint.2013.07.130.

CURRIE, P.J., 2000, Possible evidence of gregarious behavior in tyrannosaurids: Gaia v, 15 p. 123–133.

CUTLER, A. H. and FLESSA, K. W. 1990, Fossils out of sequence: Computer simulations and strategies for dealing with stratigraphic disorder: Palaios, v. 5, p. 227, doi:10.2307/3514941.

DODSON, P., 1971, Sedimentology and taphonomy of the Oldman Formation (Campanian), Dinosaur Provincial Park, Alberta (Canada): Palaeogeography, Palaeoclimatology, Palaeoecology, v.10, p. 21–74.

DODSON, P., 1973, The significance of small bones in paleoecological interpretation.
Contributions to Geology: University of Wyoming v. 12, p. 15–19.

EBERTH, D.A., D.S BERMAN, S.S. SUMIDA, and H. HOPF., 2000, Lower Permian terrestrial
paleoenvironments and vertebrate paleoecology of the Tambach Basin (Thuringia,
Central Germany): The upland holy grail: Palaios, v. 15 p. 293–313.

EBERTH, D.A., and GETTY, M.A., 2005, Ceratopsian bonebeds: occurrence, origins, and
significance *in* Currie P.J. and Koppelhus E.B. (eds.), Dinosaur Provincial Park: a
spectacular ancient ecosystem revealed, Indiana University Press, Bloomington, Indiana,
p. 501–536.

EBERTH, D. A., ROGERS, R. R., and FIORILLO, A. R., 2007, A Practical Approach to the Study of
Bonebeds, *in* Bonebeds: Genesis, analysis, and paleobiological significance, University
of Chicago Press, Chicago.

FARLOW, J. O., STEINMETZ, J. C., DECHURCH, D., ARGAST, A., and SUNDERMAN, J. A., 2010,
Geology of the late Neogene Pipe Creek sinkhole (Grant County, Indiana), Indiana
University, Indiana Geological Survey, Bloominton, IN.

FIORILLO, A.R., 1991, Taphonomy and depositional setting of Careless Creek Quarry (Judith
River Formation), Wheatland County, Montana, U.S.A.: Palaeogeography,
Palaeoclimatology, Palaeoecology, v. 81, p. 281–311.

FRISCIA, A., VAN VALKENBURGH, B., SPENCER, L. and HARRIS, J., 2008, Chronology and Spatial
Distribution of Large Mammal Bones in Pit 91, Rancho La Brea. Palaios, v. 23, p.35-42.

GIBSON, M. L., 2011, Population Structure Based on Age-Class Distribution of *Tapirus polkensis* from the Gray Fossil Site, Tennessee (Unpublished master's thesis). East Tennessee State University.

GIUSTI, D. and ARZARELLO, M., 2016, The need for A taphonomic perspective in spatial analysis: Formation processes at the early Pleistocene site of Pirro Nord (P13), Apricena, Italy: Journal of Archaeological Science: Reports, v. 8, p. 235-249, doi:10.1016/j.jasrep.2016.06.014.

GIUSTI, D., TOURLOUKIS, V., KONIDARIS, G.E., THOMPSON, N., KARKANSAS, P., PANAGOPOULOU, E., and HARVATI, K., 2018, Beyond Maps: Patterns of formation processes at the middle Pleistocene open-air site of Marathousa 1, Megalopolis Basin, Greece: Quaternary International, v. 497, p. 137–53.

GORHAM, E., and SANGER, J., 1972, Fossil pigments in the surface sediments of a meromictic lake: Limnology and Oceanography, v. 17, p. 618-622, doi:10.4319/lo.1972.17.4.0618.

HEWITT, R.J., PARFITT, S.A., and WENBAN-SMITH, F.F., 2018, Rose diagrams and statistical tests for archaeological orientation data: A case applied to the Southfleet Road Elephant site, Ebbsfleet, UK. doi:10.31235/osf.io/f2vzs

HILL, A.P., 1979, Disarticulation and scattering of mammal skeletons: Paleobiology, v. 5, p. 261– 274.

HILL, A.P., and BEHRENSMEYER A.K., 1984, Disarticulation patterns of some modern East African mammals: Paleobiology, v. 10, p. 366–376.

HILL, K., SWIFT, J. N., HOWARD, C., FARRELL, A., and LINDSEY, E. L., 2020, 3D Visualization of Subsurface Objects from La Brea Tar Pits, Los Angeles, CA: Digital Applications in Archaeology and Cultural Heritage, v. 20. doi:10.1016/j.daach.2020.e00167

HUNT JR., R.M., 1990, Taphonomy and sedimentology of Arikaree (lower Miocene) fluvial, eolian, and lacustrine paleoenvironments, Nebraska and Wyoming: A paleobiota entombed in fine-grained volcaniclastic rocks, *in* Lockley M.G. and Rice A. (eds.), Volcanism and fossil biotas, special paper, Geological Society of America, Boulder, Colorado, p. 69–111.

JASINSKI, S. E., 2018, A New Slider Turtle (Testudines: Emydidae: Deirochelyinae: *Trachemys*) from the Late Hemphillian (Late Miocene/Early Pliocene) of Eastern Tennessee and the Evolution of the Deirochelyines: PeerJ, 6. doi:10.7717/peerj.4338

KEENAN, S.W., and ENGEL, A.S., 2017, Reconstructing diagenetic conditions of bone at the Gray Fossil Site, Tennessee, USA: Palaeogeography, Palaeoclimatology, Palaeoecology, v. 471, p. 48-57, doi:10.1016/j.palaeo.2017.01.037.

KEENAN, S.W., WIDGA, C., DEBRUYN, J., SCHAEFFER, S., ENGEL, A.S., and HATCHER, R.D., 2018, Nutrient hotspots through time: A field guide to modern and fossil taphonomy in east Tennessee, Geological Society of America, p. 61-74.

KETCHUM, W., 2011, Using Geographical Information Systems to investigate spatial patterns in fossils of *Tapirus polkenis* from the Gray Fossil Site, Washington County, Tennessee. (Master's Thesis). East Tennessee State University. Johnson City, TN.

LANDIS, J.R., and KOCH, G.G., 1977, The Measurement of Observer Agreement for Categorical Data: Biometrics, v. 33, p. 159, doi:10.2307/2529310.

LANCASTER, S.T., UNDERWOOD, E.F., and FRUEH, W.T., 2010, Sediment reservoirs at mountain stream confluences: Dynamics and effects of tributaries dominated by debris-flow and fluvial processes: Geological Society of America Bulletin, v. 122, p. 1775-1786, doi:10.1130/b30175.1.

LANDLER, L., RUXTON, G.D., and MALKEMPER E.P., 2019, The Hermans-Rasson test as a powerful alternative to the Rayleigh test for circular statistics in biology: BMC Ecology, v. 19, p. 30.

LEWIS Jr., W.M., 1983, A revised classification of lakes based on mixing: Canadian Journal of Fisheries and Aquatic Sciences. v. 40, p. 1779-1787, doi:10.1139/f83-207.

LIEN, D., CAVIN, J., JOHNSON, S., and HERBEL, C., 2002, Interactive field mapping: Using the Pentax total station and Arcview for the analysis of fossil bed accumulations: Journal of Vertebrate Paleontology v. 22, p. 79A.

LIU, Y. and JACQUES, F.M., 2010, *Sinomenium macrocarpum* sp. nov. (Menispermaceae) from the Miocene–Pliocene transition of Gray, Northeast Tennessee, USA: Review of Palaeobotany and Palynology, v. 159, p. 112-122 doi:10.1016/j.revpalbo.2009.11.005.

LYMAN, R.L., 1994, Vertebrate taphonomy: Cambridge manuals in archaeology, Cambridge University Press, Cambridge, 524 p.

MACKIE, M.E., SUROVELI, T.A., O'BRIEN, M., KELLY, R.L., PELTON, S., HAYNES, C.V., Mackie M E, Surovell T A, O'Brien M, Kelly R L, Pelton S, Haynes Jr. C V, Frison G C, Yohe R M, Teteak S, Rockwell H M, and MAHAN, S., 2020, Confirming a cultural Association at the la PRELE Mammoth Site (48CO1401), converse County, Wyoming: American Antiquity, v. 85, p. 554-572, doi:10.1017/aaq.2020.8.

MARR, J.G., SHANMUGAM, G., and PARKER, G., 2001, Experiments on Subaqueous Sandy Gravity Flows: The Role of Clay and Water Content in Flow Dynamics and Depositional Structures: Bulletin of the Geological Society of America v. 113, p. 1377–86.

MILLER, I.M., PIGATI, J.S., ANDERSON, R.S., JOHNSON, K.R., MAHAN, S.A., AGER, T.A., BAKER, R.G., BLAAUW, M., BRIGHT, J, BROWN, P.M., BRYANT, B., CALAMARI Z.T., CARRARA, P.E., CHERNEY, M.D., DEMBOSKI, J.R., ELIAS, S.A., FISHER, D.C., GRAY, H.J., HASKETT D.R., HONKE, J.S., JACKSON, S.T., JIMENEZ-MORENO, G., KLINE, D., LEONARD, E.M., LIFTON, N.A., LUCKING, C., MCDONALD, H.G., MILLER, D.M., MUHS, D.R., NASH, S.E., NEWTON, C., PACES, J.B., PETRIE, L., PLUMMER, M.A., PORINCHU, D.F., ROUNTREY, A.N., SCOTT, E., SERTICH, J.J.W, SHARPE, S.E., SKIPP, G.L., STRICKLAND, L.E., STUCKY, P.R.K., THOMPSON, R.S., and WILSON, J., 2014, Summary of the Snowmastodon Project Special Volume. A High-Elevation, Multi-Proxy Biotic and Environmental Record of MIS 6-4 from the Ziegler Reservoir Fossil Site, Snowmass Village, Colorado, USA: Quaternary Research, v. 82, p. 618–34.

NAVE, J.W., ALI, T.A., AND WALLACE, S.C., 2005, Developing a GIS Database for the Gray Fossil Site, Tennessee, Based on Modern Surveying: Surveying & Land Information Science, v. 5, p. 259–264.

107

ORGANISTA, E., DOMINGUES-RODRIGO, M., YRAVERDA, J., URIBELARREA, D., ARRIAZA, M.C.,
ORTEGA, M.C., Mabulla, A., Gidna, A., BAQUEDANO, E., 2017, Biotic and abiotic
processes affecting the formation of BK level 4C (BED II, Olduvai GORGE) and their
bearing on hominin behavior at the site: Palaeogeography, Palaeoclimatology,
Palaeoecology, v. 488, p. 59-75, doi:10.1016/j.palaeo.2017.03.001.

PIERSON, T. C., 2005, Distinguishing between debris flows and floods from field evidence in
small watersheds: Fact Sheet, doi:10.3133/fs20043142.

ROGERS, R.R., 2005, Fine-grained debris flows and extraordinary vertebrate burials in the Late
Cretaceous of Madagascar: Geology, v. 33, p. 297–300.

ROGERS, R.R. and KIDWELL, S.M., 2007, A conceptual framework for the genesis and analysis of
vertebrate skeletal concentrations, in: Rogers, R.R., Eberth, D.A., Fiorillo, A.R. (Eds.),
Bonebeds: Genesis, Analysis, and Paleobiological Significance: The University of
Chicago Press, Chicago, p. 499.

SAMUELS, J.X., BREDHOEFT, K.E., and WALLACE, S.C., 2018, A New Species of *Gulo* from the
Early Pliocene Gray Fossil Site (Eastern United States); Rethinking the Evolution of
Wolverines: PeerJ, v. 6. doi:10.7717/peerj.4648

SCHUSTER, R. L. and HIGHLAND, L. M., 2007, Overview of the effects of mass wasting on the
natural environment: Environmental and Engineering Geoscience, v. 13(1) p. 25-44.
doi:10.2113/gseegeosci.13.1.25

SHIPMAN, P.G., 1981, Life history of a fossil: An introduction to taphonomy and paleoecology. Harvard University Press, Cambridge.

SHOTWELL, J.A., 1955, An approach to the paleoecology of mammals: Ecology, v. 36, p. 327-337.

SHUNK, A.J., DRIESE, S.G., and CLARK, G.M., 2006, Latest Miocene to earliest Pliocene sedimentation and climate record derived from paleosinkhole fill deposits, Gray Fossil Site, northeastern Tennessee, U.S.A.: Palaeogeography, Palaeoclimatology, Palaeoecology, v. 231, p. 265–278.

SHUNK, A., DRIESE, S., and DUNBAR, J., 2009, Late Tertiary paleoclimatic interpretation from lacustrine rhythmites in the Gray Fossil Site, northeastern Tennessee, USA: Journal of Paleolimnology, v. 42, p. 11–24, https://doi.org/10.1007/s10933-008-9244-0.

STEWART, K., WALKER, K., and LIKENS, G., 2009, Meromictic lakes: Encyclopedia of Inland Waters, p. 589-602, doi:10.1016/b978-012370626-3.00027-2.

SYME, C. and SALISBURY, S., 2017, Patterns of Aquatic decay and disarticulation in Juvenile Indo-Pacific crocodiles (*Crocodylus Porosus*), and implications for the taphonomic interpretation of fossil Crocodyliform material, doi:10.31233/osf.io/szyeb.

TOOTS, H., 1965, Orientation and distribution of fossils as environmental indicators, *in* R.H. DeVoto and R.K. Bitter (eds.), Sedimentation of Late Cretaceous and Tertiary outcrops, Rock Springs Uplift: 19th annual field conference guidebook. Wyoming Geological Association, Casper, p. 219–229.

VARRICCHIO, D.J., 1995, Taphonomy of Jack's Birthday Site, a diverse dinosaur bonebed from the Upper Cretaceous Two Medicine Formation of Montana: Palaeogeography, Palaeoclimatology, Palaeoecology, v. 114, p. 297–323.

VOORHIES, M.R., 1969, Taphonomy and population dynamics of an early Pliocene fauna, Knox County, Nebraska: University of Wyoming Contributions to Geology, Special Papers, v. 1, p. 1-69.

WALKER, K.F. and LIKENS, G.E., 1975, Meromixis and A Reconsidered typology of Lake circulation patterns: SIL Proceedings, 1922-2010, v. 19, p. 442-458, doi:10.1080/03680770.1974.1189608.

WALLACE, S.C. and WAND X., 2004, Two New Carnivores from and Unusual Late Tertiary Fossil Biota in Eastern North America: Nature, v. 431, p. 556-559.

WHITELAW, J.L., MICKUS, K., WHITELAW, M.J., and NAVE, J., 2008, High-resolution gravity study of the Gray Fossil Site: Geophysics, v. 732, doi:10.1190/1.2829987.

WIDGA, C., HAUGRUD, S., SCHUBERT, B., WALLACE, S. C., COMPTON, B., MEAD, J., 2018, Mastodons, Vertebrate Taphonomy and Nutrient Cycling at the Gray Fossil Site: Geological Society of America *Abstracts with Programs.* V. 50 (3), doi: 10.1130/abs/2018SE-311962
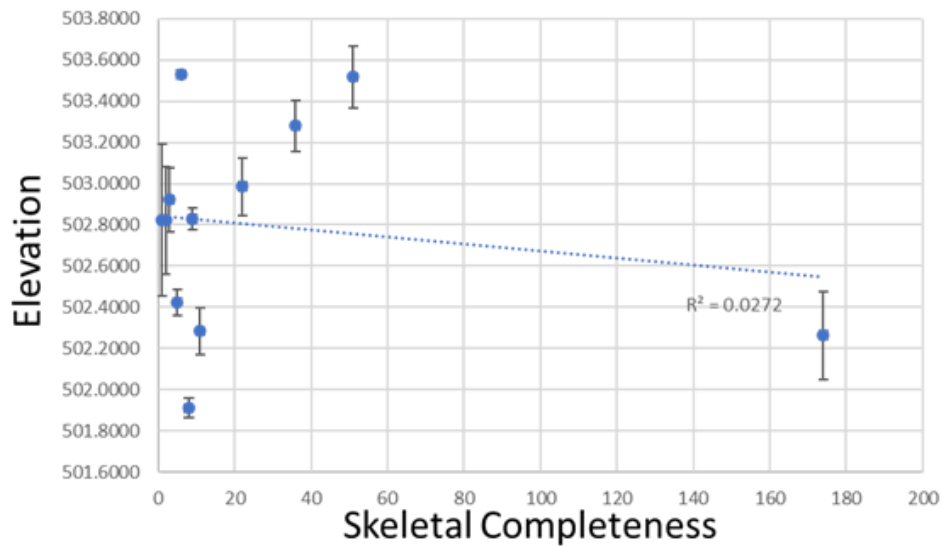
Chapter 3 Supplemental Data

3.1 Skeletal Completeness/Mean Elevation Plots and Trend Lines with R^2 Values. Error bars are based off Standard Deviations.
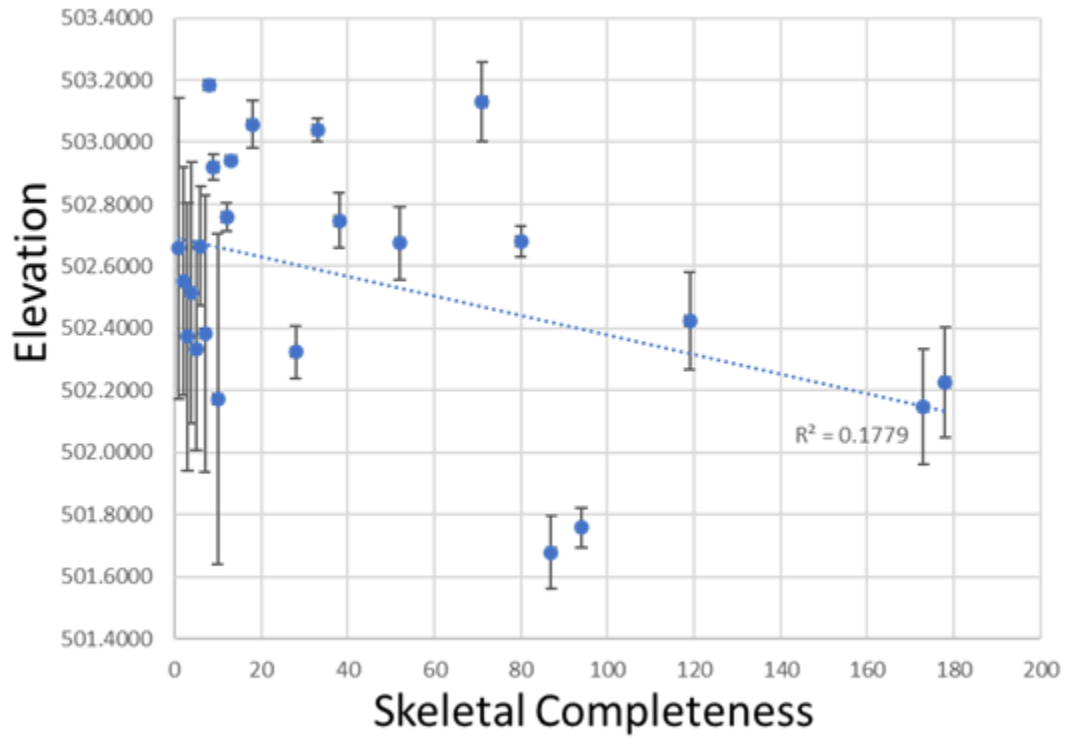
A Mastodon Pit
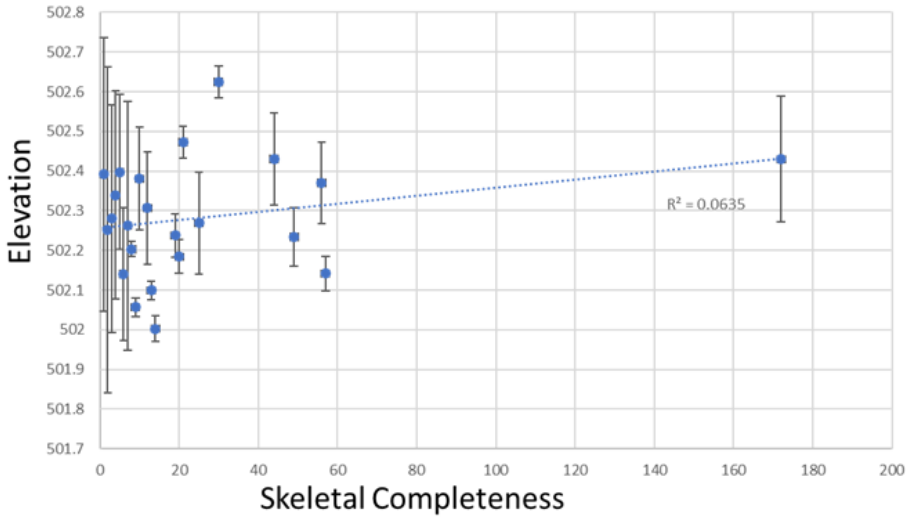
B Mulch Pit

C Rhino Pit

CHAPTER 4. CONCLUSIONS

Recommendations for Field Collection

Once datasets are created in excel, they can be edited in ArcGIS Pro to incorporate more data and visualize the data. This expedited some workflows as I relied on computing power to complete repetitive calculations for the large datasets. Measurements such as volume, weight, length, strike, and plunge are all valuable information, but take time to manually record in the field. Much of this information can be accurately calculated from the Total Station data. With this information, many above mentioned dimensional data can be calculated (although the accuracy of some measurements is dependent on the number of points collected on individual specimens). ArcGIS Pro is ideal for creating dimensional spatial data as the software comes with many tools to create this type of data.

Digital computation of dimensional data can be very efficient, but one step in the workflow to create datasets for ArcGIS Pro was very time-consuming. This step was the transfer of handwritten field note records to an Excel spreadsheet. Thousands of records were typed into spreadsheets, exacerbating the possibility of transcription errors. This step was extremely time intensive, ultimately taking weeks of manual data entry from digital scans of the field notes. Thankfully, the field notes recorded at GFS over the past seventeen years were quite consistent. Consistent formatting, information, and recorded details allow the data to be organized into rows and columns on a spreadsheet. The "=VLOOKUP" function in excel was then used to link newly created spreadsheets to the master spatial dataset created by the total station. This step merges the two pieces of field data so that the final datasets include what was found (taxa, skeletal element, placement on element) and where it was found (northing value, easting value, and depth).

Due to the labor-intensive data entry process, data redundancy, and the potential for transcription errors, the information contained in field notes would be an ideal candidate for conversion to a digital worksheet. This was actually proposed by early researchers at GFS. Nave et al. (2005) suggested that Microsoft Access forms be incorporated into field data collection. With technological tools such as rugged field tablets becoming less expensive with increased battery life, it is recommended that digital worksheets be incorporated into field data collection at GFS. Survey123 (3.12, ArcGIS) is an example of such a form that would work well as it is customizable and easily linked to ArcGIS Pro (Figure 4.1). The form can include drop down menus for certain entries to limit responses in order to keep data as consistent as possible. Open text fields can also be added to detail unique observations on what is being collected.

Figure 4.1 An example of a digital Survey 123 form that could be incorporated into field data collection at GFS. Drop-down menus can be incorporated to limit user responses. In this case, a form will be created for every single survey point collected by the total station. Forms can then be transferred to one spreadsheet where all data are collected and organized.

Hand drawn sketches of *in situ* material along with placement of survey points noted in the sketch were also important to gathering data on associated specimens for this assessment. Sketches are a great way to simplify information and highlight important observations noted. With digital field notes, hand drawn sketches can still be incorporated as an image field can be added to digital forms. A hand drawn sketch can be photographed with the camera on a tablet and uploaded to the digital form in the field. An alternative solution would be to create an

annotated photograph of observed specimens. Photographs of *in situ* features can overcomplicate

observations noted; however, annotations made on the photographs can help highlight the

important features.

A second recommendation for the field data collection methods would be to create a

more consistent field number. Figure 2.2 breaks down the unique field number created for each

point recorded by the total station. The format of the field number lends itself well to coding,

which is becoming increasingly popular and useful in GIS applications. A critical part of coding

is consistency, and this is important when it comes to the number of characters (digits) associated

with a code. If a code is always the same number of characters, coding becomes much easier. In

Figure 2.2, the orange and green parts of the code are always six digits followed by a dash and

then three digits. After this portion of the field number, the character lengths become more

variable.

A skeletal element is designated by a letter(s) depending on the order in which it is

recovered. For example, if a tapir left femur was the first uncovered element from an associated

tapir, it will receive an "A" as the element designation. All other spatial points taken on the

Tapir's left femur will receive an A as well, but once the second element has been recovered, it

will be designated by a "B". Letters "I" and "O" are skipped to avoid confusion with numbers

"1" and "0". This provides 24 unique characters for recovered elements coming from the same

individual. If an associated individual has more than 24 skeletal elements preserved, the entry

restarts at A and a second character is added to designate the element by running through the

alphabet a second time (i.e. "Y", "Z", "AA", "AB", "AC"… etc.). To keep the number of

characters consistent, it is recommended to start this portion of the field number with two letters

("AA") and continue as normal from there. This will provide a total of 576 unique entries for a

given associated specimen at a character length of 2. Mammalian skeletons rarely exceed 250 skeletal elements, but with this format, something even like an abundance of osteoderms could also be recorded in the system. The final portion of the field number designating the point number placed on the given skeletal element. This character can be variable as it is the final portion included in the code. With this new format, the first three portions of the code (date, specimen number, specimen element) will stay a consistent length at 12 characters followed by 1-3 characters for the survey point placement on skeletons. Point placement rarely exceeds 1 digit, but some elements recorded in the field notes were represented by hundreds of points though these were fragments thought to be associated to a single element.

This leads to the next limitation of the field number format, which is its inability to account for fragmentation in the fossil material. There is no part of the code that designates material at the fragment level (i.e., two pieces from a skeletal element that broke apart from each other). Rather than come up with a system to incorporate this information into the code, it is recommended that field documentation continue to rely on field sketches to understand fragmentation of specific elements. This is time-consuming, but it would also be time-consuming to the total station operator. It would be all too possible for the operator to type in the wrong information and ultimately lead to incorrect data. It is also felt that observations of fragmentation are only necessary for detailed studies of individuals much like it was observed for ETMNH 305 for this study. Perhaps a scalar fragmentation field in the digital notes would add meaningful data to the spreadsheet.

What's next?

Working to create a more consistent, potentially digital, method for field data collection can facilitate faster post-processing. Eventually, a workflow could be designed to automate the

entire workflow. This is an instance where coding can have an impact on the science carried out at GFS as the time taken to prepare data to be analyzed is drastically shortened.

Where to Dig Next?

Considering the potential implications of a mass wasting feature in a sinkhole may aid field crews when making decisions in where to dig next. Most of the excavation pits at GFS contain the black clay rhythmites that infilled the sinkhole. These deposits are representing the interior of the sinkhole rather than the sinkhole edge/bank. The geologic feature identified in the Mastodon Pit has oxidized sediments that may reflect more of the sinkhole margin. The two most fossiliferous excavation pits at the site thus far are the Mastodon Pit and the Rhino Pit adjacent to it. Perhaps they are more fossiliferous as they are reflecting animals preserved near the edges. Furthermore, there are fewer aquatic animals present in these two deposits when compared to others that contain aquatic turtles, fish, and alligators. Those types of animals are seldom found in the Mastodon and Rhino Pits even though they are the most fossiliferous deposits. The Mulch Pit has been thoroughly excavated and lies just to the north of both the Mastodon and Rhino Pits. The Mulch Pit contains typical rhythmites and fossils that are mostly disarticulated. The deposits just south of the Mastodon and Rhino Pits remain unexcavated as they were under a hill. As of 2019, much of this portion of the hill has been removed, allowing access to the sinkhole deposits at lower depths. It is recommended that this area is explored by field crews as this area may be approaching the edge of the sinkhole and will be more fossiliferous. If the sinkhole margin is identified and proves to be productive, GFS field workers would be able to follow the marginal deposits leading to more information about the sinkhole such as its dimensions.

Final Overall Conclusions

- Workflows were proposed to create digital representatives of features and surface observed at the Gray Fossil site:

  o Objects can be featured as point-based, line-based, and polygon-based shapefiles within ArcGIS Pro.

  o Excavation surfaces can be mapped in high resolution with UAV imagery and processed in multiple programs to create 3D raster surfaces for mapped features to interact with.

- Taphonomy of GFS was assessed:

  o Bones with a distinct long axis are often oriented in multimodal directions for all excavation pits included in this study, with slightly stronger directional preference noted in the Rhino Pit.

  o The inclination of the bones with a distinct long axis had plunges of 11-12° in the Mulch and Rhino pits while the Mastodon Pit where plunges were greater at 15-17°, and the inclinations in each pit have minimal preference in direction.

  o Mean carcass completeness of tapir remains in the Mulch and Mastodon Pits is 1.7 and 1.8 respectively, with higher values in the Rhino and Tortoise Pits (2.3 and 2.2, respectively).

  o Unassociated and associated tapirs in the adjacent excavation pits do not appear to be deposited at distinctly different depths, but the organization of associated tapir individuals is clearly different between the Mastodon Pit and the Mulch and Rhino Pits.

- o Percentages of Voorhies Groups of tapir material are not significantly different between the excavation pits.

- o Sedimentary evidence and the distribution of bones and boulders suggest that the Mastodon Pit was the site of a mass wasting event.

- o The Mastodon, ETMNH 305 displays similar characteristics of other bones from the Mastodon Pit, however there are some qualitative observations that add detail to this interpretation.

- Recommendations for field data collection include:

  - o Incorporating digital field notes.

  - o Creating a more consistent Field Number format for improved machine learning applications.

REFERENCES

Abler W L. 1984. A three-dimensional map of a paleontological quarry. Contributions to

Geology (University of Wyoming) 23: 9-14.

Agenbroad L D. 1984. Hot Springs, South Dakota: entrapment and taphonomy of Columbian

Mammoth. In Martin P S and Klein R G, (eds.). Quaternary extinctions: a prehistoric

revolution. Tucson: University of Arizona Press. p. 113-127.

Agisoft Metashape. https://www.agisoft.com/pdf/PS_1.3%20-Tutorial%20(BL)%20-

%20Orthophoto,%20DEM%20(GCPs).pdf

Akersten W, Shaw C A, and Jefferson G T. 1983. Rancho La Brea: Status and future.

Paleobiology. 9: 211–217.

Alberdi M T, Alonso M A, Azanza B., Hoyos M, and Morales J. 2001. Vertebrate taphonomy in

circum-lake environments: Three cases in the Guadix-Baza Basin (Granada, Spain).

Palaeogeography, Palaeoclimatology, Palaeoecology, 165(1-2): 1-26. doi:10.1016/s0031-

0182(00)00151-6.

Albert G, Botfalvai G, and Ősi A. 2018. Mapping the past: GIS and intrasite spatial analyses of

fossil deposits in paleontological sites and their applications in taxonomy, taphonomy and

paleoecology. Palaeontologia Electronica, 21(3). doi:10.26879/8120031-0182(00)00151-

6

Ali S H, Omar N Q, and Abujayyab S K. 2016. Investigation of the accuracy of surveying and buildings with the pulse (non-prism) total station. International Journal of Advanced Research, 4(3): 2320-5407.

Allison P A and Broggis D E. 1991. Taphonomy of Nonmineralized Tissues: Topics in Geobiology, 25(70): doi:10.1007/978-1-4899-5034-5_2

Allmendinger R. 2020. StereoNet V.11.3.0. Rick Allmendinger's Stuff. (n.d.). Cornell University. Retrieved December 30, 2020, from https://www.rickallmendinger.net/

Apollonio F I, Gaiani M, and Benedetto Benedetti B. 2012. 3D Reality-Based Artefact Models for the Management of Archaeological Sites Using 3D GIS: A Framework Starting from the Case Study of the Pompeii Archaeological Area. Journal of Archaeological Science 39(5): 1271-1287. https://doi.org/10.1016/j.jas.2011.12.034

Badgley C. 1986. Taponomy of mammalian fossil remains from Siwalik rocks of Pakistan. Paleobiology, 12:119–142.

Badgley C., Bartels W S, Morgan M E, Behrensmeyer A K, and Raza S. 1995. Taphonomy of vertebrate assemblages from the Paleogene of northwestern Wyoming and the Neogene of northern Pakistan. Palaeogeography, Palaeoclimatology, Palaeoecology. 115(1-4), 157-180. doi:10.1016/0031-0182(94)00110-t

Batty M. 2018. Inventing future cities. doi:10.7551/mitpress/11923.001.0001

Behrensmeyer A K. 1975. The taphonomy and paleoecology of Plio-Pleistocene vertebrate
assemblages east of Lake Rudolph, Kenya. Bulletin of the Museum of Comparative
Zoology. 146:473–578.

Behrensmeyer A K. 1982. Time resolution in fluvial vertebrate assemblages. Paleobiology.
8:211–228.

Behrensmeyer A. 1988. Fossils in the making. Chicago: Chicago Univ. Press.

Behrensmeyer A K. 1991. Terrestrial vertebrate accumulations. In Allison P A and Briggs D E
G, (eds.). Taphonomy: Releasing the data locked in the fossil record. Plenum, New York,
Blackwell Scientific Publications, Oxford. p. 291–335.

Bertog J, Jeffery D, Coode K, Hester W, Robinson D, and Bishop J. 2014. Taphonomic patterns
of a dinosaur accumulation in a lacustrine delta system in the Jurassic Morrison
Formation, San Rafael Swell, Utah, USA. Palaeontologia Electronica. doi:10.26879/372

Blob R W. 1997. Relative hydrodynamic dispersal potentials of soft-shelled turtle elements;
implications for interpreting skeletal sorting in assemblages of nonmammalian terrestrial
vertebrates. Palaios. 12:151–164.

Bourque J R and Schubert B W. 2015. Fossil Musk Turtles (Kinosternidae, Sternotherus) from
the Late Miocene-Early Pliocene (Hemphillian) of Tennessee and Florida. Journal of
Vertebrate Paleontology 35(1):1–19.

Bramble K, Burns M E, and Currie P J. 2014. Enhancing bonebed mapping with GIS technology
using the Danek Bonebed (Upper Cretaceous Horseshoe Canyon Formation, Edmonton,

Alberta, Canada) as a case study. Canadian Journal of Earth Sciences. 51(11): 987-991.

doi:10.1139/cjes-2014-0056

Brown C M, Herridge-Berry S, Chiba K, Vitkus A, and Eberth D A. 2020. High-resolution

(centimetre-scale) GPS/GIS-based 3D mapping and spatial analysis of in situ fossils in

two horned-dinosaur bonebeds in the Dinosaur Park Formation (Upper Cretaceous) at

Dinosaur Provincial Park, Alberta, Canada. Canadian Journal of Earth Sciences. 1-22.

doi:10.1139/cjes-2019-0183

Burdick K, Wallace SC, Nave J. 2002. State of the art GIS applications at the Miocene age fossil

site in Gray, Tennessee. Journal of Vertebrate Paleontology 22(3, supplement):117A.

Bunn H T. 1989. Diagnosing Plio-Pleistocene hominid activity with bone fracture evidence. In

Bonnichsen R and Sorg M H, (eds.). Bone modification, Orono: University of Maine

Center for the Study of the First Americans. p. 299-315.

Cobo-Sánchez L, Aramendi J, and Domínguez-Rodrigo M. 2014. Orientation patterns of

wildebeest bones on the LAKE masek floodplain (Serengeti, Tanzania) and their

relevance to interpret anisotropy in the Olduvai lacustrine floodplain. Quaternary

International. 322-323, 277-284. doi:10.1016/j.quaint.2013.07.130

Currie P J. 2000. Possible evidence of gregarious behavior in tyrannosaurids. Gaia 15:123–133.

Cutler A H and Flessa K W. 1990. Fossils out of SEQUENCE: Computer simulations and

strategies for dealing with Stratigraphic disorder. PALAIOS. 5(3): 227.

doi:10.2307/3514941

Dodson P. 1971. Sedimentology and taphonomy of the Oldman Formation (Campanian), Dinosaur Provincial Park, Alberta (Canada). Palaeogeography, Palaeoclimatology, Palaeoecology. 10:21–74.

Dodson P. 1973. The significance of small bones in paleoecological interpretation. Contributions to Geology, University of Wyoming 12:15–19.

Eberth D A. 1990. Stratigraphy and sedimentology of vertebrate microfossil sites in the uppermost Judith River Formation (Campanian), Dinosaur Provincial Park, Alberta, Canada. Palaeogeography, Palaeoclimatology, Palaeoecology. 78:1–36.

Eberth D A, Berman D S, Sumida S S, and Hopf H. 2000. Lower Permian terrestrial paleoenvironments and vertebrate paleoecology of the Tambach Basin (Thuringia, Central Germany): The upland holy grail. Palaios. 15:293–313.

Eberth D A and Getty M A. 2005. Ceratopsian bonebeds: occurrence, origins, and significance. In Currie P J and Koppelhus E B (eds.). Dinosaur Provincial Park: a spectacular ancient ecosystem revealed. Indiana University Press, Bloomington, Indiana. p. 501–536.

Eberth D A, Rogers R R, and Fiorillo A R. 2007. A Practical Approach to the Study of Bonebeds. In Bonebeds: Genesis, analysis, and paleobiological significance. Chicago: University of Chicago Press. Efremov I A. 1940. Taphonomy: a new branch o f paleontology. Pan-American Geologist 74: 81-93.

Esri 3D GIS. ArcGIS Capabilities. Available: https://www.esri.com/en-us/arcgis/3dgis/overview. Esri Orthomosaic workflow.

https://doc.arcgis.com/en/imagery/workflows/tutorials/createdrone-imagery-products-ortho-mapping.htm

Estrada Belli F. 1999. The archaeology of complex societies in Southeastern Pacific coastal GUATEMALA: A Regional GIS Approach. doi:10.30861/9781841711195

Farlow J O, Steinmetz J C, DeChurch D, Argast A, and Sunderman J A. 2010. Geology of the late Neogene Pipe Creek sinkhole (Grant County, Indiana). Bloominton, IN: Indiana University, Indiana Geological Survey.

Fiorillo A R. 1991. Taphonomy and depositional setting of Careless Creek Quarry (Judith River Formation), Wheatland County, Montana, U.S.A. Palaeogeography, Palaeoclimatology, Palaeoecology. 81:281–311.

Friscia A, Van Valkenburgh B, Spencer L, and Harris J. 2008. Chronology and Spatial Distribution of Large Mammal Bones in Pit 91, Rancho Le Brea. Palaios. 23(1): 35- 42.

Gibson M L. 2011. Population Structure Based on Age-Class Distribution of Tapirus polkensis from the Gray Fossil Site, Tennessee (Unpublished master's thesis). East Tennessee State University.

Gilmore C W. 1936. Osteology of Apatosaurus, with special reference to specimens in the Carnegie Museum. Memoirs of the Carnegie Museum. 11(4): 175–300.

Giusti D and Arzarello M. 2016. The need for A taphonomic perspective in spatial analysis: Formation processes at the early Pleistocene site of Pirro Nord (P13), Apricena, Italy:

Journal of Archaeological Science: Reports, 8: 235-249,
doi:10.1016/j.jasrep.2016.06.014.

Giusti D, Tourloukis V, Konidaris E, Thompson N, Karkanas P, Panagopoulou E, and Harvati K.
2018. Beyond hill Maps: Patterns of Formation Processes at the Middle Pleistocene
Open-Air Site of Marathousa 1, Megalopolis Basin, Greece. Quaternary International.
497:137–53.

Gorham E and Sanger J. 1972. Fossil pigments in the surface sediments of a meromictic lake.
Limnology and Oceanography. 17(4): 618-622. doi:10.4319/lo.1972.17.4.0618

Grieves M. 2014. Digital Twin: Manufacturing Excellence through Virtual Factory Replication.
Digit Twin White Pap. Accessed November 17, 2019.

Grieves, M. 2019. "Digital Twin."Arup 18:80.

Hewitt R J, Parfitt S A, and Wenban-Smith F F. 2018. Rose diagrams and statistical tests for
archaeological orientation data: A case applied to the Southfleet Road Elephant site,
Ebbsfleet, UK. doi:10.31235/osf.io/f2vzs19901991

Hill A P. 1979. Disarticulation and scattering of mammal skeletons. Paleobiology. 5: 261– 274.

Hill A P and Behrensmeyer A K. 1984. Disarticulation patterns of some modern East African
mammals. Paleobiology. 10: 366–376.

Hill K, Swift J N, Howard C, Farrell A, and Lindsey E L. 2020. 3D Visualization of Subsurface

Objects from La Brea Tar Pits, Los Angeles, CA. Digital Applications in Archaeology

and Cultural Heritage. doi:10.1016/j.daach.2020.e00167

Hunt, R M Jr. 1990. Taphonomy and sedimentology of Arikaree (lower Miocene) fluvial, eolian,

and lacustrine paleoenvironments, Nebraska and Wyoming: A paleobiota entombed in

fine-grained volcaniclastic rocks. In Lockley M G and Rice A, (eds.). Volcanism and

fossil biotas. Special paper 244.Geological. Society of America, Boulder, Colorado. p.

69–111

Jasinski S E. 2018. A New Slider Turtle (Testudines: Emydidae: Deirochelyinae: Trachemys)

from the Late Hemphillian (Late Miocene/Early Pliocene) of Eastern Tennessee and the

Evolution of the Deirochelyines. PeerJ, 6. doi:10.7717/peerj.4338

Keenan S W and Engel A S. 2017. Reconstructing diagenetic conditions of bone at the Gray

Fossil Site, Tennessee, USA. Palaeogeography, Palaeoclimatology, Palaeoecology. 471:

48-57. doi:10.1016/j.palaeo.2017.01.037

Keenan S W, Widga C, Debruyn J, Schaeffer S, Engel A S, and Hatcher R D. 2018. Nutrient

hotspots through time: A field guide to modern and fossil taphonomy. In east Tennessee.

Geological Society of America. p. 61-74.

Ketchum W. 2011. Using Geographical Information Systems to Investigate Spatial Patterns in

Fossils of Tapirus polkenis from the Gray Fossil Site, Washington County, Tennessee.

(Master's Thesis). East Tennessee State University. Johnson City, TN.

Kvamme K L. 1995. A view from across the water: the North American experience in

    archaeological GIS. In Archaeology and Geographical Information Systems: A European

    Perspective. Pennsylvania: Taylor & Francis. p. 1–14.

Landis J R and Koch G G. 1977. The Measurement of Observer Agreement for Categorical Data.

    Biometrics. 33(1): 159. doi:10.2307/2529310

Lancaster S T, Underwood E F, and Frueh W T. 2010. Sediment reservoirs at mountain stream

    confluences: Dynamics and effects of tributaries dominated by debris-flow and fluvial

    processes. Geological Society of America Bulletin. 122(11-12): 1775-1786.

    doi:10.1130/b30175.1

Landler L, Ruxton G D, and Malkemper E P. 2019. The Hermans-Rasson test as a powerful

    alternative to the Rayleigh test for circular statistics in biology. BMC Ecology. 19:30.

Lewis W M Jr. 1983. A revised classification of lakes based on mixing. Canadian Journal of

    Fisheries and Aquatic Sciences. 40(10): 1779-1787. doi:10.1139/f83-207

Lien D, Cavin, J, Johnson S, and Herbel C. 2002. Interactive field mapping: Using the Pentax

    total station and Arcview for the analysis of fossil bed accumulations. Journal of

    Vertebrate Paleontology. 22(3): 79A

Liu Y and Jacques F M. 2010. Sinomenium macrocarpum sp. nov. (Menispermaceae) from the

    Miocene–Pliocene transition of gray, northeast Tennessee, USA. Review of Palaeobotany

    and Palynology. 159(1-2): 112-122. doi:10.1016/j.revpalbo.2009.11.005

Lyman R L. 1994. Vertebrate taphonomy. Cambridge manuals in archaeology. Cambridge
University Press, Cambridge.

Mackie M E, Surovell T A, O'Brien M, Kelly R L, Pelton S, Haynes C V, Mahan S. 2020.
Confirming a cultural Association at the la Prele Mammoth Site (48CO1401), converse
County, Wyoming. American Antiquity. 85(3): 554-572. doi:10.1017/aaq.2020.8

Marr J G, Shanmugam G, and Parker G. 2001. Experiments on Subaqueous Sandy Gravity
Flows: The Role of Clay and Water Content in Flow Dynamics and Depositional
Structures. Bulletin of the Geological Society of America. 113(11): 1377–1386.

Mead J I, Schubert B W, Wallace S C, Swift S L. 2012. Helodermatid lizard from the
MioPliocene oak-hickory forest of Tennessee, eastern USA, and a review of
monstersaurian osteoderms. Acta Palaeontologica Polonica. 57:111–121
doi:10.4202/app.2010.0083

Miller I M, Pigati J S, Anderson R S, Johnson K R, Mahan S A, Ager T A, Baker R G, Blaauw
M, Bright J, Brown P M, et al. 2014. Summary of the Snowmastodon Project Special
Volume. A High-Elevation, Multi-Proxy Biotic and Environmental Record of MIS 6-4
from the Ziegler Reservoir Fossil Site, Snowmass Village, Colorado, USA. Quaternary
Research (United States). 82(3): 618–34.

Nave J W, Ali T A, and Wallace S C. 2005. Developing a GIS Database for the Gray Fossil Site,
Tennessee, Based on Modern Surveying. Surveying & Land Information Science. 65(4):
259–264.

Nigro J D, Ungar P S, Ruiter D J, and Berger L R. 2003. Developing a Geographic Information System (GIS) for Mapping and Analysing Fossil Deposits at Swartkrans, Gauteng Province, South Africa. Journal of Archaeological Science. 30(3): 317-324. doi:10.1006/jasc.2002.0839

Ochoa D, Zavada M, Liu Y, and Farlow J. 2016. Floristic implications of two contemporaneous inland upper Neogene sites in the eastern US: Pipe Creek Sinkhole, Indiana, and the Gray Fossil Site, Tennessee (USA). Palaeobiodiversity and Palaeoenvironments. 96: 239-254.

Organista E, Domínguez-Rodrigo M, Yravedra J, Uribelarrea D, Arriaza M C, Ortega M C, Baquedano E. 2017. Biotic and abiotic processes affecting the formation of BK level 4C (BED II, Olduvai GORGE) and their bearing on hominin behavior at the site. Palaeogeography, Palaeoclimatology, Palaeoecology. 488: 59-75. doi:10.1016/j.palaeo.2017.03.001

Parmalee P W, Klippel WE, Meylan P A, and Holman J A. 2002. A late Miocene–early Pliocene population of Trachemys (Testudines: Emydidae) from east Tennessee. Annals of Carnegie Museum. 71: 233–239.

Pierson T C. 2005. Distinguishing between debris flows and floods from field evidence in small watersheds. Fact Sheet. doi:10.3133/fs20043142

Rogers R R. 1994. Vertebrate paleontological techniques. In Leiggi P. and May P. (eds.). Vertebrate paleontological techniques. Cambridge England: Cambridge University Press. p. 47-58.

Rogers R R and Kidwell S M. 2000. Associations of vertebrate skeletal concentrations and

   discontinuity surfaces in terrestrial and shallow marine records: A test in the Cretaceous

   of Montana. Journal of Geology. 108: 131–154.

Ryan M J, Russell A P, Eberth D A, and Currie P J. 2001. The taphonomy of a Centrosaurus

   (Ornithischia: Ceratopsidae) bone bed from the Dinosaur Park Formation (Upper

   Campanian), Alberta, Canada, with comments on cranial ontogeny. Palaios. 16: 482–506.

Safrel I, Julianto E N, and Usman N Q. 2018. Accuracy Comparison between GPS Real Time

   Kinematic (RTK) Method and Total Station to Determine the Coordinate of an Area.

   Unnes Journals. 20(2): 123-130. doi:10.15294/jtsp.v20i2.16284

Samuels J, Bredehoeft K, and Wallace S. 2018. A new species of Gulo from the Early Pliocene

   Gray Fossil Site (Eastern United States); rethinking the evolution of wolverines. PeerJ. 6.

   doi:10.7717/peerj.4648

Schrotter G and Hürzeler C. 2020. The digital twin of the city of Zurich for urban planning. PFG

   – Journal of Photogrammetry, Remote Sensing and Geoinformation Science. 88(1): 99-

   112. doi:10.1007/s41064-020-00092-2

Schuster R L and Highland L M. 2007. Overview of the effects of mass wasting on the natural

   environment. Environmental and Engineering Geoscience. 13(1): 25-44.

   doi:10.2113/gseegeosci.13.1.25

Shipman P G. 1981. Life history of a fossil: An introduction to taphonomy and paleoecology.

   Harvard University Press, Cambridge.

Shotwell J A. 1955. An approach to the paleoecology of mammals. Ecology. 36: 327-337.

Shunk A J, Driese S G, and Clark G M. 2006. Latest Miocene to earliest Pliocene sedimentation
    and climate record derived from paleosinkhole fill deposits, Gray Fossil Site,
    northeastern Tennessee, U.S.A. Palaeogeography, Palaeoclimatology, Palaeoecology.
    231(3): 265–278.

Shunk A, Driese S, and Dunbar J. 2009. Late Tertiary paleoclimatic interpretation from
    lacustrine rhythmites in the Gray Fossil Site, northeastern Tennessee, USA. Journal of
    Paleolimnol. 42(1): 11–24. https://doi.org/10.1007/s10933-008-9244-0

Stewart K, Walker K, and Likens, G. 2009. Meromictic lakes. Encyclopedia of Inland Waters. p.
    589-602. doi:10.1016/b978-012370626-3.00027-2

Syme C and Salisbury S. 2017. Patterns of Aquatic decay and disarticulation in Juvenile Indo-
    Pacific crocodiles (*Crocodylus Porosus*), and implications for the taphonomic
    interpretation of fossil Crocodyliform material. doi:10.31233/osf.io/szyeb.

Toots H. 1965. Orientation and distribution of fossils as environmental indicators. In DeVoto R
    H and Bitter R K (eds.). Sedimentation of Late Cretaceous and Tertiary outcrops, Rock
    Springs Uplift. 19th annual field conference guidebook. Wyoming Geological
    Association, Casper. p. 219–229

Varricchio D J. 1995. Taphonomy of Jack's Birthday Site, a diverse dinosaur bonebed from the
    Upper Cretaceous Two Medicine Formation of Montana. Palaeogeography,
    Palaeoclimatology, Palaeoecology. 114:297–323.

Voorhies M R. 1969. Taphonomy and population dynamics of an early Pliocene fauna, Knox

    County, Nebraska. University of Wyoming Contributions to Geology, Special Papers. 1:

    1-69.

Walker K F and Likens G E. 1975. Meromixis and A Reconsidered typology of Lake circulation

    patterns. SIL Proceedings 1922-2010. 19(1): 442-458.

    doi:10.1080/03680770.1974.11896084

Wallace S C, Nave J W and Burdick K M. 2002. Preliminary report on the recently discovered

    Gray Fossil Site (Miocene), Washington Co., Tennessee: with comments on observed

    paleopathologies–The advantages of a large sample. Journal of Vertebrate Paleontology.

    22: 117.

Wallace S and Wang X. 2004. Two new carnivores from an unusual late Tertiary forest biota in

    eastern North America. Nature. 431(7008): 556-559.

Whitelaw J L, Mickus K, Whitelaw M J, and Nave J. 2008. High-resolution gravity study of the

    Gray Fossil Site. Geophysics. 73(2). doi:10.1190/1.2829987

Widga C, Haugrud S, Schubert B, Wallace S C, Compton B, Mead J. 2018. Mastodons,

    Vertebrate Taphonomy and Nutrient Cycling at the Gray Fossil Site: Geological Society

    of America Abstracts with Programs. 50 (3). doi: 10.1130/abs/2018SE-311962

Zobaa M K, Zavada M S, Whitelaw M J, Shunk A J, and Oboh-Ikuenobe F E. 2011. Palynology

    and palynofacies analyses of the Gray Fossil Site, eastern Tennessee: Their role in

understanding the Basin-fill history. Palaeogeography, Palaeoclimatology,

Palaeoecology. 308(3-4): 433-444. doi:10.1016/j.palaeo.2011.05.051

VITA

DAVID G. CARNEY

Education:	M.A. Geosciences, East Tennessee State University, Johnson City, Tennessee, 2021
	B.A. Environmental Earth Sciences, Eastern Connecticut State University, Willimantic, Connecticut, 2013
	Public Schools, Glastonbury, Connecticut
Professional Experience:	Graduate Assistant, East Tennessee State University, College of Arts and Sciences, 2019-2021
	Recreational Technician, Belt Creek Forest Service Ranger Station; Nihart, Montana, 2018-2019
	Crew Co-Leader, Montana Conservation Corps, Bozeman, Montana, 2016
Honors and Awards:	Viewer's Choice Award (TNGIC), 2021
	Best Interactive Map Award (TNGIC), 2021
	Best Student Map Award (TNGIC), 2021
	Geoscience's excellence in Teaching Award for Earth thru Time Lecture and Lab courses (ETSU), 2021
	Russ McCarty Student Travel Grant (AMMP), 2021
	Congressional Award (Americorps NCCC), 2015